Pro-survival function of the mitochondrial Hsp90 homolog, TRAP1, in cancer cells and insight into cancer therapy

Hye-Kyung Park

School of Life Sciences

(Biological Sciences)

Graduate School of UNIST

2015

Pro-survival function of the mitochondrial Hsp90 homolog, TRAP1, in cancer cells and insight into cancer therapy

Hye-Kyung Park

School of Life Sciences

(Biological Sciences)

Graduate School of UNIST

Pro-survival function of the mitochondrial Hsp90 homolog, TRAP1, in cancer cells and insight into cancer therapy

A thesis submitted to the Graduate School of UNIST

in partial fulfillment of the requirements

for the degree of Doctor of Science

Hye-Kyung Park

01. 05. 2015

Approved by

_____

Advisor

Byoung Heon Kang

Pro-survival function of the mitochondrial Hsp90 homolog, TRAP1, in cancer cells and insight into cancer therapy

Hye-Kyung Park

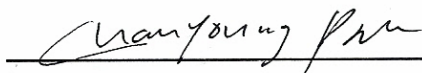This certifies that the thesis of H. K. Park is approved.
01. 05. 2015

Advisor: Byoung Heon Kang

Byoung Heon Kang

Chan Young Park

Taejoo Park

Changwook Lee

Sung Hoon Back

Abstract

Heat shock protein (Hsp90) is an ATP dependent chaperone that regulates folding of a wide range of client proteins or substrates, which are involved in cellular signaling pathways for tumorigenesis. The most of Hsp90 is localized in cytoplasm but mitochondrial Hsp90 homologue, tumor necrosis factor receptor-associated protein 1 (TRAP1), has been reported. The TRAP1 is highly elevated in many cancer cell types and human cancer patients compared to normal cells. TRAP1 plays important roles in tumorigenesis including the neoplastic metabolic shift to aerobic glycolysis, tumor cell invasion and metastatasis, inhibition of cell death and development of drug resistance.

A class of TRAP1 inhibitors, named gamitrinibs (GA mitochondrial matrix inhibitors), has been developed through combinatorial chemistry. Gamitrinib consist of geldanamycin, a competitive inhibitor of the ATPase pocket of Hsp90 and TRAP1, conjugated with tandem repeats of tetracyclic guanidinium or triphenylphosphonium for mitochondrial targeting. Gamitrinib not only trigger massive cell death in cultured cancer cells *in vitro* but also strongly suppress tumor growth in various cancer xenograft or genetic mouse model *in vivo*. The gamitrinib induced cytotoxicity is attributed to the reactivation of cyclophilin D (CypD), an opener of the permeability transition pore (PTP) located in the mitochondrial inner membrane. PTP opening by CypD activation is often suppressed in cancer cells to avoid cell death by interaction with mitochondrial Hsp90s even under stressful cellular environment. Furthermore, gamitrinibs have been shown to induce organelle-specific stress response and dysregulation of bioenergetics in mitochondria of cancer cells.

Resistance to cell death in the presence of stressful stimuli is one of hallmarks of cancer cells acquired during multistep tumorigenesis, and knowledge of the molecular mechanism of stress adaptation can be exploited to develop cancer-selective therapeutics. Mitochondria and the endoplasmic reticulum (ER) are physically interconnected organelles that can sense and exchange various stress signals. Although there have been many studies on stress propagation from the ER to mitochondria, reverse stress signals originating from mitochondria have not been well reported. In this study, we showed that mitochondrial heat shock protein 90 (Hsp90) suppresses mitochondria-initiated calcium-mediated stress signals propagating into the ER in cancer cells. Mitochondrial Hsp90 inhibition with gamitrinib triggers the calcium signal by opening the mitochondrial permeability transition pore and, in turn, the ER ryanodine receptor, via calcium-induced calcium release. Subsequent depletion of ER calcium activates unfolded protein responses in the ER, thereby increasing the expression of a pro-apoptotic transcription factor, CEBP homologous protein (CHOP). Combined treatment of the ER stressor thapsigargin with the mitochondrial Hsp90 inhibitor gamitrinib augments interorganelle stress signaling by elevating CHOP expression, and showed synergistic cytotoxic activity exclusively in cancer cells *in vitro* and *in vivo*.

1

Collectively, the mitochondrial Hsp90s confer apoptosis resistance to cancer cells by suppressing the mitochondria-initiated calcium-mediated interorganelle stress response. Next, the mitochondria stress inducer, gamibrinib has been exploited, for combination cancer therapy with clinical cancer drug doxorubicin (DOX). DOX, an anthracycline antibiotic with the trade name Adrimycin, is one of the most effective anticancer drugs and has been widely used to treat cancer patients in various combination chemotherapeutic regimens. The antitumor activities of DOX and closely related anthracycline analogs are primarily attributed to DNA damage resulting from the inhibition of DNA topoisomearse II. DOX has also been reported to increase oxygen derived free radicals, which contributes not only to its anticancer activities but also induce a major side effect, irreversible cardiomyopathy in the patients. To mitigate the cardiotoxic side effects of DOX, we explored the efficacy of combination treatment of DOX with gamitrinib. The combination treatment with DOX and gamitrinib showed synergistically increased anticancer activities at suboptimal cytotoxic dose *in vitro* and *in vivo*, without augmenting the cardiotoxic side effects. The mechanism of the action is involved in stimulation of cellular stress signaling mediating JNK of CHOP pathways and activation of proapoptotic protein Bim. Depending on cellular context of disparate cancer cell types, the combination treatment induced CHOP and Bim expression and phosphorylation of JNK and Bim, which leads to enhance accumulation of Bim and Bad in the mitochondria. These mechanisms were independent of ROS production and synergistically enhanced apoptosis exclusively in cancer cells *in vitro* and *in vivo*. In summary, combined treatment of TRAP1 inhibitors can unleash the full potential of the anticancer activity of various anticancer drugs.

CONTENTS

List of figures

Abbreviations

Δ Ψm: mitochondrial membrane potential

17AAG: 17-allylamino-17-demethoxygeldanamycin

BAPTA: 1,2-bis(o-aminophenoxy)ethane-N,N,N',N'-tetraacetic acid acetoxymethylester

Bim: Bcl-2 interacting mediator

CHOP: C/EBP homologous protein

CI: combination index

CICR: calcium induced calcium release

CPK: creatine phosphokinase

CsA: cyclosporine A

Cyp-D: cyclophilin D

DOX: doxorubicin

DR5: death receptor 5

eIF2 α: eukaryotic translation initiation factor 2 α

ER: endoplasmic reticulum

FCCP: carbonyl cyanide 4-(trifluoromethoxy) phenylhydrazone

Gamitrinib: GA mitochondrial matrix inhibitor

Hsp90: heat shock protein 90

IP 3R: inositol 1,4,5-trisphosphate receptors

JNK: c-Jun N-terminal kinase

MOMP: mitochondrial outer membrane permeabilization

MTT: 3(4,5-dimethyl-thyzoyl-2-yl)2,5 diphenyltetrazolium bromide

PTP: permeability transition pore

RyR: ryanodine receptor

Thap: thapsigargin

TMRM: tetramethylrhodamine methyl ester

TRAP1: tumor necrosis factor receptor-associated protein 1

UPR: unfolded protein response

XBP1: X-box binding protein

Chapter 1. Introduction

1-1. Molecular characteristic of chaperones

1-1-1. Functions of chaperones

Molecular chaperones are proteins that assist the disassembly or assembly and the unfolding or the non-covalent folding of other molecular structures and described first in the literature in 1978 [1]. In the cellular biology, proteins are structurally complex and versatile macromolecule which are synthesized on ribosome and folded in their native state [2]. Generally the chaperones aid in the co-translational folding of newly synthesized proteins and helps the conformational change of macromolecules [3]. Some chaperones are linked to remodelling of non-native proteins and other chaperones prevent or slow protein aggregation or misfolding. Therefore they are essential for protein quality control network [4, 5]. They are not highly expressed in normal biological condition. In non-native state as under cellular stress, proteins are easy to aggregate by misfolding, unfolding or disassembly. Since the chaperones capture misfolded or unfolded polypeptide and stabilize them, they are strongly increased to minimize protein aggregation in stressed cells. The chaperones have been reported that have function as foldase, holdase and involved in translocation, protein degradation, signal transduction, receptor maturation, protein trafficking, immunity and so on [6-10].

1-1-2. Heat shock proteins

Many chaperones are heat shock proteins because protein folding is severely affected by cellular stresses or temperatures [11]. Upon heat shock response, heat shock proteins are dramatically increased in transcriptional level by increased Heat shock factor 1 activity [12-15]. The heat shock proteins (HSP) are named depending on their molecular weight such as Hsp40, Hsp60, Hsp70, Hsp90 and Hsp100. Most of HSPs localized in cytosol or ER but Hsp60, Hsp70, Hsp90 are also expressed in mitochondria. Hsp100s are ATP dependent proteins and capture misfolded proteins and associated in stress tolerance [16]. Hsp90s has ATP binding domain and clamp into their client proteins depend on binding ATP [17, 18]. Hsp70s are well characterized 70kDa proteins and assisted by Hsp40s. Their client proteins are involved in survival factor therefore decreased Hsp70 results in apoptosis [19, 20].

Hsp40s is also called chaperone DnaJ and is the crucial partner of Hsp70 chaperones (Table.1) [21-23].

1-2. Heat shock protein 90 (Hsp90)

1-2-1 Transcriptional regulation of Hsp90

Hsp90 is highly abundant in the cytoplasm, where it occupies 1-2% of total protein level and its expression about doubles in response to cellular stress in most eukaryotes. Its inducible transcription is regulated by the transcription factor heat shock factor1 (HSF1) [12, 14, 19], which controls approximately hundreds of target genes in response to cellular stress. HSF1 is not only a client protein of Hsp90 but also regulated by complex with Hsp90 and Hsp70 negatively [19, 24]. HSF1 monomer held in inactive complex with Hsp90 and Hsp70 but this interaction is broken under cellular stress. Hsp90 capture misfolded protein and other client proteins which is increased in stressed cells and HSF1 can be released from Hsp90 complex (Fig.1) [14, 24]. Therefore, Hsp90 regulates its own transcription [19] .

1-2-2. Cellular location of Hsp90

Most of Hsp90 is localized in cytoplasm but some Hsp90 is translocated to the nucleus under cellular stress [25-27]. Its translocation occurs by co-transport with its client protein because Hsp90 has no a nuclear localization sequences. In addition, it found in mitochondria in malignant tumour cells and inhibition of Hsp90 function induces apoptosis [28].

1-2-3. Structure of Hsp90

Hsp90 is a dimeric protein and very conserved in evolution. Each monomer consists of three part such as amino-terminal domain (NTD), middle domain and carboxy- terminal domain (CTD). ATP binds in NTD of Hsp90 and hydrolyzed after interaction with Hsp90 and client proteins. The Hsp90 middle domain is connected to the NTD by a charged linker and consists of two αβα motif. The middle domain is thought to have essential role in client recognition. The CTD of Hsp90 has less conserved in sequence than NTD or middle domain and it is involved in dimerization. It is mixed α and β domain structurally and end of CTD has the tetratricopeptide repeat (TRP) motif recognition site [29]. TRP motif consist of

MEEVD(Met-Glue-Glue-Val-Asp) residue and is responsible for interaction with many co-chaperones [30, 31].

1-2-4. The function of Hsp90

In normal cells, Hsp90 plays a many roles including in protein folding, maintenance, intracellular transport as well as protein degradation. Generally, Hsp90 suppresses aggregation of client protein and helps correct conformational changes. Furthermore, Hsp90 is needed to keep correct structure of 26s proteosome. The 26s proteosome is involved protein degradation for polyubiquitinated proteins so Hsp90 can control protein quality in a macro aspects.[32]

Hsp90 has above 20 client proteins and various cellular functions according to client protein such as cellular signal transduction, tumorigenesis, protein trafficking, Heat shock response, cell mobility, cell cycle and proliferation and immunity [33-36].

1-3. Heat shock protein 90 (Hsp90) homologue proteins

1-3-1. Hsp90 homolgues in other cellular compartments

In mammalians, Hsp90 family can be divided into 3 sub families: cytosolic Hsp90A, endoplasmic reticulum (ER) localized Hsp90B and mitochondrial TNF receptor associated protein 1(TRAP1) [37-39]. HSP90A is the most studied of the Hsp90 families and consists of two sub-family such as inducible expressed HSP90AA and constitutive expressed HSP90 AB. They are abundant in cytosol and some HSP90A can be translocated to nucleus under cellular stress. The ER localized HSP90B proteins is also known Grp94 in human and controls in ER protein quality [40]. The function of TRAP1 is poorly understood of the other families but many papers reported that human TRAP1 protect cells from cellular stress (Fig. 2).

1-3-2. Mitochondrial HSP90 homologue (TRAP1) in cancer

TRAP1is highly up regulated in cancer cells compared to normal cells and protect cells against oxidative stress and apoptosis [41, 42]. This pathway is involved in mitochondrial permeability transition (MPT). TRAP1 binds to cyclopphilin D (CypD) which is key molecule in permeability transition (PT) pore complex and their interaction results to inactive CypD so blocked PT pore opening [43]. In addition, TRAP1 may play a role in

organelle homeostasis by involving protein folding quality control [44]. TRAP1 preserve Hexokinase II (HK II) and stability of succinate dehydrogenase (SDHB) [45-48]. HK II is a key mediator of glycolysis and SDHB is associated with oxidative phosphorylation. Both of enzymes play important roles in cellular homeostasis and metabolic network. Inhibition of TRAP1 by genetically or pharmacologically impairs both oxidative phosphoryalation and glycolysis. The TRAP1 has a quite different cellular functions and client proteins from the cytosolic Hsp90 protein. Through reprogramming cancer cell metabolism, TRAP1 are involved in cytoprotection, tumour progression and multidrug resistance [46-48].

1-3-3. Inhibitors against TRAP1

A class of mitochondrotropic Hsp90 inhibitors, named gamitrinibs (GA mitochondrial matrix inhibitors), has been developed through combinatorial chemistry. Gamitrinib consist of geldanamycin, a competitive inhibitor of the ATPase pocket of Hsp90 and TRAP1, conjugated with tandem repeats of tetracyclic guanidinium or triphenylphosphonium for mitochondrial targeting (Fig.3). Gamitrinib not only trigger massive cell death in cultured cancer cells in vitro but also strongly suppress tumor growth in various cancer xenograft or genetic mouse model in vivo. The gamitrinib induced cytotoxicity is attributed to the reactivation of cyclophilin D (cypD), an opener of the permeability transition pore (PTP) located in the mitochondrial inner membrane. CypD inactivation is often suppressed in cancer cells by interaction with mitochondrial Hsp90s because the opening of the PTP can be lethal. Furthermore, gamitrinibs have been shown to induce organelle-specific stress response and dysregulation of bioenergetics in mitochondria of cancer cells (Fig.4) [49-52].

HSPs family	Cellular location	Functions
Small Hsps	cytosol	Heat inactivation, Suppress aggregation
Hsp40	Cytosol	Crucial co-chaperone activity with Hsp70
Hsp60	Mitochondria Cytosol	Refold and prevent aggregation
Hsp70	ER, mitochondria Cytosol	Interorganellar transport, Antiapoptotic activity Autoregulation of the heat shock response
Hsp90	ER, cytosol	Signal transduction i cell cycle and proliferation Refold and regulation client protein Protein trafficking
Hsp100	cytosol	Control stress tolerance

Table 1-1. Family of Heat shock proteins and their functions

family	Subcelluar location	type	
HSP90A (Hsp90a)	Cytosol	Hsp90AA (inducible)	
		Hsp90AB (constitutive)	
HSPB (Hsp90b, Grp94)	ER		
TRAP1	mitochondria		

Table 1-2. Family of Heat shock protein 90 (Hsp90)
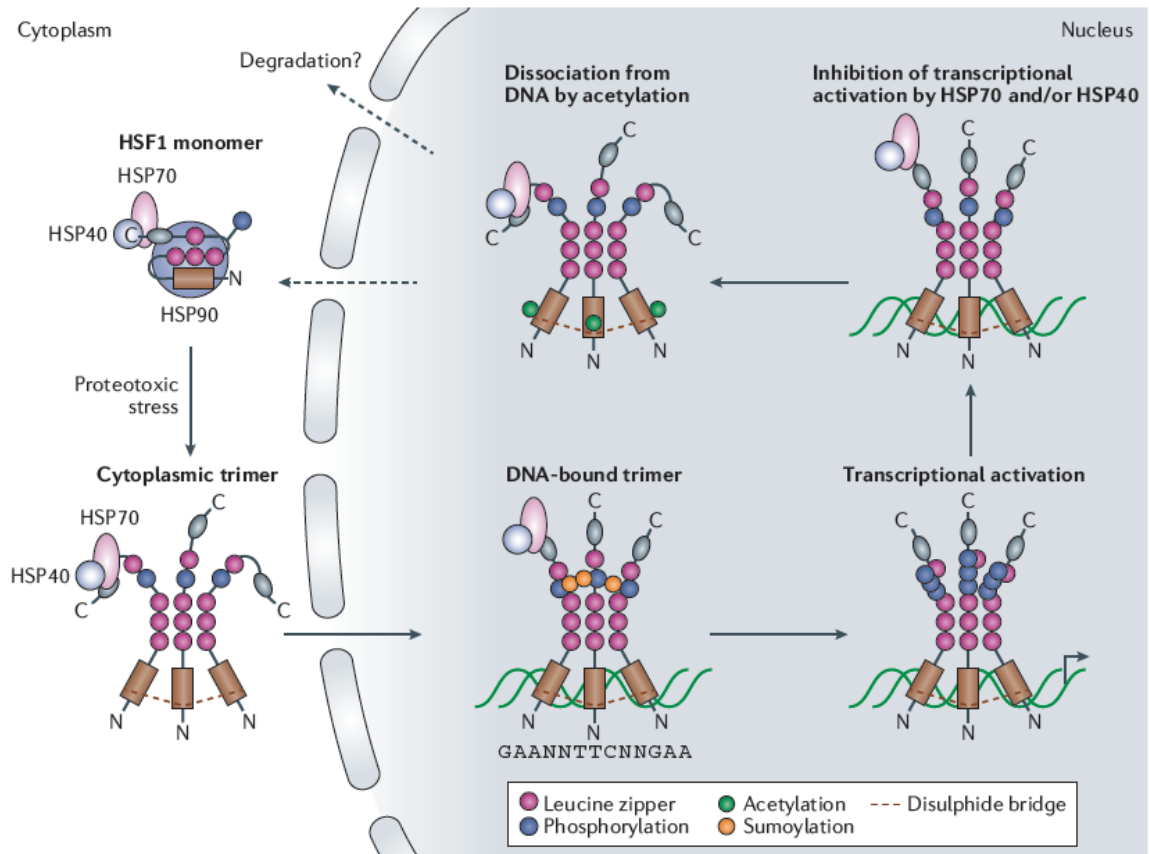
Figure 1-1. HSF1 activation and attenuation cycle [24]

Nature Reviews Drug Discovery **10**, 930-944
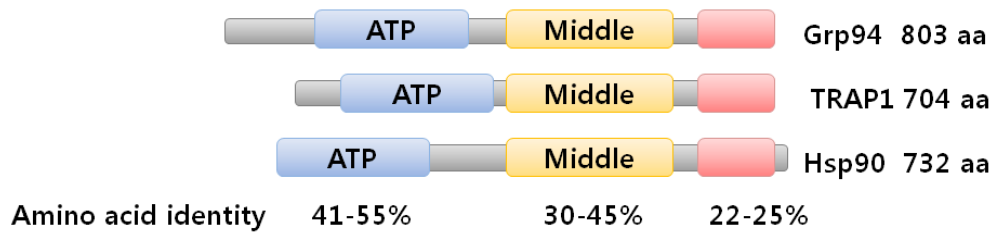
Figure 1-2. Hsp90 homologue proteins
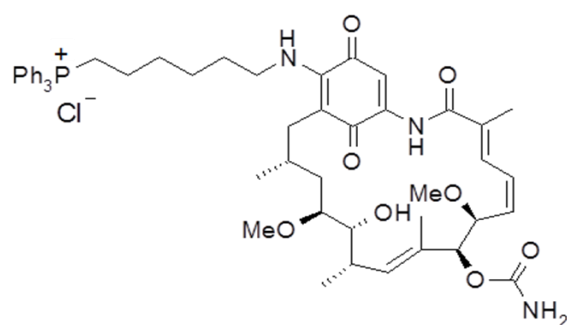
TPP-GA
MW: 891.09 (Phosphonium ion)
     926.54 (Cl salt)

Figure 1-3. The structure of Gamitrinib
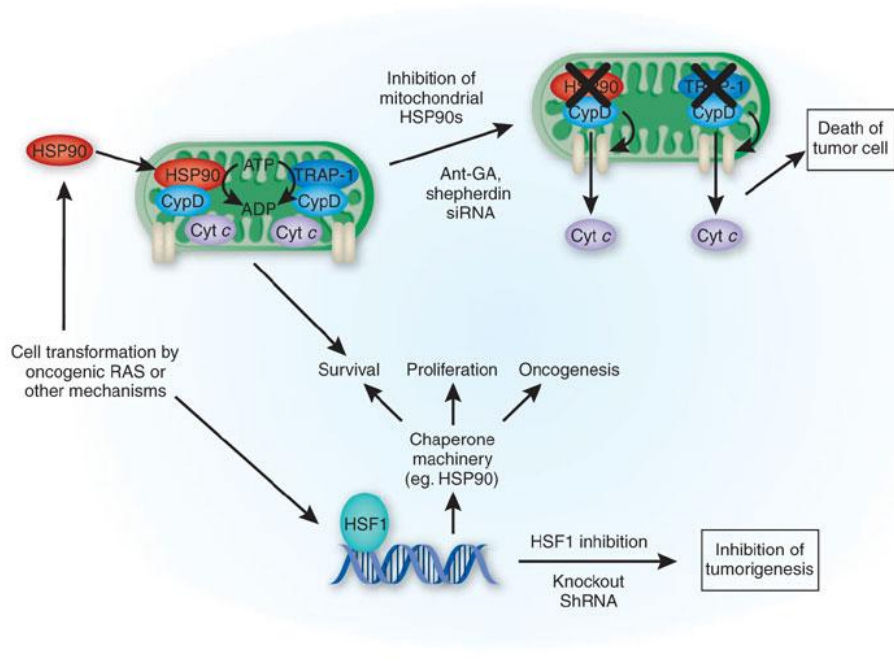
Figure 1-4. Hsp90 and TRAP1 regulates tumour cell survival [43]

Nature Medicine 13, 1415 - 1417 (2007)

1-4. References

1.   Ellis, R.J., *Discovery of molecular chaperones.* Cell Stress Chaperones, 1996. **1**(3): p. 155-60.

2.   Richardson, R.T., et al., *Nuclear autoantigenic sperm protein (NASP), a linker histone chaperone that is required for cell proliferation.* J Biol Chem, 2006. **281**(30): p. 21526-34.

3.   Ellis, R.J., *Molecular chaperones: assisting assembly in addition to folding.* Trends Biochem Sci, 2006. **31**(7): p. 395-401.

4.   Ellis, R.J., *Protein misassembly: macromolecular crowding and molecular chaperones.* Adv Exp Med Biol, 2007. **594**: p. 1-13.

5.   Fenton, W.A. and A.L. Horwich, *Chaperonin-mediated protein folding: fate of substrate polypeptide.* Q Rev Biophys, 2003. **36**(2): p. 229-56.

6.   Hoffmann, J.H., et al., *Identification of a redox-regulated chaperone network.* EMBO J, 2004. **23**(1): p. 160-8.

7.   DeFranco, D.B., C. Ramakrishnan, and Y. Tang, *Molecular chaperones and subcellular trafficking of steroid receptors.* J Steroid Biochem Mol Biol, 1998. **65**(1-6): p. 51-8.

8.   Brown, M.A., et al., *Hsp90--from signal transduction to cell transformation.* Biochem Biophys Res Commun, 2007. **363**(2): p. 241-6.

9.   Richter, K. and J. Buchner, *Hsp90: chaperoning signal transduction.* J Cell Physiol, 2001. **188**(3): p. 281-90.

10.   Pratt, W.B., *The hsp90-based chaperone system: involvement in signal transduction from a variety of hormone and growth factor receptors.* Proc Soc Exp Biol Med, 1998. **217**(4): p. 420-34.

11.   Ellis, R.J. and S.M. van der Vies, *Molecular chaperones.* Annu Rev Biochem, 1991. **60**: p. 321-47.

12.   Zou, J., et al., *Repression of heat shock transcription factor HSF1 activation by HSP90 (HSP90 complex) that forms a stress-sensitive complex with HSF1.* Cell, 1998. **94**(4): p. 471-80.

13.   Wang, X., et al., *Phosphorylation of HSF1 by MAPK-activated protein kinase 2 on serine 121, inhibits transcriptional activity and promotes HSP90 binding.* J Biol Chem, 2006. **281**(2): p. 782-91.

14.   Marunouchi, T., et al., *Possible involvement of HSP90-HSF1 multichaperone complex in impairment of HSP72 induction in the failing heart following myocardial infarction*

in rats. J Pharmacol Sci, 2013. **123**(4): p. 336-46.

15. Donnelly, N., et al., *HSF1 deficiency and impaired HSP90-dependent protein folding are hallmarks of aneuploid human cells.* EMBO J, 2014. **33**(20): p. 2374-87.

16. Zeymer, C., et al., *The molecular mechanism of Hsp100 chaperone inhibition by the prion curing agent guanidinium chloride.* J Biol Chem, 2013. **288**(10): p. 7065-76.

17. Niknejad, H., et al., *Inhibition of HSP90 could be possible mechanism for anti-cancer property of amniotic membrane.* Med Hypotheses, 2013. **81**(5): p. 862-5.

18. Hostein, I., et al., *Inhibition of signal transduction by the Hsp90 inhibitor 17-allylamino-17-demethoxygeldanamycin results in cytostasis and apoptosis.* Cancer Res, 2001. **61**(10): p. 4003-9.

19. Nakamura, M., et al., *Expression of hsp70, hsp90 and hsf1 in the reef coral Acropora digitifera under prospective acidified conditions over the next several decades.* Biol Open, 2012. **1**(2): p. 75-81.

20. Aghdassi, A., et al., *Heat shock protein 70 increases tumorigenicity and inhibits apoptosis in pancreatic adenocarcinoma.* Cancer Research, 2007. **67**(2): p. 616-625.

21. Shukla, H.D. and B.R. Singh, *Identification of a 40 kDa heat shock protein in Clostridium botulinum type A as DnaJ like chaperone.* Abstracts of Papers of the American Chemical Society, 1998. **216**: p. U561-U561.

22. Bustard, K. and R.S. Gupta, *The sequences of heat shock protein 40 (DnaJ) homologs provide evidence for a close evolutionary relationship between the Deinococcus-Thermus group and cyanobacteria.* Journal of Molecular Evolution, 1997. **45**(2): p. 193-205.

23. Cuellar, J., et al., *Structural Insights into the Chaperone Activity of the 40-kDa Heat Shock Protein DnaJ BINDING AND REMODELING OF A NATIVE SUBSTRATE.* Journal of Biological Chemistry, 2013. **288**(21): p. 15065-15074.

24. Neef, D.W., A.M. Jaeger, and D.J. Thiele, *Heat shock transcription factor 1 as a therapeutic target in neurodegenerative diseases.* Nature Reviews Drug Discovery, 2011. **10**(12): p. 930-944.

25. Gallo, L.I., et al., *The 90-kDa heat-shock protein (Hsp90)-binding immunophilin FKBP51 is a mitochondrial protein that translocates to the nucleus to protect cells against oxidative stress.* J Biol Chem, 2011. **286**(34): p. 30152-60.

26. Suetsugu, S. and T. Takenawa, *Translocation of N-WASP by nuclear localization and export signals into the nucleus modulates expression of HSP90.* J Biol Chem, 2003. **278**(43): p. 42515-23.

27. Galigniana, M.D., et al., *Hsp90-binding immunophilins link p53 to dynein during p53 transport to the nucleus.* J Biol Chem, 2004. **279**(21): p. 22483-9.

28. Vanden Berghe, T., et al., *Disruption of HSP90 function reverts tumor necrosis factor-induced necrosis to apoptosis.* J Biol Chem, 2003. **278**(8): p. 5622-9.

29. Didenko, T., et al., *Hsp90 structure and function studied by NMR spectroscopy.* Biochim Biophys Acta, 2012. **1823**(3): p. 636-47.

30. Pearl, L.H. and C. Prodromou, *Structure and mechanism of the Hsp90 molecular chaperone machinery.* Annu Rev Biochem, 2006. **75**: p. 271-94.

31. Li, J. and J. Buchner, *Structure, function and regulation of the hsp90 machinery.* Biomed J, 2013. **36**(3): p. 106-17.

32. Nathan, D.F. and S. Lindquist, *Mutational analysis of Hsp90 function: interactions with a steroid receptor and a protein kinase.* Mol Cell Biol, 1995. **15**(7): p. 3917-25.

33. Pratt, W.B. and D.O. Toft, *Regulation of signaling protein function and trafficking by the hsp90/hsp70-based chaperone machinery.* Exp Biol Med (Maywood), 2003. **228**(2): p. 111-33.

34. Bagatell, R. and L. Whitesell, *Altered Hsp90 function in cancer: a unique therapeutic opportunity.* Mol Cancer Ther, 2004. **3**(8): p. 1021-30.

35. McClellan, A.J., et al., *Diverse cellular functions of the Hsp90 molecular chaperone uncovered using systems approaches.* Cell, 2007. **131**(1): p. 121-35.

36. Liu, Y., et al., *Molecular chaperone Hsp90 associates with resistance protein N and its signaling proteins SGT1 and Rar1 to modulate an innate immune response in plants.* J Biol Chem, 2004. **279**(3): p. 2101-8.

37. Altieri, D.C., et al., *TRAP-1, the mitochondrial Hsp90.* Biochim Biophys Acta, 2012. **1823**(3): p. 767-73.

38. Chen, B., et al., *The HSP90 family of genes in the human genome: insights into their divergence and evolution.* Genomics, 2005. **86**(6): p. 627-37.

39. Chen, B., et al., *The expression of the HSP90 gene in response to winter and summer diapauses and thermal-stress in the onion maggot, Delia antiqua.* Insect Mol Biol, 2005. **14**(6): p. 697-702.

40. Marzec, M., D. Eletto, and Y. Argon, *GRP94: An HSP90-like protein specialized for protein folding and quality control in the endoplasmic reticulum.* Biochim Biophys Acta, 2012. **1823**(3): p. 774-87.

41. Kang, B.H., *TRAP1 regulation of mitochondrial life or death decision in cancer cells and mitochondria-targeted TRAP1 inhibitors.* BMB Rep, 2012. **45**(1): p. 1-6.

42. Kang, B.H., et al., *Regulation of tumor cell mitochondrial homeostasis by an organelle-specific Hsp90 chaperone network.* Cell, 2007. **131**(2): p. 257-70.

43. Workman, P. and E. de Billy, *Putting the heat on cancer.* Nat Med, 2007. **13**(12): p. 1415-7.

44. Nakagawa, T., et al., *Cyclophilin D-dependent mitochondrial permeability transition regulates some necrotic but not apoptotic cell death.* Nature, 2005. **434**(7033): p. 652-8.

45. Chae, Y.C., et al., *Control of tumor bioenergetics and survival stress signaling by mitochondrial HSP90s.* Cancer Cell, 2012. **22**(3): p. 331-44.

46. Siegelin, M.D., et al., *Exploiting the mitochondrial unfolded protein response for cancer therapy in mice and human cells.* J Clin Invest, 2011. **121**(4): p. 1349-60.

47. Chae, Y.C., et al., *Landscape of the mitochondrial Hsp90 metabolome in tumours.* Nat Commun, 2013. **4**: p. 2139.

48. Boland, M.L., A.H. Chourasia, and K.F. Macleod, *Mitochondrial dysfunction in cancer.* Front Oncol, 2013. **3**: p. 292.

49. Kang, B.H., et al., *Preclinical characterization of mitochondria-targeted small molecule hsp90 inhibitors, gamitrinibs, in advanced prostate cancer.* Clin Cancer Res, 2010. **16**(19): p. 4779-88.

50. Kang, Y.J., et al., *Inhibition of doxorubicin chronic toxicity in catalase-overexpressing transgenic mouse hearts.* Chem Res Toxicol, 2002. **15**(1): p. 1-6.

51. Kang, B.H., et al., *Combinatorial drug design targeting multiple cancer signaling networks controlled by mitochondrial Hsp90.* J Clin Invest, 2009. **119**(3): p. 454-64.

52. Yoshida, S., et al., *Molecular chaperone TRAP1 regulates a metabolic switch between mitochondrial respiration and aerobic glycolysis.* Proc Natl Acad Sci U S A, 2013. **110**(17): p. E1604-12.

Chapter 2. Mitochondrial Hsp90s suppress calcium-mediated stress signals propagating from mitochondria to the ER in cancer cells

2-1. Introduction

Molecular chaperones help the conformational changes and correct folding of their substrates, called client proteins, and minimize their aggregation and misfolding [1]. Heat shock protein 90 (Hsp90) is an ATP-dependent molecular chaperone which regulates the function and the stability of client proteins which are associated with signal transduction during malignant transformation and progression [2, 3]. Organelle-resident Hsp90 family proteins are mainly expressed in the endoplasmic reticulum(ER) and mitochondria, where they control protein homeostasis [4, 5]. The mitochondrial Hsp90s, tumor necrosis factor receptor-associated protein 1 (TRAP1), are abundant in the mitochondria of many cancer cells [6, 7], and their client proteins, cellular functions and regulation are quite different from the cytoplasmic Hsp90 pool [4, 6]. TRAP1 are involved in cytoprotection, tumor progression, and multidrug resistance by reprogramming metabolic network of cancer cell [8-12] and sustaining mitochondrial membrane integrity [6, 13, 14]. Mitochondria integrate vital and lethal signals emanating from various cellular compartments to bring about cell death through inner and outer membrane permeabilization [15]. Although the molecular mechanism is not clear, cyclophilin D (Cyp-D) is reported to regulate the permeability transition pore (PTP) in the mitochondrial inner membrane [16-20]. TRAP1 expression is elevated in cancer cells, which suppresses Cyp-D function to suppress the deadly increase of membrane permeability in the organelle [6]. PTP opening upon Cyp-D activation increases mitochondrial inner membrane permeability toward small molecules (<1,500 Da), resulting in loss of mitochondrial membrane potential ($\Delta\Psi$m), discharge of matrix calcium stores, and swelling and rupture of the mitochondrial outer membrane [15, 21]. Calcium, a ubiquitous second messenger, is associated in a broad variety of physiological events via its interaction with effectors responsible for calcium-dependent processes [22]. The mitochondria and ER are the major intracellular calcium stores, regulating calcium signaling and homeostasis [23, 24]. They have a largely interconnected architecture with numerous contacts, which facilitates inter-organelle calcium transport by generating calcium hotspots proximal to open calcium channels [25-27]. Both the ER and mitochondria contain calcium-triggered calcium release channels that can activate each other via positive feedback, including ryanodine receptors (RyRs) and inositol 1,4,5-trisphosphate receptors (IP3Rs) [15, 28]. There is

a growing consensus that ER-mitochondria calcium crosstalk can coordinate signaling for metabolism and cell death between the organelles [24]. Although calcium signaling has been intensively studied, reports of "mitochondria-initiated" calcium crosstalk between mitochondria and the ER are scarce. Here, we demonstrate a novel function of mitochondrial Hsp90s that confers resistance to cancer cell death by inhibiting the propagation of mitochondrial-origin calcium signals to the ER.

2-2. Materials and methods

Cells and culture condition

  HeLa, MDA-MB-231, and NCI-H460 cells were purchased from the Korean Cell Line Bank and 22Rv1 from the American Type Culture Collection. Cell lines were maintained as recommended by supplier. Cells were cultured in DMEM or RPMI medium (Lonza) containing 10% fetal bovine serum (FBS; GIBCO) and 1% penicillin/streptomycin (GIBCO) at 37℃ in a 5% CO2 humidified atmosphere.

Chemicals, plasmids and antibodies

  Gamitrinib conjugated with triphenylphosphonium was prepared as described previously[29]. MitoTracker, Fura-2-AM, and tetramethylrhodamine methyl ester (TMRM) were purchased from Molecular Probes, Ryanodine was from Santa Cruz Biotechnology. Mn(III) tetrakis (1-methyl-4-pyridyl) porphyrin (MnTMPyP) was from Calbiochem. 1,2-bis(o-aminophenoxy) ethane-N,N,N',N'-tetraacetic acid acetoxymethyl ester (BAPTA), cyclosporine A (CsA), carbonyl cyanide 4-(trifluoromethoxy) phenylhydrazone (FCCP), tetracaine, and thapsigargin(Thap), and N-acetylcysteine (NAC) and all other chemicals were from Sigma, Anti-CEBP homologous protein (CHOP) antibodies were obtained from Cell Signaling; anti-RyR, anti-IP3R,anti-eIF2α and anti-cytochrome c antibodies from Santa Cruz Biotechnology; anti-cyclopholin D from Calbiochem; anti-eIF2α[pS52] from Invitrogen; anti-β-actin from MP Biomedicals; and anti-TRAP1 from BD Biosciences.

Astrocyte preparation

  Primary cultures of astrocytes were prepared as previously described[30]. Briefly, the mouse brain cortex, after removing the meninges, was dissected and dissociated with moderate

pipetting. Cells were plated on 100-mm dishes coated with 10 μg/ml poly-D-lysine (Sigma) and grown to confluence in DMEM supplemented with 10% FBS, 10% horse serum (GIBCO), 100 units/ml penicillin, and 100 μg/ml streptomycin at 37°C in a 5% CO2 humidified atmosphere. Afterward, astrocytes were trypsinized and plated on 6-well plates coated with poly-D-lysine to administer drugs.

siRNA treatment

Small interfering RNAs (siRNA) against TRAP1, RyR2, IP3R, and CHOP were synthesized by Genolution (Korea) as follows:
RyR2-#1, 5′-AAGTGGTTCTGCAGTGCACCG; RyR2-#2,5′-AAGTACGAGTTGGAGATG ACC; TRAP1-#1, 5′- AAACATGAGTTCCAGGCCGAG;TRAP1-#2, 5′- CCCGGTCCCTGT ACTCAGAAA; IP3R1-#1, 5′-GAGAATTTCCTTGTAGACATCTGCA; IP3R1-#2, 5′-GGCC TGAGAGTTACGTGGCAGAAAT; IP3R2, 5′-GAGAAGGCTCGATGCTGAGACTTGA; IP3R3, 5′-CCGAGATGACAAGAAGAACAAGTTT;CHOP-#1, 5′-AGAACCAGCAGAGG TCACAA;CHOP-#2,5′-AAGAGAATGAACGGCTCAAGC; control, 5′-ACUCUAUCUGCA CGCUGAC.

Cells were cultured on 6-well plates at 50–75% confluence, transfected with 20 nM siRNA mixed with G-Fectin (Genolution) for 48 hours, and then analyzed or treated with drugs. Analysis of cell viability and apoptosis induction Cells (5×10^3 cells/well) were cultured in 96-well plates overnight and treated with gamitrinib and Thap alone or in combination for 24 hours. To determine cell viability, cells were exposed to 3 (4,5-dimethyl-thyzoyl-2-yl)2,5 diphenyltetrazolium bromide (MTT), and crystallized formazan was quantified by measuring the absorbance at 595 nm with an Infinity M200 microplate reader (TECAN). Absorbance data were compared with that of vehicle control and expressed as percent viability. Alternatively, after treatment with drugs, DNA content (propidiumiodide, red fluorescence) and caspase activation (DEVDase activity, green fluorescence) of the cells were analyzed using the CaspaTag in situ apoptosis detection kit (Millipore). Labeled cells were analyzed using the FACS Calibur™ system (BD Biosciences). Data were processed using FlowJo software (TreeStar).

CHOP reporter assay

To generate a CHOP reporter stable cell line, PC 3 cells were co-transfected with 8 μg of a promoter construct (CHOP::GFP)[31] obtained from Addgene (Addgene plasmid 21898) and

800 ng of puromycin linearized selection marker (Clontech) using Lipofectamin (Invitrogen) per manufacturer's instructions. Transfected PC3 cells were cultured in RPMI (Lonza) with 1 μg/ml puromycin (Clontech) for 3 weeks and colonies were picked using cloning cylinders. GFP expression was monitored in the IncuCyte™ imaging system (Essen Bioscience) at an excitation wavelength of 450–490 nm and an emission of 500–530 nm, and analyzed by Image J software (National Institutes of Health).

Live cell imaging for intracellular calcium

HeLa cells were incubated with 5 μM Fura-2-AM for 30 min at 37℃ and 5% CO2. After washing with Hank's Buffer, the cells were incubated with calcium-free Locke's solution (154 mM NaCl, 5.6 mM KCl, 3.2 mM MgCl2, 5 mM HEPES, 10 mM glucose, 0.2 mM EGTA; pH 7.4). Fluorescence changes were monitored every 5 minutes using an IX81 ZDC microscope (Olympus) at an emission wavelength of 510 nm with dual excitation at 340 nm and 380 nm. Images of the 340/380 fluorescence ratio were generated and analyzed by the Xcellence software package (Olympus). Imaging D1ER and mtCameleon Fluorescence resonance energy transfer (FRET) measurements were performed using an FV1000 laser confocal scanning microsope (Olympus) with a FRET module and a UPLSAPO 100× oil immersion objective with a 1.40 numerical aperture. HeLa cells were seeded on a Lab Tek II slide chamber at 40–80% confluency in DMEM (Lonza) supplemented with 10% FBS and 1% penicillin/streptomycin at 37℃ and 5% CO2. D1ER or mtCameleon constructs (kind gifts from Dr. R.Y. Tsien, University of San Diego) [32] were transfected into HeLa cells using the Lipofectamine transfection reagent (Invitrogen) per manufacturer's instructions. Cells were imaged at 24 or 48 hours after transfection. All analyses were performed under the same conditions. D1ER and mtCameleon, containing FRET donor (CFP) and acceptor (citrine) components, were excited with a 440-nm diode laser source; the emitted fluorescence bands were separated by a grating and detected by photomultiplier tubes in the CFP channel (480 nm) and FRET channel (535 nm). The FRET ratio (R_{FRET}) was calculated as described previously[33] from confocal images using FV10-ASW 3.1 software (Olympus) by pixel-by-pixel quantification of fluorescence intensity:

$R_{FRET} = I_{FRET}/I_{CFP}$, where I_{FRET} and I_{CFP} represent the fluorescence intensities from the FRET and CFP channels, respectively. The FRET ratio (relative units) was plotted after comparing R_{FRET} values.

RNA extraction and reverse transcript-PCR

Total RNA was prepared from cells suspended in cold PBS using the RNeasy mini kit

(QIAGEN), and cDNA was synthesized using the ProtoScript® First Strand cDNA Synthesis Kit (New England Biolabs) using an oligo(dT) primer. The PCR reaction was performed in a Mastercycler PCR machine (Eppendorf) with the following sets of oligonucleotide primers: glyceraldehyde phosphate dehydrogenase (GAPDH), 5′-CGGGAAGCTTGTCATCAATGG-3′ and 5′-GGCAGTGATGGCATGGACTG-3′; CHOP, 5′- CTTTCTCCTTCGGGACACTG-3′ and 5′-AGCCGTTCATTCTCTTCAGC-3′; TRAP1, 5′-ATGGCGCGCGAGCTGCGG-3′ and 5′-CAGTCGTCCTGCCTGCAA-3′; X-box binding protein 1 (XBP1), 5′-CCTTGTAGTTGAGAA CCAGG-3′ and 5′-GGGGCTTGGTATATATGTGG-3′.

Xenograft tumor models

All experiments involving animals were approved by UNIST (IACUC-12-003-A). 22Rv1 (7 × 106) cells suspended in sterile PBS (200 μl) were injected subcutaneously into both flanks of 6-week-old BALB/c nu/nu male mice (Japan SLC Inc.) and allowed to grow to an average volume of approximately 100 mm3. Animals were randomly divided into four groups (two tumors/mouse, five mice/group). Gamitrinib or vehicle (DMSO) dissolved in 20% Cremophor EL (Sigma) in PBS was injected intraperitoneally, and Thap dissolved in 0.9% NaCl in PBS intravenously. The mice were administered 10 mg/kg gamitrinib and 0.2 mg/kg Thap twice a week. Tumors were measured daily with a caliper, and tumor volume was calculated using the formula: $V = 1/2 \times (width)2 \times length$. At the end of experiment, animals were euthanized, and organs including brain, heart, kidney, liver, lung, spleen, and tumor were collected for histology or western blotting. For histological analysis, harvested organs were fixed in 10% formalin and embedded in paraffin. Sections (5 μm) were placed on high-adhesive slides, stained with H&E, and scanned using the Dotslide system (Olympus) with 10× magnification. For western blot analysis, tissue samples were lysed in RIPA buffer (50 mM Tris, pH 8.0, 150 mM NaCl, 1% NP-40, and 0.25% N-deoxycholate) containing protease inhibitor and phosphatase inhibitor cocktails (Calbiochem) using a homogenizer (IKA).

Statistical analysis of data

All MTT experiments were duplicated and repeated independently at least three times. Statistical analyses were performed using the software program Prism 5.0 (GraphPad). In an unpaired t-test, $p < 0.05$ was considered significant.

2-3. Results

Mitochondrial Hsp90s regulate the mitochondrial calcium store

To investigate whether mitochondrial Hsp90s regulate mitochondrial calcium stores, we used the mitochondriatargeted Hsp90 inhibitor gamitrinib, a conjugated of triphenylphosphonium (a mitochondria-targeting moiety) and geldanamycin (an Hsp90 inhibitor) [29, 34]. A cytotoxic dose (30 μM) of gamitrinib dramatically increased the intracellular calcium concentration within an hour in human cervical (HeLa), prostate (22Rv1), and breast (MDA-MB-231) cancer cell lines in calcium-free medium (Fig. 2-1A and B). A non-targeted Hsp90 inhibitor, 17-allylamino-17-demethoxygeldanamycin (17AAG), did not increase cytosolic calcium (Fig. 2-1D), consistent with a previous report that gamitrinib is specific to mitochondrial Hsp90 without affecting cytosolic Hsp90 function [29]. After gamitrinib treatment, PTP opening and loss of mitochondrial membrane potential ($\Delta\Psi m$) occurred within 30 minutes (Fig. 2-2A, TMRM staining), whereas cytochrome c release (Fig. 2-2B, cytochrome c staining) were not prominent until after 2 hours. Caspase activation and cell death occured after 4 hours (Fig. 2-1C, DEVDase activity and PI staining), and it suggested that calcium flux concurs with PTP opening, prior to mitochondrial outer membrane permeabilization (MOMP). Consistently, cytosolic calcium elevation was inhibited by cyclosporin A (CsA) (Fig. 2-1C), a potent Cyp-D inhibitor, blocking PTP opening [15]. Thus, mitochondrial Hsp90 inhibition immediately induces PTP opening, loss of $\Delta\Psi m$, and discharge of the calcium stored in the mitochondrial matrix. Thereafter, a cascade of MOMP, cytochrome c release, and caspase activation ensues (Fig. 2-2D).

Mitochondrial calcium release results in depletion of ER calcium

The PTP opening has been shown to immediately discharge calcium stored in the mitochondria [35]; however, after mitochondrial Hsp90 inhibition in this study, calcium release continued even after a significant drop in $\Delta\Psi m$ (Fig. 2-1A and 2-2A), suggestive of additional sources of calcium flux. We postulated that the primary calcium-storing organelle, the ER, contributes to the cytosolic calcium increase after gamitrinib treatment. To prove this, we directly measured calcium depletion using the calcium sensor protein, Cameleon, targeted to mitochondria and the ER (mtCameleon and D1ER, respectively) [32]. Gamitrinib treatment resulted in FRET signal loss in both mtCameleon- and D1ER-transfected HeLa cells, comparable to that seen with FCCP or Thap treatment (Fig. 2-3A and B), clearly indicating calcium depletion in the ER as well as in mitochondria. FCCP is used to observe as positive control which can affect

mitochondria specifically and Thapsigargin is used to release stored Calcium as an inhibitor of the Ca^{2+}-ATPase of the ER (Fig. 2-3C and D). Consistent with previous reports [29], the non-targeted Hsp90 inhibitor 17AAG did not affect the mtCameleon FRET signal (Fig. 2-4A and B) and gamitrinib has no effect on the $\Delta\Psi$m of a normal MCF10A breast cell (Fig. 2-5A and B). Calcium depletion in the ER evokes the unfolded protein response and induces CHOP activation Gamitrinib has been reported to trigger the unfolded protein response in mitochondria, and, through unknown mechanisms, to subsequently activate CHOP, the proapoptotic transcription factor often induced during unfolded protein responses in the ER (UPRER) [4, 36-38]. siRNA knockdown of the mitochondrial Hsp90 homolog TRAP1 results in spliced XBP1 mRNA production and eukaryotic translation initiation factor 2α (eIF2α) phosphorylation (Fig. 2-6A and B), suggesting activation of UPRER sensor proteins such as inositol-requiring protein1α (IRE1α) and PKR-like ER kinase[39, 40]. Consistently, pharmacological inactivation of mitochondrial Hsp90s by gamitrinib also triggered eIF2α phosphorylation and XBP1mRNA splicing (Fig. 2-6C and 2-7). In addition to UPRER sensor protein activation, CHOP induction was clearly seen after both pharmacological and genetic inhibition of mitochondrial chaperones (Fig. 2-6D). To investigate the critical involvement of mitochondrial calcium discharge through the PTP for the ER stress response, gamitrinib was administered in the presence or absence of the PTP inhibitor CsA and the calcium chelator BAPTA. Both substances compromised UPRER induction, resulting in a dramatic reduction in eIF2α phosphorylation and CHOP expression (Fig. 2-7).

Ryanodine receptors mediate mitochondrial calcium-induced calcium depletion in the ER

IP3Rs and RyRs are ER membrane channels responsible for calcium release from the organelle [22]. Silencing IP3R1, the major isoform in HeLa cells [41] (Fig. 2-8A), did not affect the elevation of cytosolic calcium and the induction of CHOP after gamitrinib treatment (Fig. 2-8B and C), but was enough to compromise lysophosphatidic acid-induced ER calcium release in calcium-free medium (Fig. 2-8D). By contrast, specific RyR inhibitors such as ryanodine (100 μM) and tetracaine (300 μM)[42] strongly inhibited gamitrinib-induced ER calcium release, similar to the PTP inhibitor CsA (Fig. 2-9A). Genetic knockdown of RyR2 the dominant RyR isoform in HeLa cells [43-45], also blocked gamitrinib-induced cytoplasmic calcium increase (Fig. 2-9B and C). Consistently, ryanodine and RyR2-specific siRNAs inhibited eIF2α phosphorylation and the subsequent CHOP induction (Fig. 2-9B and D). Collectively, our data suggest that RyR, not IP3R, is the ER sensor that propagates the signal initiated by discharged calcium from mitochondria in cancer cells. Although Reactive oxygen species (ROS) has known

as a factor to release ER calcium but ROS did not affect gamitrinib-induced calcium release and CHOP induction in this mechanism (Fig. 2-10). Mitochondria-initiated calcium signaling plays an important role in setting up the cell death threshold impaired mitochondrial function [12] and slightly elevated cytoplasmic calcium (Fig. 2-11, Fluo-4 staining) were frequently found in gamitrinib-treated cells, even at non-toxic dose of the drug. Therefore, we hypothesized that calcium-mediated stress propagation can render cells sensitive to additional stresses, i.e. lowering the cell death threshold. A representative UPRER inducer, Thap, was combined with gamitrinib to test this hypothesis. Gamitrinib sensitized cancer cells to Thap treatment at various concentrations, while the nontargeted Hsp90 inhibitor 17AAG did not (Fig. 2-12A and C). Consistent with pharmacological data, TRAP1knockdown also sensitized cancer cells to Thap treatment (Fig. 2-12B and D). The combination drug treatment of gamitrinib and Thap elevate time dependent CHOP expression and the CHOP expression induced by combination treatment was faster and higher compared to single-agent treatment (Fig. 2-13A). A cell-based reporter assay also showed elevated CHOP transcription activity following combination treatment (Fig. 2-13B). siRNA-mediated knockdown of either CHOP significantly suppressed this increased cytotoxic activity, but did not affect the toxicity seen with single agent treatment (Fig. 2-13C). The combination drug induced CHOP expression was a RyR-dependent manner and siRNA-mediated knockdown of RyR significantly suppressed the CHOP expression and the cytotoxic activity (Fig. 2-14A and B). It suggests important roles of RyR and CHOP in the drug combination effect (Fig. 2-13C and 14A) and RyR opening is an essential upstream event in the stress response elevating CHOP expression. The combination of gamitrinib and Thap synergistically induced apoptotic cell death, causing a dramatic increase in caspase activity (Fig. 2-15A). CHOP-dependent death receptor 5 (DR5) expression [46] has been reported before, but was not involved in the drug combination, considering marginal elevation of DR5 expression and no activation of caspase-8 (Fig. 2-15B and C) [47]. Collectively, our data argue that gamitrinib lowers the cellular threshold against ER stresses by increasing CHOP expression in an RyRdependent manner.

Combined synergistic anticancer activities in vivo

The mitochondrial Hsp90 pool is dramatically elevated in many cancer cells to cope with various stresses, but expression is very low or undetectable in most normal tissues except brain and testis [6, 7, 48-50]. To test whether mitochondrial Hsp90-regulated interorganelle calcium signaling is functional in normal cells, we examined primary astrocytes from mouse brain, where Hsp90 expression in mitochondria is higher than in other tissues [6]. Gamitrinib did not

affect CHOP induction and eIF2α phosphorylation (Figure 2-16A), whereas Thap increased CHOP expression in astrocytes (Fig. 2-16C). Gamitrinib treatment in combination with Thap did not sensitize astrocytes (Fig. 2-16B), possibly due to very low expression of both TRAP1 and Cyp-D in astrocytes compared to cancer cells (Fig. 2-16D). Collectively, gamitrinib does not affect the cell death threshold in astrocytes, probably due to the limited contribution of the chaperones to PTP opening in normal cells; this is in stark contrast with data from cancer cells (Fig. 2-12A and C). Next, the gamitrinib and Thap combination was further examined using a xenograft of relapsed prostate cancer cells (22Rv1) [51], to test whether the cancer cell-specific lowering of the cell death threshold occurs in vivo. Because Thap has been reported to be highly toxic in vivo [52], we administered a very low dose of the drug. Suboptimal individual doses of Thap and gamitrinib did not result in significant inhibition of tumor growth, whereas combined treatment inhibited tumor growth (Fig. 2-17A) without remarkable histological abnormalities and body weight changes (Fig. 2-18A and B). Individual treatment with either gamitrinib or Thap slightly elevated CHOP expression, whereas combined treatment further elevated CHOP expression synergistically in cancer cells, but not in the brain or liver (Fig. 2-17B and 18C). Therefore, similar to the in vitro data, mitochondrial Hsp90 inhibition lowers the cell death threshold of cancer cells to Thap treatment in vivo (Fig. 2-19).

2-4. Discussion

Mitochondria are integrators of various cellular stress signals that eventually make life-or-death decisions. We show here that mitochondria can also produce calcium mediated stress signals and propagate them to neighboring organelles. For calcium signaling, interplay between the permeability transition pore (PTP) in mitochondria and ryanodine receptor (RyR) in ER was essential, and the mitochondrial Hsp90 pool negatively modulates signal commencement in cancer cells to protect them from cellular stresses. TRAP1 knockdown by siRNA showed a similar phenotype to simultaneous inactivation of both Hsp90 and TRAP1 by gamitrinib. Considering functional overlap between Hsp90 and TRAP1 in the regulation of PTP in cancer cells [6, 53], the lack of functional compensation by the mitochondrial Hsp90 is quite unexpected, and may suggest different protein interaction networks between Hsp90 and TRAP1, or alternatively, that TRAP1 functionally dominates over Hsp90 in cancer mitochondria. There is growing consensus that mitochondrial Hsp90 and TRAP1 play important roles in neoplastic

progression by modulating a variety of mitochondrial pathways: metabolic reprogramming, mitochondrial dynamics, reactive oxygen species, autophagy, and cell death [53, 54]. Thus, to clearly address their roles in mitochondrial homeostasis and tumorigenesis, the relative contribution of the chaperones to the mitochondrial signal pathways and the functional relationship between them should first be discovered.

Calcium, in such stress signaling, does not merely mediate mitochondria-ER communication, but is also critical for PTP and RyR calcium channel opening. Calcium released through one of the channels can trigger the opening of the other through calcium-induced calcium release (CICR) [15, 28], which can eventually amplify signals even with minute perturbation of mitochondrial chaperone functions.

Interestingly, IP3Rs, major ER calcium channels allegedly requiring the ligand IP3 as well as calcium for CICR [42], are not involved in mitochondria-initiated calcium signaling, which further argues that the mitochondria-initiated pathway occurs through genuine CICR that is solely dependent on discharged calcium. Interplay and subsequent signal amplification between the calcium channels are crucial to signaling, as inhibition of either the PTP or RyR blocked calcium signaling. The unknown mechanism of CHOP induction after inactivation of mitochondrial Hsp90s in previous reports[4, 36-38] can be explained by this interplay. Furthermore, local calcium increases, seen as calcium hot-spots after low-dose gamitrinib treatment (Fluo-4 staining in Figure 2-5A), seem to be the consequence of the calcium channel interplay, which is sufficient to provoke global mitochondrial membrane potential reduction and UPR ER induction. Without a large increase in cytoplasmic calcium concentration, this is sufficient to propagate the stress response, probably due to the closely apposed architecture of the mitochondria and ER [23, 26, 27]. Thus, mitochondriainitiated calcium signaling might be further supported by the physical interconnection between mitochondria and the ER, which forms a specialized microdomain of transient calcium [24, 55] and can facilitate reciprocal PTP and RyR activation via CICR. Target-centered anticancer drugs often show limited efficacies, poor safety, and resistance profiles due to complicated signaling networks in many cancer cells [56, 57]. Multicomponent and system-oriented therapeutics development approaches could provide a solution [58, 59]. The target proteins of gamitrinib and Thap have fundamentally different functions in distinct organelles [6, 60, 61]. When combined, their anticancer activities were enhanced and non-toxic doses of the drugs were sufficient in vitro and in vivo to kill cancer, but not normal cells, through calcium-mediated coordination of compartmentalized signaling networks and synergistic elevation of CHOP expression. These pharmacological data further support the function of mitochondrial Hsp90s as important regulators of inter organelle

crosstalk, increasing the stress threshold, and identify these proteins as drug targets for the development of novel combination cancer therapy. Thus, we believe that mitochondrial Hsp90 inhibitors require further system-oriented investigation to facilitate the development of an effective and better multi component anticancer regimen by combining antitumor drugs or even non-antitumor drugs capable of inducing organelle stress.

In conclusion, Mitochondria-initiated and calcium-mediated propagation of the stress signal plays an important role in coordinating ER and mitochondrial stress responses, and is implicated in lowering the cell death threshold in cancer cells. Therefore, targeting the coordinated calcium stress signaling pathway often suppressed in cancer cells might be a feasible and effective strategy for the rational development of cancer therapeutics.
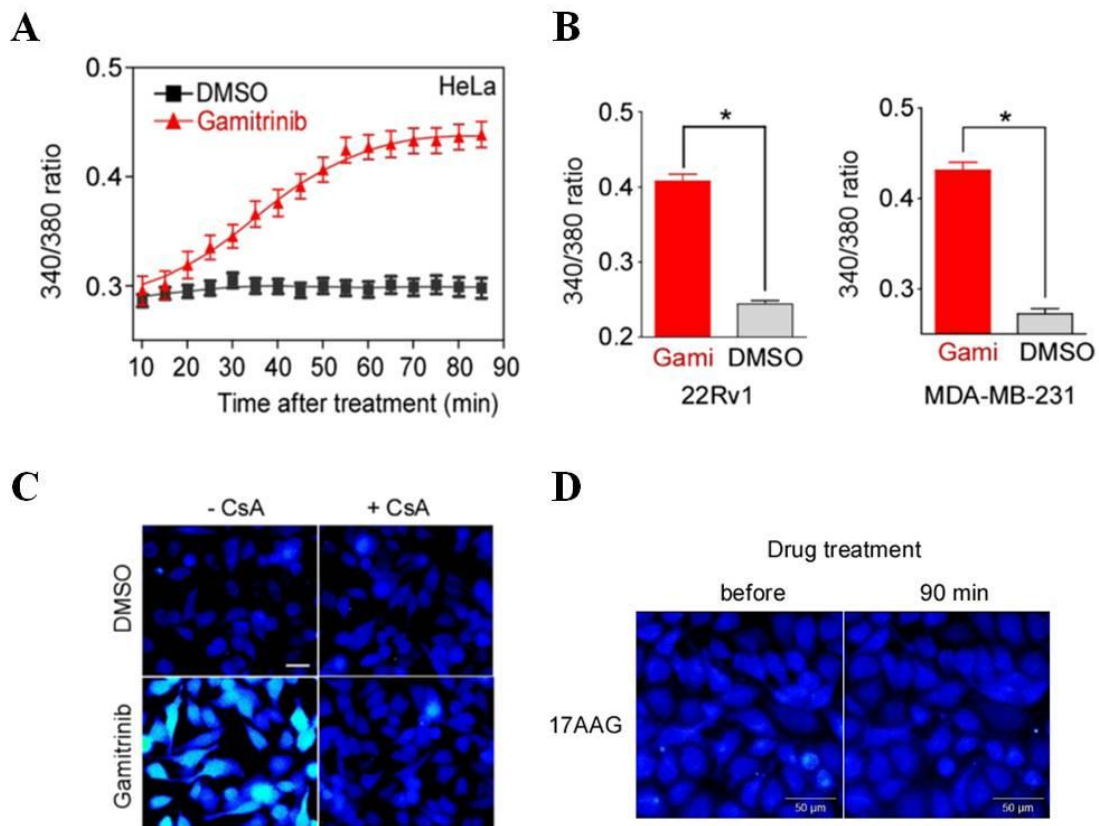
Figure 2-1. Mitochondrial Hsp90s modulate the mitochondrial calcium store

(A) Time course of cytosolic calcium increase. The ratio of the emission fluorescence intensities at 340 and 380 nm excitation of Fura-2 labeled HeLa cell in calcium-free medium was measured after 30 μM gamitrinib treatment as described in Materials and Methods. (B) Increase of cytosolic calcium in 22Rv1 and MDA-MB-231 cells. Fura-2 fluorescence ratio after 30 μM gamitrinib (Gami) treatment for 1 hour was calculated. Data are the mean ± SEM of duplicated experiments and collected from 40 regions of interest (ROIs). (C) Cyclosporin A (CsA) blocks cytosolic calcium increase. Cytosolic calcium changes in Fura-2-labeled HeLa cells treated for 1 hour with 5 μM CsA and/or 30 μM gamitrinib were analyzed. Bar, 50 μm. (D) No elevation of cytosolic calcium on 17AAG treatment. Fura-2 loaded HeLa cells were treated with a non-targeted Hsp90 inhibitor, 17AAG, and analyzed using a fluorescence microscope.
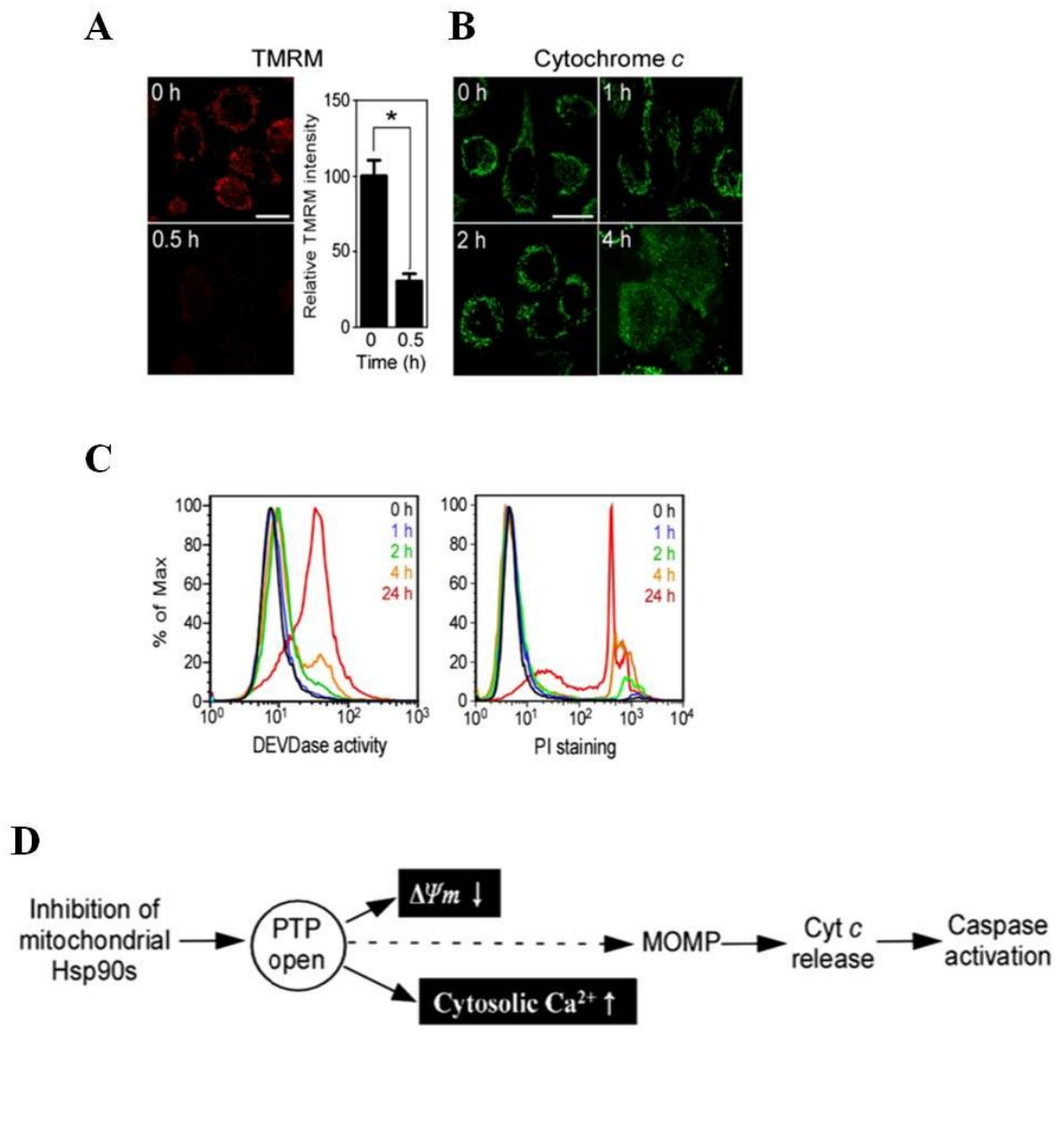
Figure 2-2. Mitochondrial Hsp90s regulate PTP opening , caspase activation and cell death
(A) Mitochondrial membrane permeabilization. TMRM-loaded HeLa cells were imaged to measure mitochondrial membrane potential depolarization ($\Delta\Psi$m). *, p< 0.0001. (B) Cytochrome c redistribution was analyzed (right) at the indicated times after 30 μM gamitrinib treatment as previously described [62]. White bar, 20 μm. (C) Caspase activation and cell death induction. After 30 μM gamitrinib treatment, HeLa cells were labeled with FITC-DEVD-fmk (left, DEVDase activity) or propidium iodide (right, PI staining) and analyzed by flow cytometry at the selected time points. (D) Summary of sequential events following mitochondrial Hsp90 inhibition. PTP opening is directly linked with the loss of $\Delta\Psi$m and

increase of cytosolic calcium. The calcium flux occurs prior to mitochondrial outer membrane permeabilization (MOMP) and cytochrome c release.
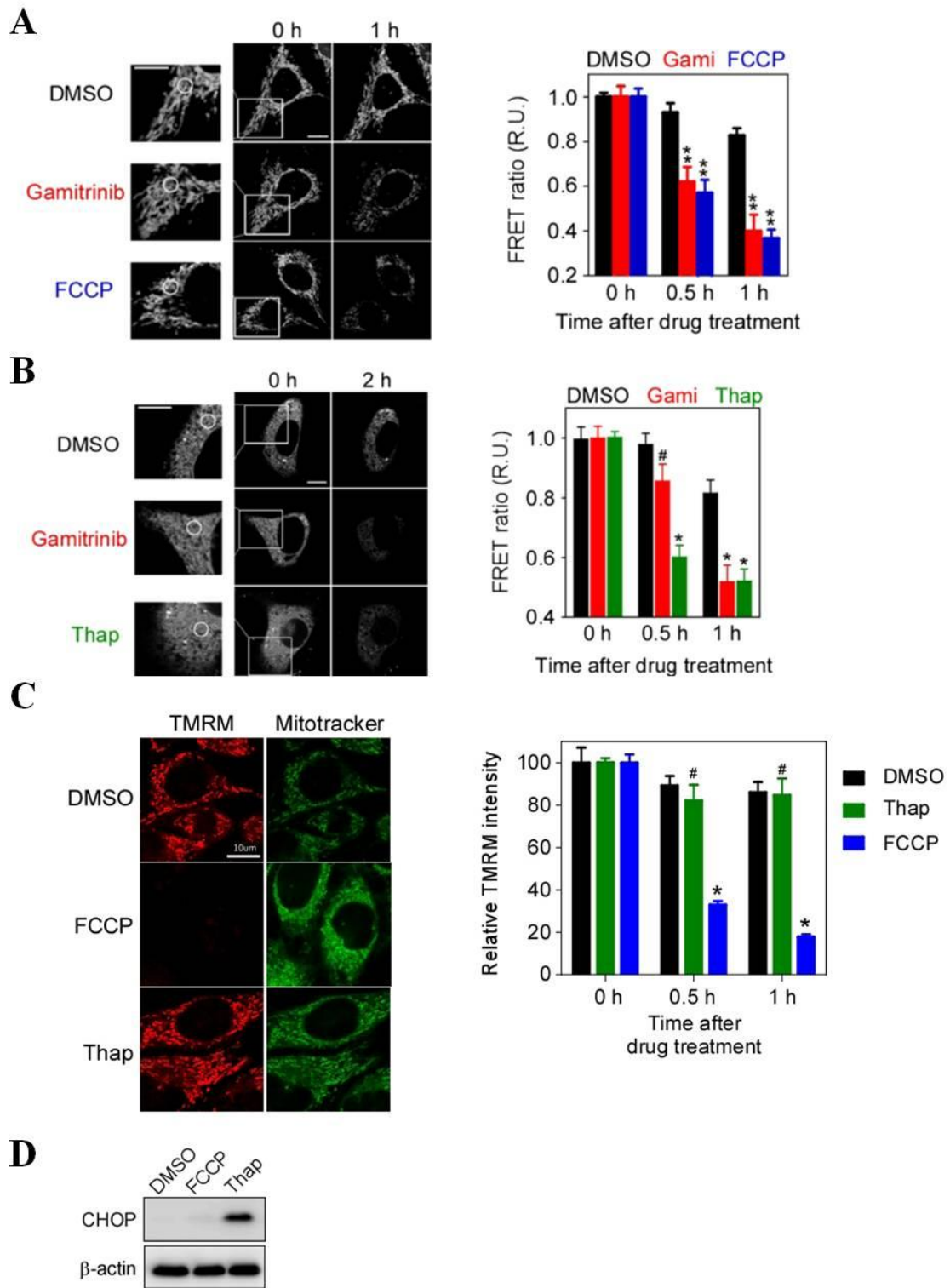
Figure 2-3. Inhibition of mitochondrial Hsp90s depletes stored calcium in both mitochondria and the ER

(A) Mitochondrial calcium depletion. After 30 μM gamitrinib and 10 μM FCCP treatment, confocal FRET images of mtCameleon-expressing HeLa cells were reconstructed from their emission fluorescence ratios at 535/480 nm with excitation at 440 nm (left). FRET ratios at the indicated time intervals were averaged and plotted (right). (B) ER calcium depletion. FRET images of HeLa cells transiently expressing D1ER were acquired at the indicated time points after gamitrinib treatment (left) and analyzed to plot the FRET ratio (right). Selected ROIs are indicated as white circles. Bar, 10 μm. Data in (A) and (B) are mean ± SEM collected from 30 ROIs. R.U., relative units. (C-D) Organelle specific effect of FCCP and Thap (C) TMRM loaded HeLa cells were treated with 10 μM FCCP or 10 μM Thap for 30 mins and analyzed by confocal microscope (left). Quantitation of the confocal microscope images (right). Data are mean ± SEM from 30 ROIs. #, not significant; *, p<0.0001. (D) HeLa cells were treated with the drugs for 2 hours and analyzed by western blotting (right).

A

Time after 17AAG treat

0 h   0.5 h   1 h
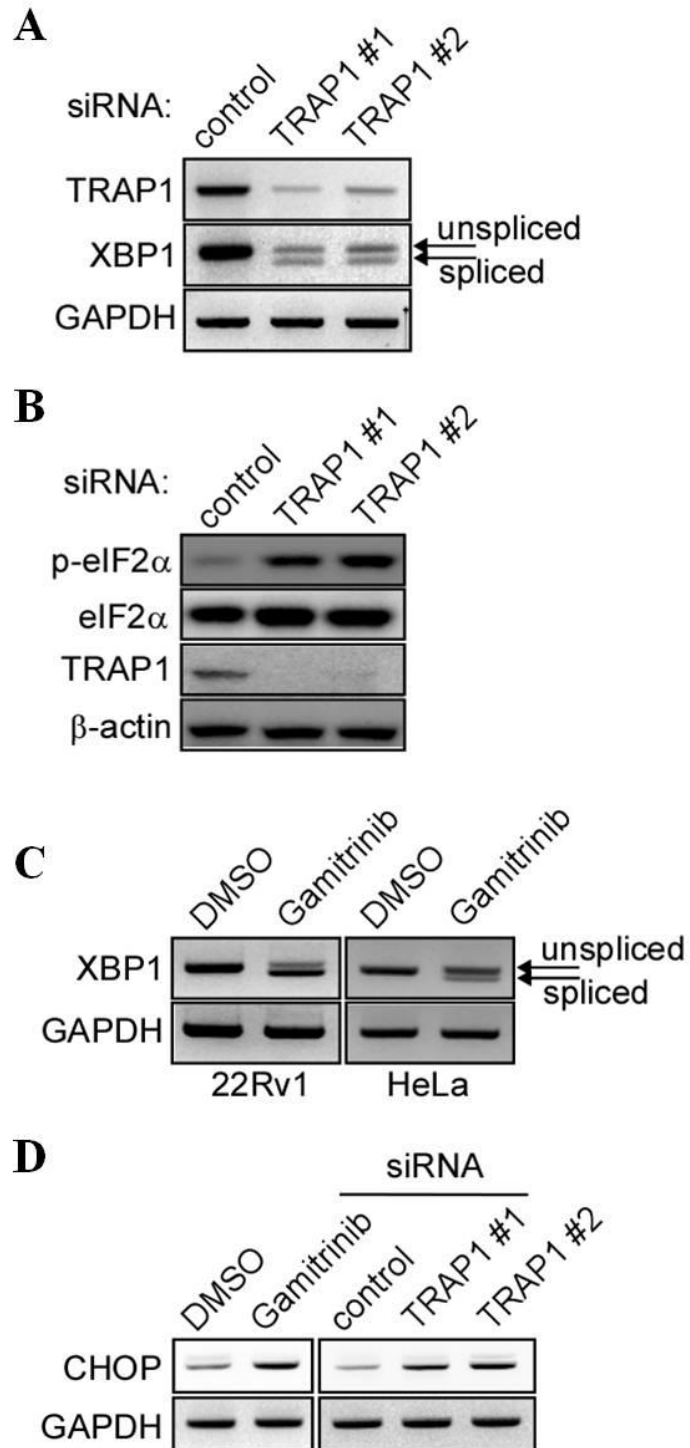

HeLa - mtCameleon

B
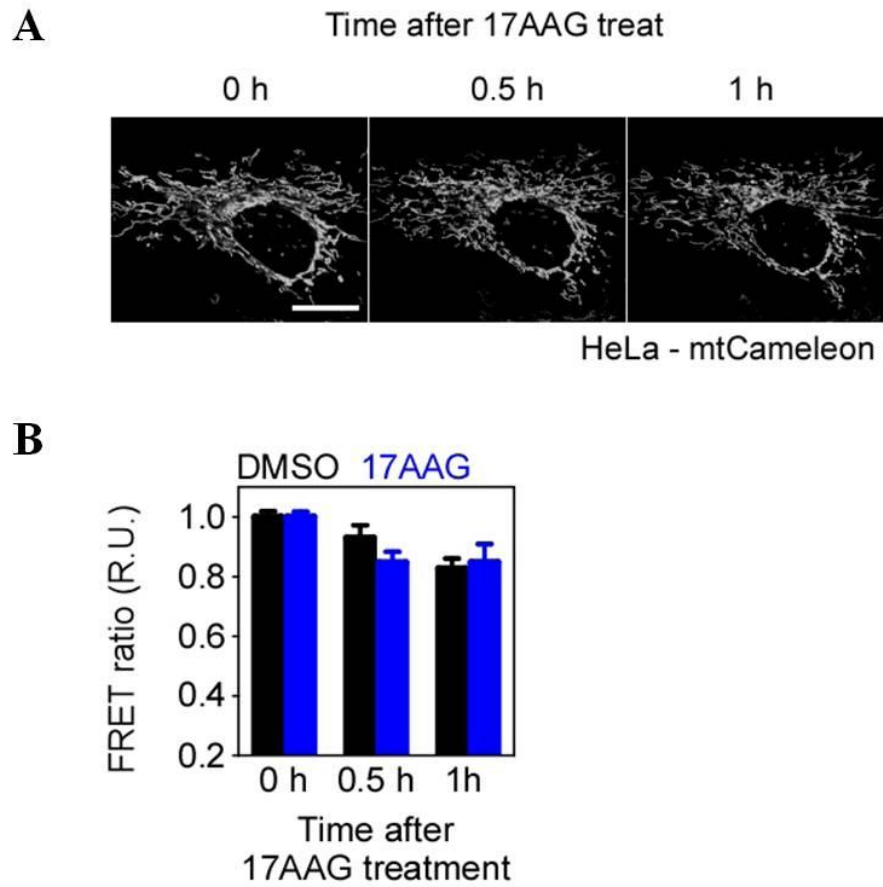
Figure 2-4. Effect of 17AAG on the mitochondrial calcium store

(A) mtCameleon was transiently expressed in HeLa cells. FRET images were acquired after 30 μM 17AAG treatment at the indicated time intervals. (B) FRET ratio was calculated and plotted (right). Data are the mean ± SEM calculated from 30 cells in two independent experiments. Bar, 10 μm. R.U., relative units.
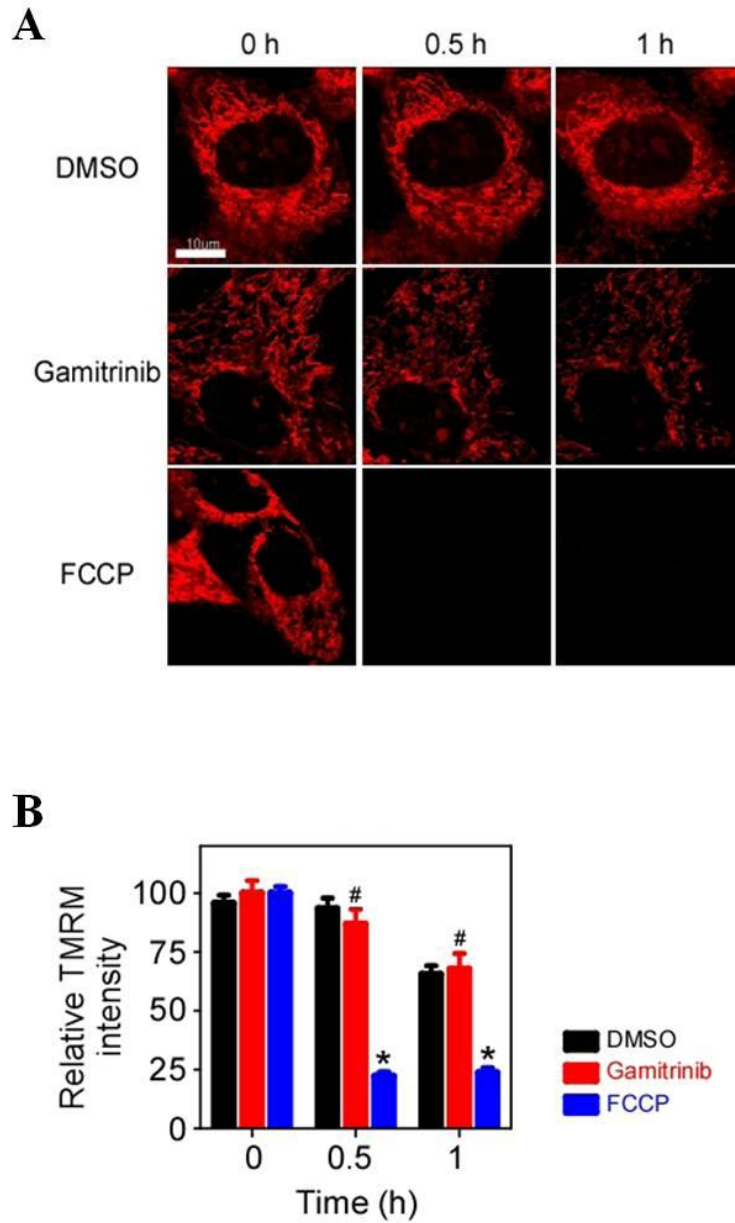
Figure 2-5. Gamitrinib effect on normal cells

(A) TMRM loaded MCF10A cells (breast normal cell line) were treated with 30 μM gamitrinib as indicated and analyzed by confocal microscope. (B) Quantitation of the images (right). Data are mean ± SEM from 40 ROIs. #, not significant; *, p<0.0001.

A

siRNA: control   TRAP1 #1   TRAP1 #2

TRAP1

XBP1 ← unspliced
      ← spliced

GAPDH

B

siRNA: control   TRAP1 #1   TRAP1 #2

p-eIF2α

eIF2α

TRAP1

β-actin

C

        DMSO   Gamitrinib   DMSO   Gamitrinib

XBP1   ← unspliced
       ← spliced

GAPDH

       22Rv1   HeLa

D

                        siRNA

DMSO   Gamitrinib   control   TRAP1 #1   TRAP1 #2
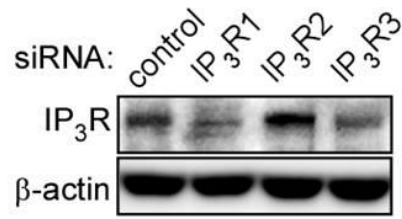
CHOP

GAPDH

40

Figure 2-6. Inhibition of mitochondrial Hsp90s activates ER stress sensors

(A) XBP1 splicing by silencing TRAP1. HeLa cells were treated with two different TRAP1 siRNAs for 24 hours. mRNA expression levels of XBP1 splicing variants, TRAP1, and GAPDH were analyzed by RT-PCR. (B) eIF2α phosphorylation upon TRAP1 silencing. After treatment of HeLa cells with two different TRAP1 siRNAs, the expression levels of eIF2α, phospho-eIF2α (p-eIF2α), TRAP1, and β-actin were analyzed by western blotting. (C) XBP1 splicing upon mitochondrial Hsp90 inhibition. After treatment with 30 μM gamitrinib for 2 hours, mRNA expression levels of XBP1 splicing variants, TRAP1, and GAPDH mRNAs were analyzed by RT-PCR. (D) Analysis of CHOP mRNA. HeLa cells were treated with 30 μM gamitrinib or TRAP1 siRNAs as indicated. CHOP and GAPDH mRNAs were analyzed by RT-PCR.
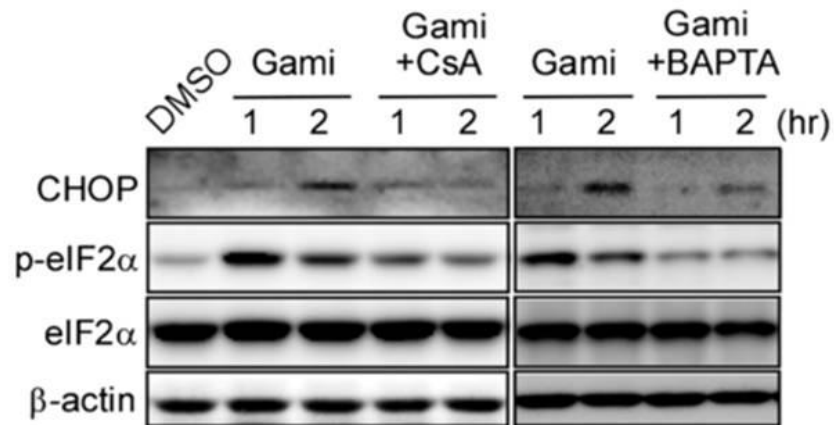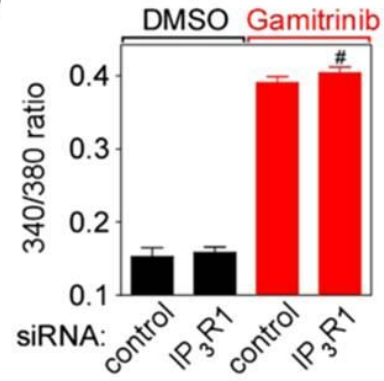
Figure 2-7. Inhibition of mitochondrial Hsp90s induce ER stress depending on calcium

CHOP induction and eIF2α phosphorylation. HeLa cells were treated with 30 μM gamitrinib, 5 μM CsA, and 10 μM BAPTA as indicated and analyzed by western blotting.
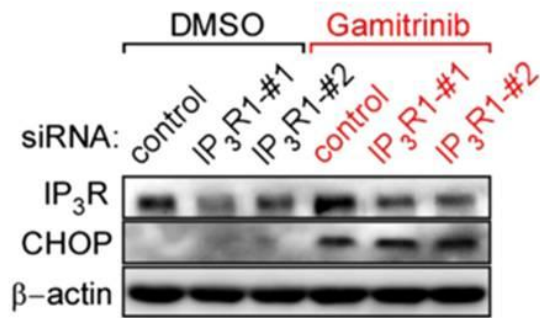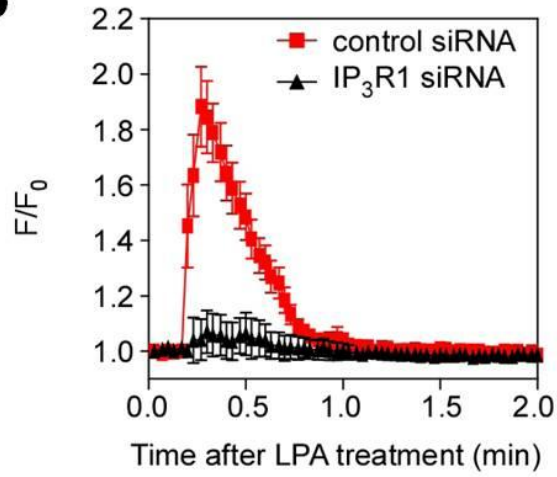
A

siRNA: control   IP$_3$R1   IP$_3$R2   IP$_3$R3

IP$_3$R

β-actin

B

C

siRNA: control   IP$_3$R1-#1   IP$_3$R1-#2   control   IP$_3$R1-#1   IP$_3$R1-#2

IP$_3$R

CHOP

β-actin

D

Figure 2-8. Gamintrinib induced cytosolic calcium elevation is not involved in IP3 receptor
(A) Silencing of IP3R isotypes. HeLa cells were treated with IP3R1-, IP3R2-, and IP3R3-specific siRNAs, and analyzed by Western blotting. (B) IP3R silencing. After IP3R siRNA treatment, Fura-2 labeled HeLa cells were treated with 30 μM gamitrinib for 1 hour. The fluorescence ratio (340/380) was plotted. The data are mean ± SEM collected from 30 ROIs in two independent experiments. (C) IP3R knockdown effect on CHOP expression. Control or IP3R1 siRNA-transfected HeLa cells were incubated with or without 30 μM gamitrinib for 2 hours. Cell extracts were analyzed by western blotting. (D) IP3R1 silencing blocked LPA-induced calcium flux. HeLa cells were treated with IP3R1 siRNA and labeled with Fura-2. After LPA treatment, cytoplasmic calcium flux was monitored. Data are the mean ± SEM calculated from 20 ROIs in two independent experiments.

A

B

C

D
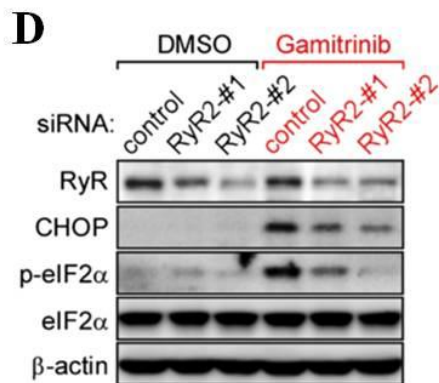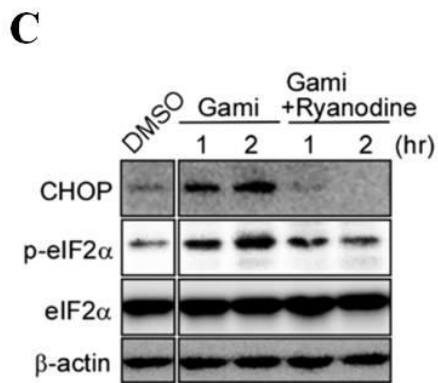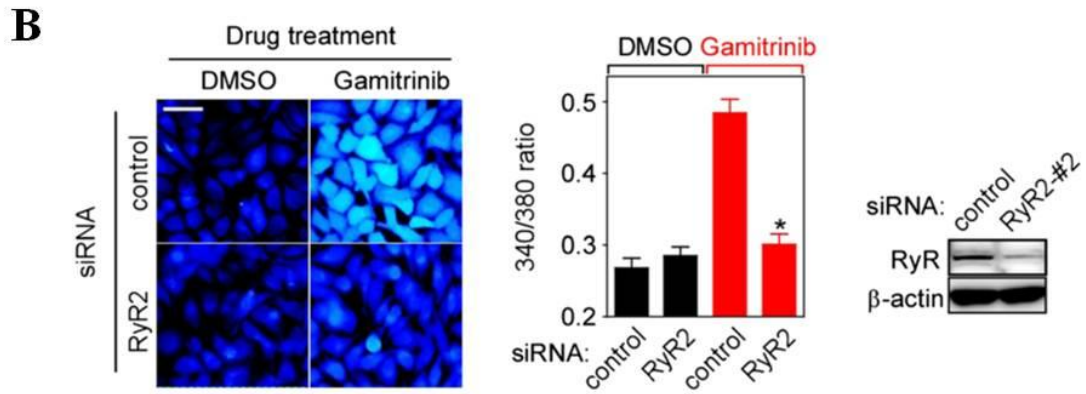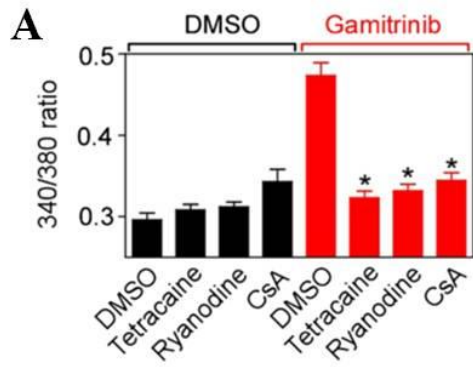
Figure 2-9. Ryanodine receptor (RyR)-mediated cytosolic calcium elevation

(A) RyR inhibitors compromise cytosolic calcium increase. Fura-2 labeled HeLa cells were treated with 30 μM gamitrinib for an hour in the presence or absence of 300 μM tetracaine, 100 μM ryanodine, and 5 μM CsA, and emission fluorescence intensity ratios (340/380 nm excitation) were measured. Data are mean ± SEM calculated from 40 ROIs in two independent experiments. (B) Fura-2 imaging and RyR2 silencing. Control or RyR2-#2 siRNA-treated HeLa cells were labeled with Fura-2 and imaged after 30 μM gamitrinib treatment for an hour (left). The fluorescence ratio (340/380) was plotted (middle). Knockdown efficiency of RyR2-#2 siRNA by western blotting (right). The data are mean ± SEM collected from 30 ROIs in two independent experiments. Bar, 50 μm. (C) Inhibition of CHOP induction by RyR inactivation. HeLa cells were treated with 30 μM gamitrinib in the presence or absence of 100 μM ryanodine. Cell extracts were analyzed by western blotting. (D) RyR2 silencing and CHOP expression. HeLa cells were treated with two different RyR2 siRNAs, incubated with 30 μM gamitrinib, for 2 hours and analyzed by western blotting.

A
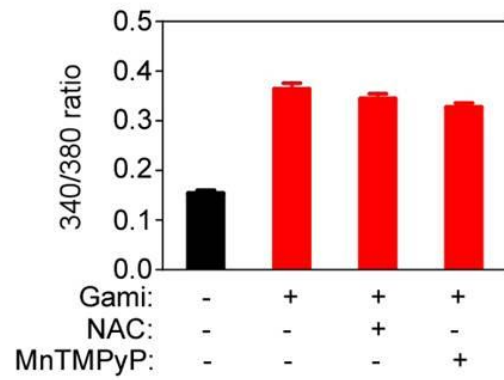
B
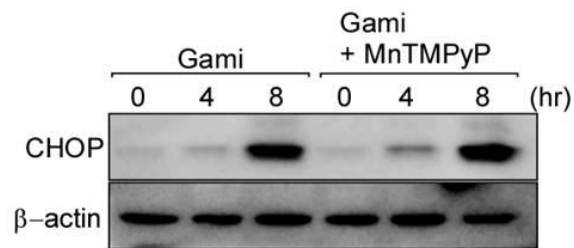
C
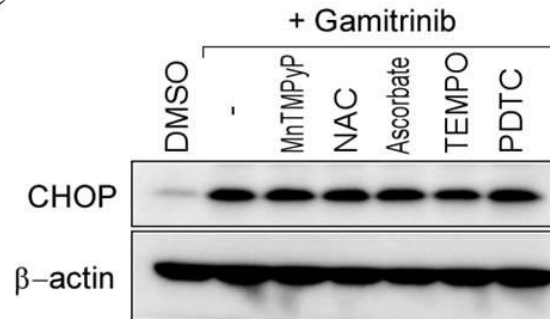
Figure 2-10. Reactive oxygen species (ROS) does not affect gamitrinib-induced calcium release and CHOP induction

(A) ROS do not affect gamitrinib-induced calcium release. Fura-2 loaded 22Rv1 cells were incubated with 30 mM N-acetylcysteine (NAC) or 30 μM MnTMPyP for 1 hour and then treated with 30 μM gamitrinib for 2 hours and analyzed by the fluorescence microscope. (B) A mitochondrial ROS scavenger effect on CHOP induction. 22Rv1 cells were treated with 20 μM gamitrinib in the presence or absence of 20 μM MnSOD for 4 and 8 hours and analyzed by western blotting. (C) A various ROS scavenger effect on CHOP induction. 22Rv1 cells were treated with 20 μM gamitrinib in the presence or absence of 0.5 mM ascorbic acid, 0.5 mM 2,2,6,6 tetramethylpiperidine 1-oxyl (TEMPO), and 20 μM pyrollidine dithiocarbamate (PDTC) for 8 hours and analyzed by western blotting.
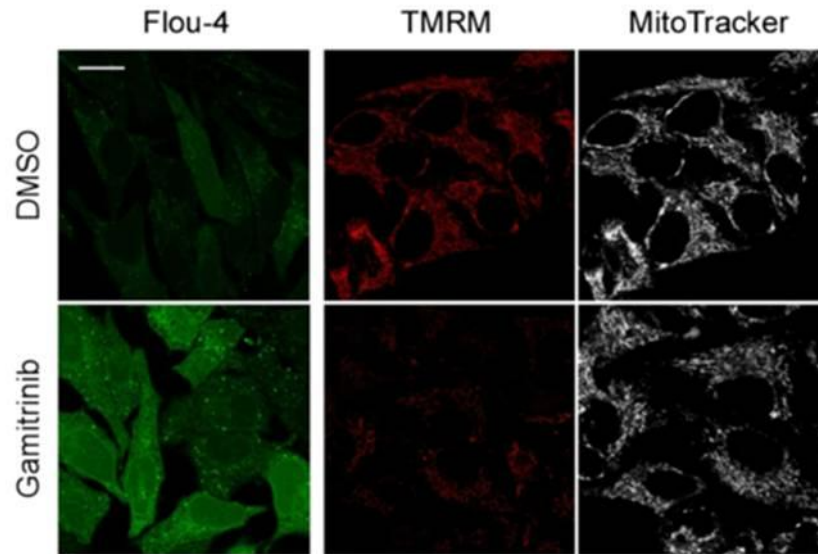
Figure 2-11. Cytoplasmic calcium and mitochondrial membrane potential by noncytotoxic dose of gamitrinib

Calcium indicated Fluo-4 or TMRM/MitoTracker-labeled HeLa cells were incubated with 5 μM gamitrinib for 24 hours and analyzed by confocal microscope. Bar, 20 μm.

A

B

C

D
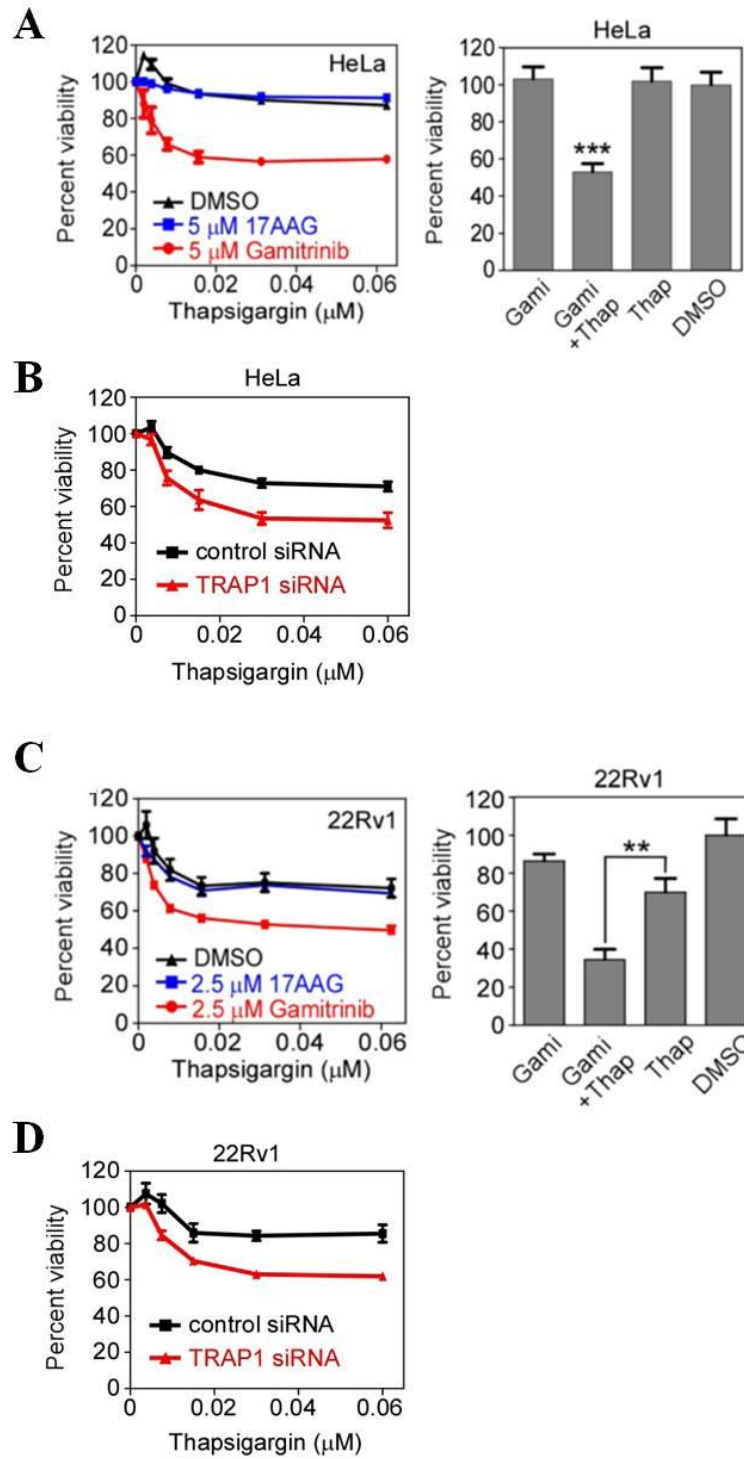
Figure 2-12. Inhibition of mitochondrial Hsp90s sensitizes HeLa cells toward thapsigargin

(A) Combination effect in HeLa. HeLa cells were treated with various concentrations of Thap in the presence of 5 μM of either 17AAG or gamitrinib, and analyzed by MTT assay (left). Alternatively, HeLa cells were treated with 5 μM gamitrinib and/or 0.06 μM Thap for 24 hours and analyzed by the MTT assay. ***, $p < 0.0001$. (B) Knockdown of TRAP1 by siRNA. After silencing of TRAP1 in HeLa with TRAP1-#1 siRNA, cells were treated with various concentrations of Thap for 24 hours and analyzed by the MTT assay. Data are from three independent duplicate experiments; data are given in terms of mean ± SEM. (C) Combination effect in 22Rv1. 22Rv1 cells were treated with various concentrations of thapsigargin in the presence of 2.5 μM of either 17AAG or gamitrinib for 24 hours, and analyzed by the MTT assay (left). Alternatively, 22Rv1 cells were treated with 2.5 μM gamitrinib (Gami) and 0.06 μM Thap as indicated for 24 hours and analyzed by the MTT assay. **, $p = 0.0006$. (D) Knockdown of TRAP1 by siRNA. After silencing of TRAP1 in 22Rv1 cells with TRAP1-#1 siRNA, cells were treated with various concentrations of Thap for 24 hours and analyzed by the MTT assay. Data are from three independent duplicate experiments; data are given in terms of mean ± SEM.

A
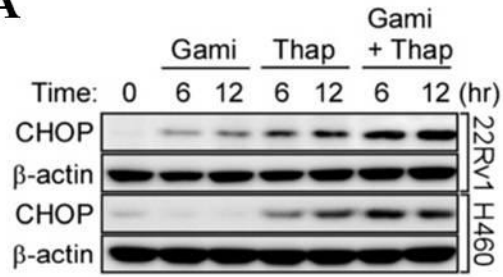
B
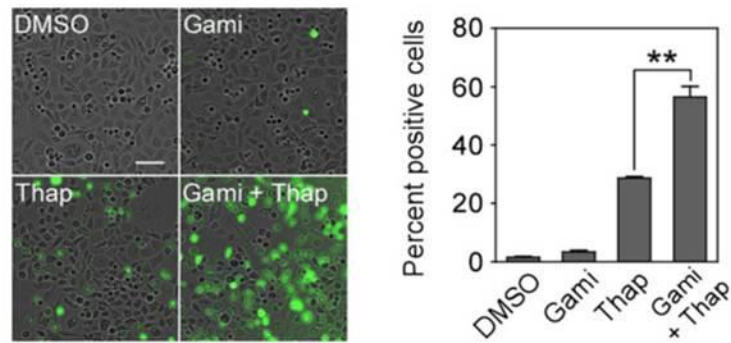
C
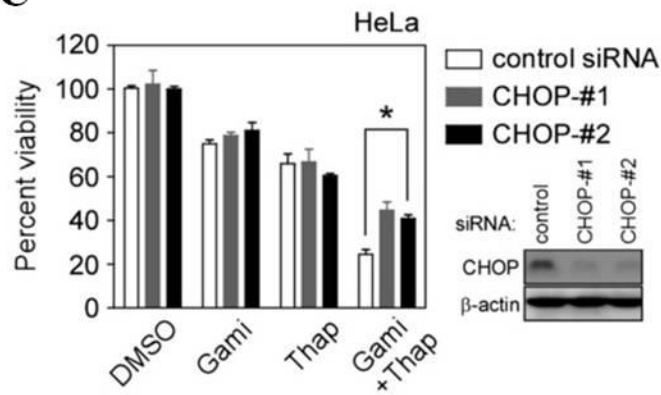
Figure 2-13. **Gamitrinib and Thap combination treatment elevates CHOP expression**

(A) Synergistic increase in CHOP induction. 22Rv1 and H460 cells were treated with 5 μM gamitrinib and 0.06 μM Thap as indicated and analyzed by western blotting. (B) CHOP reporter assay. PC3 cells stably transfected with a CHOP::GFP reporter plasmid were incubated with 2.5 μM gamitrinib and/or 0.02 μM Thap as indicated and analyzed as described in Materials and Methods (left). Cells with more than twice the background fluorescence intensity were considered as positive cells (right). Bar, 100 μm. Mean ± SEM. **, $p = 0.0036$. (C) Silencing CHOP expression. Control or CHOP siRNA-transfected HeLa cells were treated with 0.06 μM Thap and 5 μM gamitrinib for 24 hours, and analyzed by MTT assay. Knockdown efficiency analyzed by western blotting (bottom right). Mean ± SEM. *, $p < 0.05$.
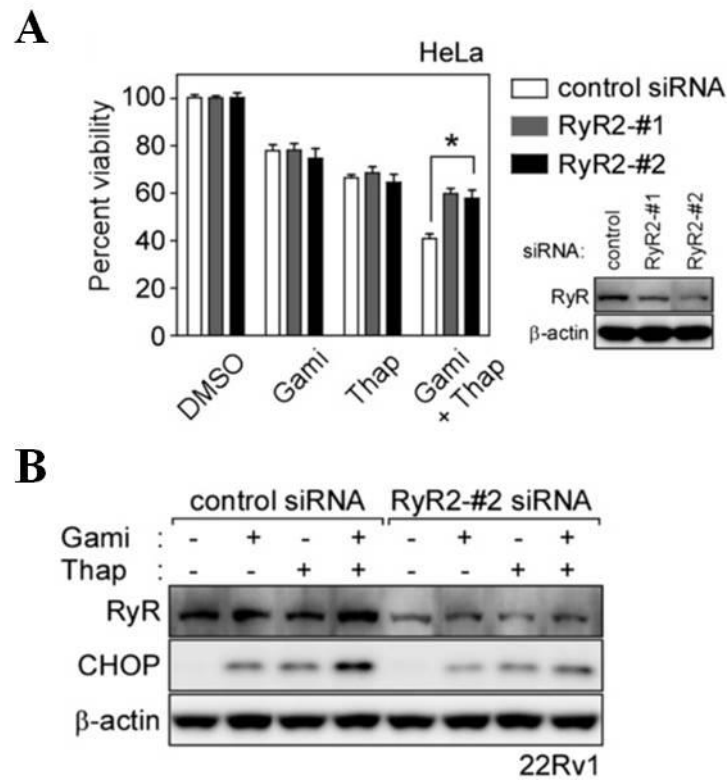
Figure 2-14. **Silencing RyR expression**

(A) Control or RyR siRNA-treated HeLa cells were incubated with 0.06 μM Thap and 5 μM gamitrinib for 24 hours, and analyzed by MTT assay. Knockdown efficiency analyzed by western blotting (bottom right). Mean ± SEM. *, $p < 0.05$. (B) Knockdown of RyR2 by siRNA. Control or RyR2 siRNA-transfected 22Rv1 cells were incubated with 2.5 μM gamitrinib and/or 0.06 μM Thap as indicated and analyzed by western blotting.
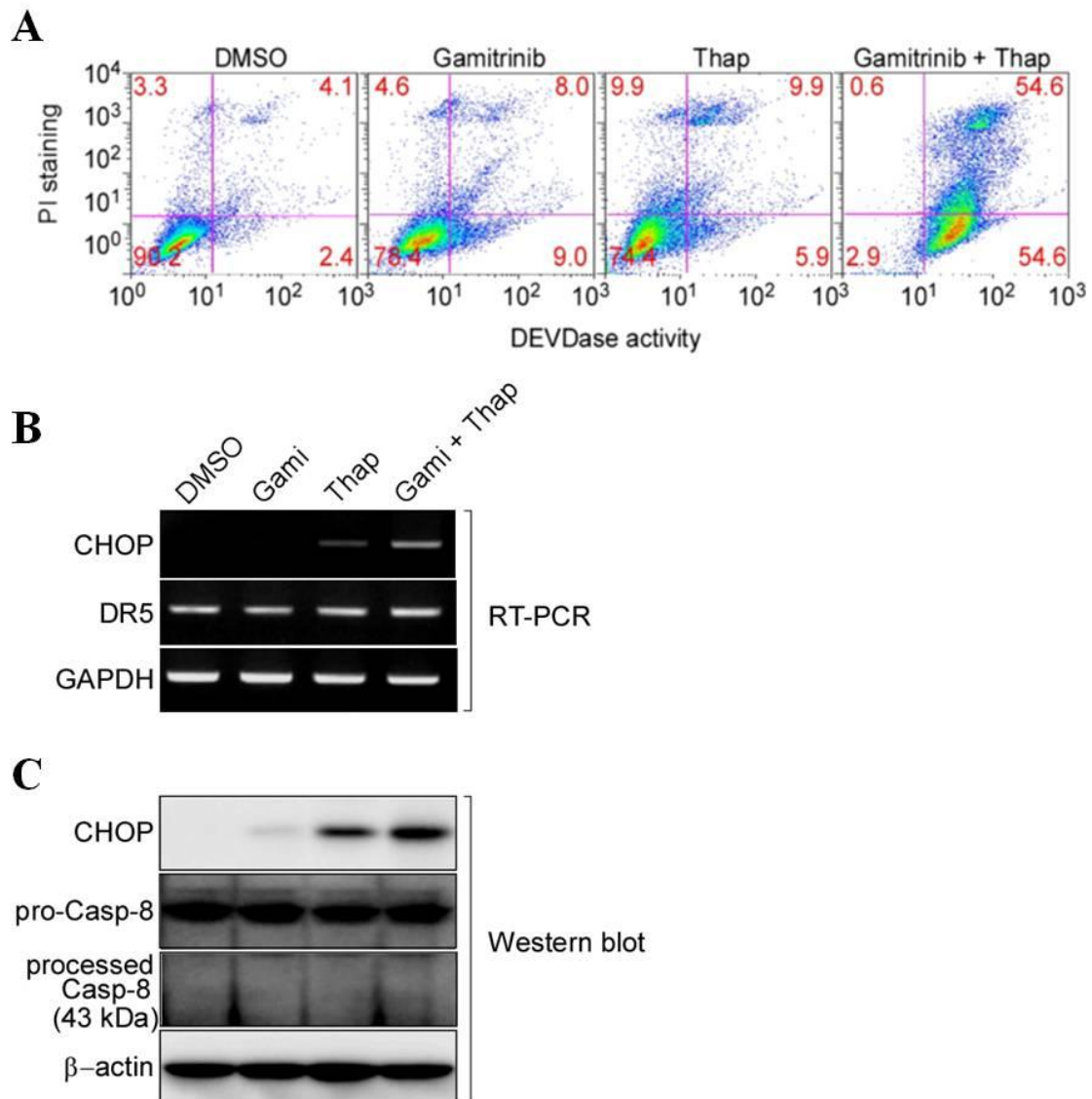
Figure 2-15. **Apoptosis induction on combination drug treated HeLa cells**

(A) Combination treatment induces apoptosis. HeLa cells were treated with 10 μM gamitrinib and 0.5 μM Thap as indicated, labeled with FITC-DEVD-fmk and propidium iodide, and analyzed by flow cytometry. (B) DR5 expression on combination drug treatment. 22Rv1 cells were treated with 2.5 μM gamitrinib and 0.06 μM Thap as indicated for 24 hours, then analyzed by reverse transcription (RT)-PCR. (C) caspase-8 activation on combination drug treatment. 22Rv1 cells were treated with 2.5 μM gamitrinib and 0.06 μM Thap as indicated for 24 hours, then analyzed by western blotting.

A

	DMSO	Gamitrinib
CHOP		
p-eIF2α		
eIF2α		
β-actin		
TRAP1		

B

C

	DMSO	Gamitrinib	Thap	
CHOP				4 hr
β-actin				
CHOP				24 hr
β-actin				

D

	astrocyte	HeLa	22Rv1	H460
TRAP1				
Cyp-D				
β-actin				
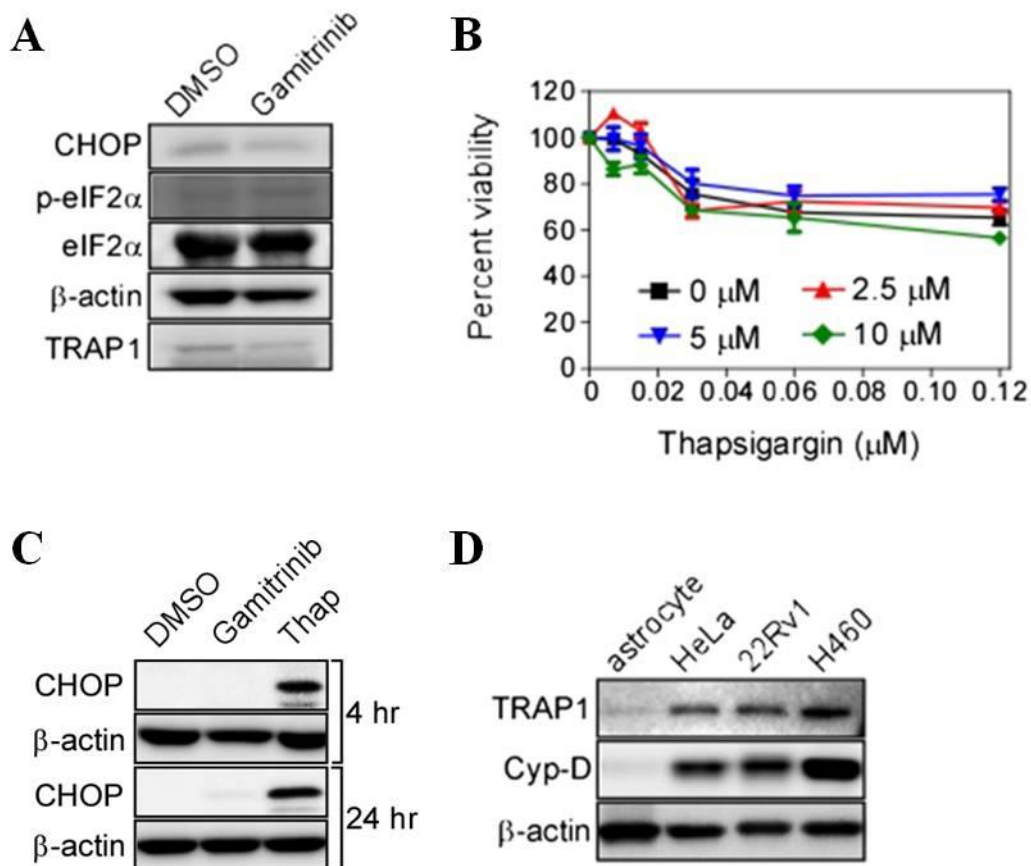
Figure 2-16. CHOP induction and cytotoxicity in astrocytes

(A) Astrocytes treated with 30 μM gamitrinib for 2 hours were analyzed by western blotting. (B) Thap in combination with gamitrinib. Astrocytes were treated with various concentrations of Thap in the presence of 0, 2.5, 5, or 10 μM gamitrinib and the cell viability was analyzed by MTT assay. Data are from three independent experiments. (C) Gamitrinib and Thap treatment in astrocytes. Astrocytes were treated with 10 μM Thap or 30 μM gamitrinib for 4 hours and 1 μM Thap or 2.5 μM gamitrinib for 24 hours, and analyzed by western blotting. (D) TRAP1 expression in astrocytes. TRAP1 and cyclophilin D (Cyp-D) expression in astrocytes isolated from mouse brain was compared with cancer cell lines by western blotting.
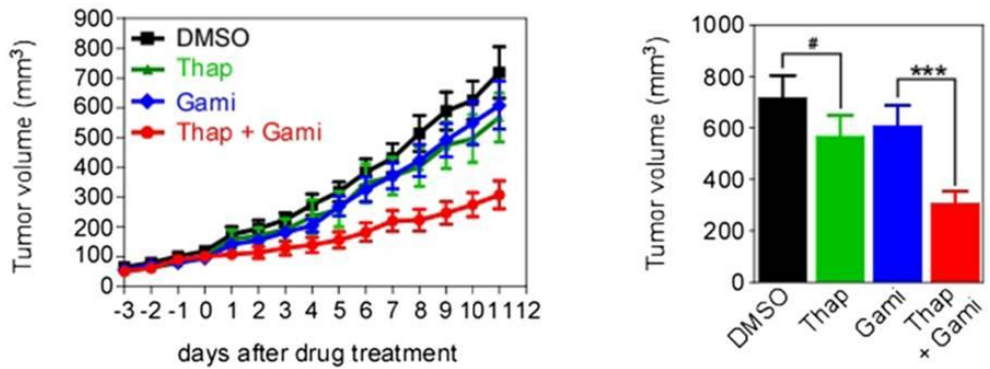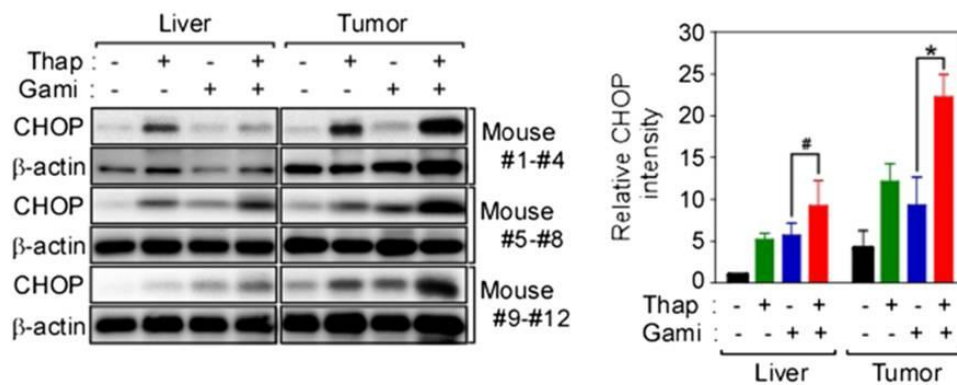
Figure 2-17. Synergistic cancer-specific cytotoxicity in vivo

(A) Tumor xenograft experiment. Subcutaneous 22Rv1 xenografts were established as described in Materials and Methods. At the end of the experiment, final tumor volumes were plotted (right). We used five mice per group and two tumors per animal. (B) Analysis of CHOP expression in liver and tumor. Liver and tumor samples from three randomly selected mice for each treatment (total 12 mice) were analyzed by western blotting (left). After normalization of CHOP band intensities with β-actin, relative CHOP intensities were calculated (right). ***, p= 0.0003; *, p = 0.039; #, p> 0.1.
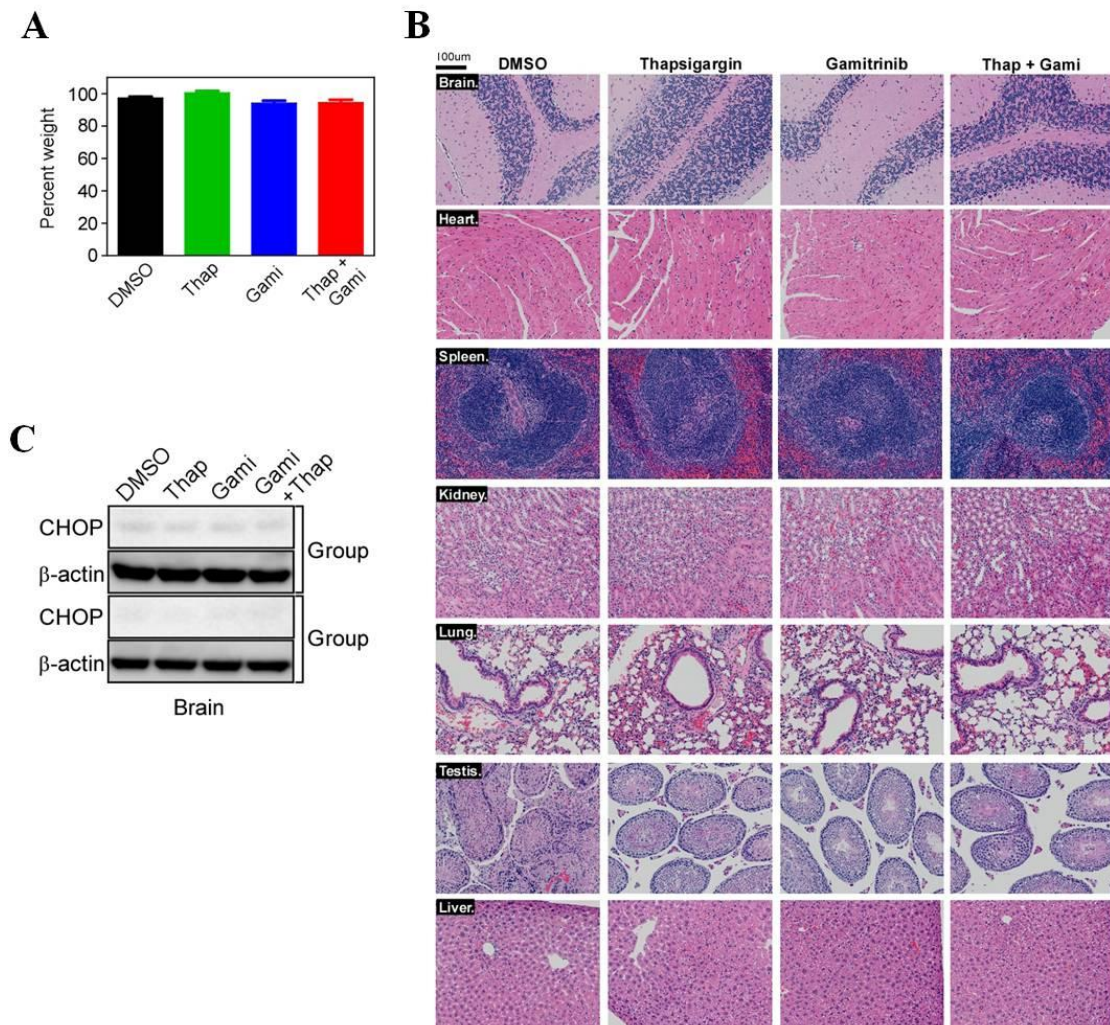
Figure 2-18. Side effect on combination drug administration in vivo

(A) Mouse body weight change. Prior to sacrificing the animals in the xenograft experiment, their body weights were measured. Data are mean ± SEM. (B) Hematoxylin and eosin staining. The animals were sacrificed at the end of the experiment, and organs were collected, fixed, stained, and analyzed under a light microscope. (C) Analysis of CHOP expression in mouse brain. Brain samples from sacrificed mice (total 8 mice) were analyzed by western blotting.
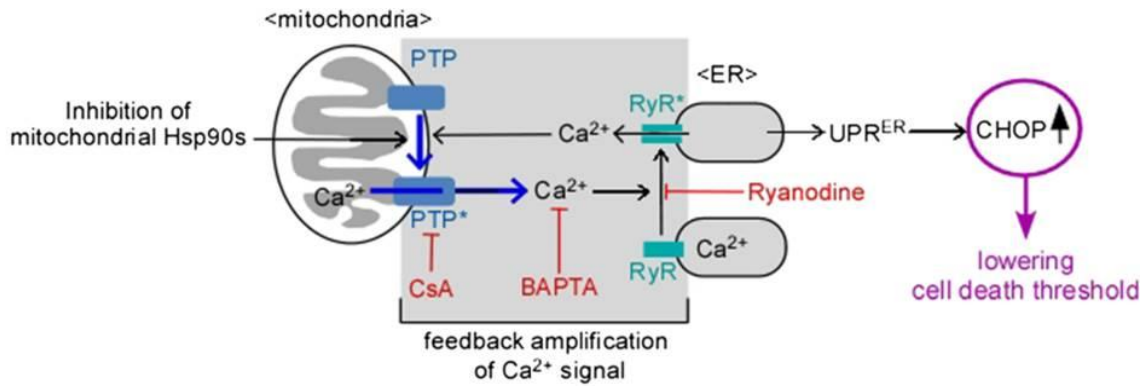
Figure 2-19. Schematic diagram of the mitochondria-initiated stress signal

Chemical inhibitors are indicated in red.

2-5. References

1. Taipale, M., D.F. Jarosz, and S. Lindquist, *HSP90 at the hub of protein homeostasis: emerging mechanistic insights.* Nat Rev Mol Cell Biol, 2010. **11**(7): p. 515-28.

2. Pearl, L.H., C. Prodromou, and P. Workman, *The Hsp90 molecular chaperone: an open and shut case for treatment.* Biochem J, 2008. **410**(3): p. 439-53.

3. Trepel, J., et al., *Targeting the dynamic HSP90 complex in cancer.* Nat Rev Cancer, 2010. **10**(8): p. 537-49.

4. Siegelin, M.D., et al., *Exploiting the mitochondrial unfolded protein response for cancer therapy in mice and human cells.* J Clin Invest, 2011. **121**(4): p. 1349-60.

5. Eletto, D., D. Dersh, and Y. Argon, *GRP94 in ER quality control and stress responses.* Semin Cell Dev Biol, 2010. **21**(5): p. 479-85.

6. Kang, B.H., et al., *Regulation of tumor cell mitochondrial homeostasis by an organelle-specific Hsp90 chaperone network.* Cell, 2007. **131**(2): p. 257-70.

7. Leav, I., et al., *Cytoprotective mitochondrial chaperone TRAP-1 as a novel molecular target in localized and metastatic prostate cancer.* Am J Pathol, 2010. **176**(1): p. 393-401.

8. Caino, M.C., et al., *Metabolic stress regulates cytoskeletal dynamics and metastasis of cancer cells.* J Clin Invest, 2013. **123**(7): p. 2907-20.

9. Chae, Y.C., et al., *Landscape of the mitochondrial Hsp90 metabolome in tumours.* Nat Commun, 2013. **4**: p. 2139.

10. Sciacovelli, M., et al., *The mitochondrial chaperone TRAP1 promotes neoplastic growth by inhibiting succinate dehydrogenase.* Cell Metab, 2013. **17**(6): p. 988-99.

11. Yoshida, S., et al., *Molecular chaperone TRAP1 regulates a metabolic switch between mitochondrial respiration and aerobic glycolysis.* Proc Natl Acad Sci U S A, 2013. **110**(17): p. E1604-12.

12. Chae, Y.C., et al., *Control of tumor bioenergetics and survival stress signaling by mitochondrial HSP90s.* Cancer Cell, 2012. **22**(3): p. 331-44.

13. Montesano Gesualdi, N., et al., *Tumor necrosis factor-associated protein 1 (TRAP-1) protects cells from oxidative stress and apoptosis.* Stress, 2007. **10**(4): p. 342-50.

14. Landriscina, M., et al., *Mitochondrial chaperone Trap1 and the calcium binding protein Sorcin interact and protect cells against apoptosis induced by antiblastic agents.* Cancer Res, 2010. **70**(16): p. 6577-86.

15. Kroemer, G., L. Galluzzi, and C. Brenner, *Mitochondrial membrane permeabilization in*

cell death. Physiol Rev, 2007. **87**(1): p. 99-163.

16. Baines, C.P., et al., *Loss of cyclophilin D reveals a critical role for mitochondrial permeability transition in cell death.* Nature, 2005. **434**(7033): p. 658-62.

17. Baines, C.P., et al., *Voltage-dependent anion channels are dispensable for mitochondrial-dependent cell death.* Nat Cell Biol, 2007. **9**(5): p. 550-5.

18. Basso, E., et al., *Properties of the permeability transition pore in mitochondria devoid of Cyclophilin D.* J Biol Chem, 2005. **280**(19): p. 18558-61.

19. Kokoszka, J.E., et al., *The ADP/ATP translocator is not essential for the mitochondrial permeability transition pore.* Nature, 2004. **427**(6973): p. 461-5.

20. Nakagawa, T., et al., *Cyclophilin D-dependent mitochondrial permeability transition regulates some necrotic but not apoptotic cell death.* Nature, 2005. **434**(7033): p. 652-8.

21. Bernardi, P. and S. von Stockum, *The permeability transition pore as a Ca(2+) release channel: new answers to an old question.* Cell Calcium, 2012. **52**(1): p. 22-7.

22. Berridge, M.J., P. Lipp, and M.D. Bootman, *The versatility and universality of calcium signalling.* Nat Rev Mol Cell Biol, 2000. **1**(1): p. 11-21.

23. Rizzuto, R. and T. Pozzan, *Microdomains of intracellular Ca2+: molecular determinants and functional consequences.* Physiol Rev, 2006. **86**(1): p. 369-408.

24. Pinton, P., et al., *Calcium and apoptosis: ER-mitochondria Ca2+ transfer in the control of apoptosis.* Oncogene, 2008. **27**(50): p. 6407-18.

25. Rizzuto, R., et al., *Close contacts with the endoplasmic reticulum as determinants of mitochondrial Ca2+ responses.* Science, 1998. **280**(5370): p. 1763-6.

26. Csordas, G., et al., *Imaging interorganelle contacts and local calcium dynamics at the ER-mitochondrial interface.* Mol Cell, 2010. **39**(1): p. 121-32.

27. Giacomello, M., et al., *Ca2+ hot spots on the mitochondrial surface are generated by Ca2+ mobilization from stores, but not by activation of store-operated Ca2+ channels.* Mol Cell, 2010. **38**(2): p. 280-90.

28. Endo, M., *Calcium-induced calcium release in skeletal muscle.* Physiol Rev, 2009. **89**(4): p. 1153-76.

29. Kang, B.H., et al., *Combinatorial drug design targeting multiple cancer signaling networks controlled by mitochondrial Hsp90.* J Clin Invest, 2009. **119**(3): p. 454-64.

30. Banker, G. and K. Goslin, *Developments in neuronal cell culture.* Nature, 1988. **336**(6195): p. 185-6.

31. Novoa, I., et al., *Feedback inhibition of the unfolded protein response by GADD34-mediated dephosphorylation of eIF2alpha.* J Cell Biol, 2001. **153**(5): p. 1011-22.

32. Palmer, A.E., et al., *Bcl-2-mediated alterations in endoplasmic reticulum Ca2+ analyzed with an improved genetically encoded fluorescent sensor.* Proc Natl Acad Sci U S A, 2004. **101**(50): p. 17404-9.

33. Palmer, A.E. and R.Y. Tsien, *Measuring calcium signaling using genetically targetable fluorescent indicators.* Nat Protoc, 2006. **1**(3): p. 1057-65.

34. Kang, B.H., *TRAP1 regulation of mitochondrial life or death decision in cancer cells and mitochondria-targeted TRAP1 inhibitors.* BMB Rep, 2012. **45**(1): p. 1-6.

35. Ichas, F., L.S. Jouaville, and J.P. Mazat, *Mitochondria are excitable organelles capable of generating and conveying electrical and calcium signals.* Cell, 1997. **89**(7): p. 1145-53.

36. Haynes, C.M. and D. Ron, *The mitochondrial UPR - protecting organelle protein homeostasis.* J Cell Sci, 2010. **123**(Pt 22): p. 3849-55.

37. Zhao, Q., et al., *A mitochondrial specific stress response in mammalian cells.* Embo J, 2002. **21**(17): p. 4411-9.

38. Matassa, D.S., et al., *Translational control in the stress adaptive response of cancer cells: a novel role for the heat shock protein TRAP1.* Cell Death Dis, 2013. **4**: p. e851.

39. Kim, I., W. Xu, and J.C. Reed, *Cell death and endoplasmic reticulum stress: disease relevance and therapeutic opportunities.* Nat Rev Drug Discov, 2008. **7**(12): p. 1013-30.

40. Zhang, K. and R.J. Kaufman, *From endoplasmic-reticulum stress to the inflammatory response.* Nature, 2008. **454**(7203): p. 455-62.

41. Tovey, S.C., et al., *Calcium puffs are generic InsP(3)-activated elementary calcium signals and are downregulated by prolonged hormonal stimulation to inhibit cellular calcium responses.* J Cell Sci, 2001. **114**(Pt 22): p. 3979-89.

42. Fill, M. and J.A. Copello, *Ryanodine receptor calcium release channels.* Physiol Rev, 2002. **82**(4): p. 893-922.

43. Querfurth, H.W., et al., *Expression of ryanodine receptors in human embryonic kidney (HEK293) cells.* Biochem J, 1998. **334 (Pt 1)**: p. 79-86.

44. Giannini, G., et al., *The ryanodine receptor/calcium channel genes are widely and differentially expressed in murine brain and peripheral tissues.* J Cell Biol, 1995. **128**(5): p. 893-904.

45. Bennett, D.L., et al., *Expression and function of ryanodine receptors in nonexcitable cells.* J Biol Chem, 1996. **271**(11): p. 6356-62.

46. Yamaguchi, H. and H.G. Wang, *CHOP is involved in endoplasmic reticulum stress-induced apoptosis by enhancing DR5 expression in human carcinoma cells.* J Biol

Chem, 2004. **279**(44): p. 45495-502.

47. Hersey, P. and X.D. Zhang, *How melanoma cells evade trail-induced apoptosis.* Nature Reviews Cancer, 2001. **1**(2): p. 142-150.

48. Maddalena, F., et al., *Resistance to paclitxel in breast carcinoma cells requires a quality control of mitochondrial antiapoptotic proteins by TRAP1.* Mol Oncol, 2013. **7**(5): p. 895-906.

49. Gao, J.Y., et al., *Correlation between mitochondrial TRAP-1 expression and lymph node metastasis in colorectal cancer.* World Journal of Gastroenterology, 2012. **18**(41): p. 5965-5971.

50. Aust, S., et al., *Role of TRAP1 and estrogen receptor alpha in patients with ovarian cancer -a study of the OVCAD consortium.* Mol Cancer, 2012. **11**: p. 69.

51. Sramkoski, R.M., et al., *A new human prostate carcinoma cell line, 22Rv1.* In Vitro Cell Dev Biol Anim, 1999. **35**(7): p. 403-9.

52. Denmeade, S.R., et al., *Prostate-specific antigen-activated thapsigargin prodrug as targeted therapy for prostate cancer.* Journal of the National Cancer Institute, 2003. **95**(13): p. 990-1000.

53. Rasola, A., L. Neckers, and D. Picard, *Mitochondrial oxidative phosphorylation TRAP(1)ped in tumor cells.* Trends in Cell Biology, 2014. **24**(8): p. 455-463.

54. Yan, C.L., et al., *The targeted inhibition of mitochondrial Hsp90 overcomes the apoptosis resistance conferred by Bcl-2 in Hep3B cells via necroptosis.* Toxicology and Applied Pharmacology, 2013. **266**(1): p. 9-18.

55. de Brito, O.M. and L. Scorrano, *An intimate liaison: spatial organization of the endoplasmic reticulum-mitochondria relationship.* Embo J, 2010. **29**(16): p. 2715-23.

56. Jia, J., et al., *Mechanisms of drug combinations: interaction and network perspectives.* Nat Rev Drug Discov, 2009. **8**(2): p. 111-28.

57. Kamb, A., S. Wee, and C. Lengauer, *Why is cancer drug discovery so difficult?* Nat Rev Drug Discov, 2007. **6**(2): p. 115-20.

58. Keith, C.T., A.A. Borisy, and B.R. Stockwell, *Multicomponent therapeutics for networked systems.* Nat Rev Drug Discov, 2005. **4**(1): p. 71-8.

59. Kitano, H., *A robustness-based approach to systems-oriented drug design.* Nat Rev Drug Discov, 2007. **6**(3): p. 202-10.

60. Siegelin, M.D., *Inhibition of the mitochondrial Hsp90 chaperone network: A novel, efficient treatment strategy for cancer?* Cancer Letters, 2013. **333**(2): p. 133-146.

61. Treiman, M., C. Caspersen, and S.B. Christensen, *A tool coming of age: thapsigargin as*

an inhibitor of sarco-endoplasmic reticulum Ca(2+)-ATPases. Trends Pharmacol Sci, 1998. **19**(4): p. 131-5.

62.   Kang, B.H., et al., *Preclinical characterization of mitochondria-targeted small molecule hsp90 inhibitors, gamitrinibs, in advanced prostate cancer.* Clin Cancer Res, 2010. **16**(19): p. 4779-88.

Chapter 3. Combination treatment with doxorubicin and gamitrinib synergistically augments anticancer activity through enhanced activation of Bim.

3-1. Introduction

Heat shock protein 90 (Hsp90) is an ATP-dependent molecular chaperone that controls folding of a wide range of protein substrates, or clients, many of which are involved in signal pathways crucial for tumorigenesis [1, 2]. The primary cellular location of Hsp90 is the cytoplasm, but a pool of Hsp90 and its isoform, tumor necrosis factor receptor-associated protein 1 (TRAP1), has been reported in mitochondria [3, 4]. The mitochondrial expression of Hsp90 and TRAP1 is often elevated in many cultured cancer cells and human cancer patients tumorigenic processes including the neoplastic metabolic shift to aerobic glycolysis [5-7] and inhibition of cell death [3]. A class of mitochondriotropic Hsp90 inhibitors, named gamitrinibs (GA mitochondrial matrix inhibitors), has been developed through combinatorial chemistry [8]. Gamitrinibs consist of geldanamycin, a competitive inhibitor of the ATPase pocket of Hsp90 and TRAP1, conjugated with tandem repeats of tetracyclic guanidinium tumor triphenylphosphonium for mitochondrial targeting [8, 9]. Gamitrinibs not only trigger massive cell death in cultured cancer cells in vitro but also strongly suppress tumor growth in various xenograft and genetic mouse cancer models in vivo [8, 10, 11]. The gamitrinib-induced cytotoxicity is attributed to the reactivation of cyclophilin D (Cyp-D), an opener of the permeability transition pore (PTP) located in the mitochondrial inner membrane [3, 12]. Because such opening of the PTP can be lethal, Cyp-D activation is often suppressed in cancer cells by interaction with mitochondrial Hsp90s, which increase resistance to various cellular stresses [3]. In addition, gamitrinibs have been shown to induce organelle-specific stress responses and dysregulation of bioenergetics in mitochondria of cancer cells, concomitantly compromising neoplastic growth [7, 13-15]. Doxorubicin (DOX), an anthracycline antibiotic with the trade name Adriamycin, is one of the most effective anticancer drugs and has been widely used in various chemotherapeutic regimens to treat patients with cancer [16]. The antitumor activities of DOX are primarily attributed to DNA damage resulting from the inhibition of DNA topoisomerase II [16, 17]. The clinical use of DOX, however, has been limited by the risk of cardiotoxicity, which is dependent on the cumulative dose/treatment schedule, typically refractory to common medications, and can be fatal [17-19]. Here, we examined whether a combination of two cytotoxic drugs with unrelated

action mechanisms, DOX (genotoxic) and gamitrinib (mitochondriotoxic), would exhibit enhanced anticancer activity without aggravating unwanted side effects. This drug combination showed synergistically increased anticancer activities in vitro and in vivo, without augmenting cardiomyocyte toxicity. The underlying mechanism of action involved the activation of a proapoptotic Bcl-2 protein following the stimulation of CHOP and JNK pathways in cancer cells.

3-2. Materials and methods

Chemicals and antibodies

Gamitrinib conjugated with triphenylphosphonium was prepared as described previously [10]. MitoTracker, JC- 1, and tetramethylrhodamine methyl ester (TMRM) were purchased from Molecular Probes. All other chemicals were purchased from Sigma. The following antibodies were used in this study: anti- JNK, anti-phospho-JNK (Thr183/Tyr185), anti-COX-IV, and anti-CHOP from Cell Signaling Technology; anticytochrome c, anti-Bim, and anti-PARP from Santa Cruz Biotechnology; anti-β-actin from MP Biomedicals; and anti-TRAP1, anti-Bax, anti-caspase-8, and anti-caspase-3 from BD Biosciences.

Cells and cell culture

Human cancer cell types that originated from ovary (SKOV3), prostate (22Rv1 and PC3), cervix (HeLa), breast (MDA-MB-231), liver (SK-HEP-1), brain (A172), kidney (ACHN), and lung (NCI-H460) were purchased from the Korean Cell Line Bank. Cells were cultured in DMEM or RPMI (GIBCO) medium containing 10% FBS (GIBCO) and 1% penicillin/streptomycin (GIBCO) at 37℃ in a 10% CO_2 humidified atmosphere.

siRNA treatment

Small interfering RNAs (siRNAs) against JNK and CHOP were synthesized by Genolution Inc (Korea). siRNA sequences used in this study were as follows:
JNK1-#1, 5′-AAAGAATGTCCTACCTTCTCT-3′; JNK1-#2, 5′-AAGCCCAGTAATATAGTA GTA-3′; CHOP-#1, 5′-AGAACCAGCAGAGGTCACAA-3′; CHOP-#2, 5′-AAGAGAATGA

ACGGCTCAAGC-3′; Bim-#1, 5′-GCAACCTTCTGATGTAAGT-3′; Bim-#2, 5′-GACCG
AGAAGGTAGACAATT-3′ and control, 5′-ACUCUAUCUGCACGCUGAC-3′.

Cells were cultured on 6-well plates to 50–75% confluence, transfected with 40 nM siRNA
mixed with G-Fectin (Genolution) for 48 hours, and then analyzed or treated with drugs.

Analysis of cell viability and apoptosis induction

Cell viability was determined using 3(4,5-dimethyl-thyzoyl-2-yl)2,5 diphenyltetrazolium
bromide (MTT) and quantified by absorbance at 595 nm. Percent viability was determined by
comparison with vehicle-treated control samples. To measure apoptosis, DNA content
(propidium iodide or sytox staining), externalized phosphatidylserine (Annexin V) and caspase
activation (DEVDase activity) of the cells were determined using the CaspaTag in situ apoptosis
detection kit (Millipore) and Dead Cell Apoptosis Kit with Annexin V APC and SYTOX®
Green (Molecular probes). Labeled cells were analyzed using a FACS Calibur™ flow cytometer
(BD Biosciences). Data were processed using FlowJo software (TreeStar).

Western blot analysis and mitochondrial fractionation

Mitochondrial fractionation from cultured cells was performed with a Mitochondrial Isolation
kit (Thermo Scientific) as described in the manufacturer's instructions. For western blot analysis,
proteins were separated on 8-12% SDS-polyacrylamide gels and transferred to polyvinyl
difluoride membranes (Millipore). Primary antibodies were diluted 100–5,000-fold, and
horseradish peroxidase-conjugated mouse or rabbit secondary antibodies (KLP Inc.) were
diluted 5,000-fold. The ECL reagent (GE Healthcare) was used for chemiluminescence
detection with a LAS 4000 imager (GE Healthcare). Tumor xenograft experiment All
experiments involving animals were approved by the Ulsan National Institute of Science and
Technology Animal Care and Use Committee (approval number:UNISTIACUC-12-003-A).
Cancer cells (7×10^6 22Rv1 or 1×10^7 MDA-MB-231) were suspended in sterile 200 μl PBS.
22Rv1 cells were injected subcutaneously into both flanks of 8-week-old BALB/c nu/nu male
mice (Japan SLC Inc.). MDA-MB-231 cells were orthotopically injected into the mammary fat
pad of 8-week-old BALB/c nu/nu female mice. Gamitrinib or vehicle (DMSO) dissolved in
20% Cremophor EL (Sigma) in PBS was injected intraperitoneally (i.p.), and DOX diluted in
PBS was injected intravenously (i.v.). The mice were treated with 10 mg/kg gamitrinib and/or 3
mg/kg DOX twice a week according to the group. Tumors were measured daily with a calliper
and tumor volume was calculated using the formula $V = 1/2 \times (width)^2 \times length$. At the end of

the experiment the animals were euthanized, and organs including brain, heart, kidney, liver, lung, spleen, stomach, intestine, and testis, and tumors were collected for histologic or western blot analyses. Blood was also collected for measurement of serum creatine phosphokinase activity using the Indiko and Konelab System CK (Thermo Scientific) according to the manufacturer's instructions.

RNA extraction and reverse transcript-PCR

Total RNA was prepared from cells suspended in cold PBS using the RNeasy mini kit (QIAGEN), and cDNA was synthesized using the ProtoScript® First Strand cDNA Synthesis Kit (New England Biolabs) using an oligo(dT) primer. The PCR reaction was performed in a Mastercycler PCR machine (Eppendorf) with the following sets of oligonucleotide primers: NOXA, 5′-GTGCCCTTGGAAACGGAAGA-3′ and 5′-CCAGCCGCCCAGTCTAATCA-3′; PUMA, 5′-CAGACTGTGAATCCTGTGCT-3′ and 5′-ACAGTATCTTACAGGCTGGG-3′; DR5,5′-TGCAGCCGTAGTCTTGATTG-3′ and 5′-GAGTCAAAGGGCACCAAGTC-3′; Bcl-2, 5′-TTTTAGGAGACCGAAGTCCG-3′ and 5′-AGCCAACGTGCCATGTGCTA-3′;Bim, 5′-ATGGCAAAGCAACCTTCTGA-3′ and 5′-GGAAGCCATTGCACTGAGA-3′; CHOP, 5′-CTTTCTCCTTCGGGACACTG-3′ and 5′-AGCCGTTCATTCTCTTCAGC-3′ GAPDH, 5′-GGGAAGCTTGTCATCAATG-3′and 5′-GCAGTGATGGCATGGACT-3′.

Statistical analyses

Data from MTT assay (triplicate experiments independently repeated at least two times) were averaged and statistically analyzed by unpaired t-test using Prism 5.0 (GraphPad). A p-value less than 0.05 was considered significant. To investigate the synergistic efficacy of the drug combination, the combination index (CI) was determined according to the Chou-Talalay method using CalcuSyn software version 2.1 (Biosoft)[20].

3-3. Results

Gamitrinib-doxorubicin combination treatment showed synergistic enhancement of cytotoxicity in various cancer cell lines

To investigate the effect of combination treatment with DOX and gamitrinib, cancer cell lines originating from cervix (HeLa), ovary (SK-OV3), and prostate (22Rv1) were treated with the drugs as single agents or in combination. Gamitrinib sensitized HeLa, SK-OV3, and 22Rv1 cells to a wide range of DOX concentrations (Fig. 3-1A). Consistently, the drug combination enhanced cytotoxic effects compared with single agent treatment and resulted in cancer cell death at suboptimal concentrations (Fig. 3-1B). In contrast to the effect on cancer cells, gamitrinib did not sensitize cardiomyocytes to DOX treatment (Fig. 3-1C), suggesting no enhancement of cytotoxicity to normal cells with the drug combination. To further examine the combination effect, we calculated the combination index (CI) in various cancer cells using the Chou-Talalay method [21, 22]. The DOX and gamitrinib combination showed synergistic anticancer activity (CI<0.9) in all cancer cell types tested at a 50% effective dose: high synergism (CI<0.7) for HeLa (Fig. 3-1D), A172 (glioblastoma), ACHN (renal cell carcinoma), SK-HEP-1 (hepatocellular carcinoma), NCI-H460 (lung carcinoma), and SK-OV-3; and moderate synergism (0.7<CI<0.9) for 22Rv1 and MDA-MB-231 cells (Table 1).

Combination of DOX and gamitrinib augments apoptotic cell death

To address the cell death mechanism of the drug combination, propidium iodide uptake and caspase activation were analyzed by flow cytometry. Single drug treatment at a suboptimal concentration did not increase caspase activity significantly compared with the DMSO-treated control, whereas the drug combination dramatically increased caspase activity and concomitant cell death (Fig. 3-2A). Cell extracts from SK-OV3 and 22Rv1 consistently showed caspase activation, i.e., decreased amount of pro-form and an increase in the mature form of caspase-3 and cleavage of the caspase substrate protein, poly (ADP-ribose) polymerase (PARP), for the combined drug treatment but not for single agent treatment (Fig. 3-2B). These data suggest that the drug combination synergistically augments apoptotic cell death by mediating caspase activation. Activation of caspase by the drug combination was completely inhibited by the pan-caspase inhibitor zVAD-fmk (Fig.3- 2B). In addition, the enhanced cytotoxic activity of the drug combination was almost completely abrogated by zVAD-fmk (Fig. 3-2C), providing further evidence that the drug combination activates caspases and triggers the apoptotic cell death program. DOX does not act directly on cancer cell mitochondria Gamitrinib is designed to

accumulate in mitochondria and open the PTP, resulting in the induction of sudden cell death in various cancer cell types[10]. Some reports have suggested that the cytotoxicity of DOX is similarly attributed to direct opening of the PTP in mitochondria [17]. Therefore, we asked whether the observed drug synergism is associated with the direct effect of DOX on mitochondria. Treatment of cultured 22Rv1 cells with 5uM gamitrinib and 0.5uM DOX had only a marginal effect on mitochondrial outer (Fig. 3-3A) and inner membrane permeabilization (Fig.3-3B), whereas combined treatment with the two drugs dramatically increased the permeability of mitochondrial membranes based on discharge of cytochrome *c* into the cytoplasm (Fig. 3-3A) and loss of mitochondrial membrane potential (Fig. 3-3B). However, with isolated mitochondria, DOX alone had no effect on the membrane, whereas gamitrinib had a direct permeabilizing effect on mitochondrial membranes (Fig. 3-3C and 3D) as previously described [10] and the drug combination did not further increase membrane permeability (Fig. 3-3C and 3D). These data suggest that DOX does not affect mitochondria directly, but instead affects signaling pathways outside the mitochondria that enhance mitochondrial membrane permeabilization and lead to mitochondrial apoptotic cell death. Confocal microscopic analysis showed that DOX was primarily accumulated in the extramitochondrial space (Fig.3-3E), further supporting indirect effects of DOX on mitochondria.

Reactive oxygen species are not involved in the cytotoxic effect of combination treatment

DOX has been reported to trigger production of reactive oxygen species (ROS), although the role of ROS in the induction of cancer cell death is controversial [17]. To examine the contribution of ROS to the cytotoxic effects of the drug combination, we examined the effect of a ROS scavenger on cytotoxic activity in HeLa cells after treatment with gamitrinib and DOX, alone or in combination. DOX alone increased the production of ROS (Fig. 3-4A, left panels), and the cytotoxic activity of DOX was not affected by co-treatment with the ROS scavenger N-acetylcysteine (NAC) (Fig. 3-4B). Gamitrinib treatment increased the production of ROS in a dose-dependent manner (Fig 3-4A, middle panels), but NAC did not inhibit the cytotoxic activities of gamitrinib (Fig 3-4C). There was no additional increase in ROS production with the drug combination compared with single agent treatment (Fig. 3-4A, right panels), and NAC did not affect the cytotoxicity of the drug combination (Fig. 3-4D). These results indicate that ROS production is not involved in the enhanced cytotoxic activities of the drug combination.

Gamitrinib and DOX combination treatment activates expression of CHOP and Bim

DOX has been reported to modulate stress signal pathways such as the c-Jun Nterminal kinase

(JNK) and ER-stress induced C/EBP homologous protein (CHOP) pathways [23-25]. Gamitrinib can also activate JNK and induce CHOP by triggering an organelle-specific stress response, the mitochondrial unfolded protein response (UPR) [16, 26]. Therefore, we investigated the effect of combined DOX and gamitrinib on stress signaling and found that JNK activation (phosphorylation) and CHOP induction were increased more by the drug combination than by single agent treatment in 22Rv1 cells (Fig. 3-5A). Treatment with CHOP-specific siRNA reduced the enhanced cytotoxicity after combined drug treatment but did not affect cytotoxicity of single agent treatment (Fig. 3-5C), whereas JNK-specific siRNA did not affect the cytotoxic activity of the drugs singly or in combination. These data suggest that induction of CHOP is required for the combination effect of the drugs in 22Rv1 cells. As a downstream effector, the proapoptotic BH3-only Bcl-2 protein, Bim, is regulated by CHOP [27]. The expression of Bim was enhanced by the drug combination in 22Rv1 cells and knockdown of CHOP compromised the up-regulation of Bim (Fig. 3-5D). Consistent with these findings, inactivation of Bim by siRNA treatment compromised the enhanced cytotoxicity of the drug combination (Fig. 3-5B). Collectively, our data indicate that simultaneous genotoxic and mitochondrial proteotoxic stresses triggered by the DOX-gamitrinib combination can synergistically induce the transcription factor CHOP, which in turn increases Bim expression leading to the induction of cell death. Bim transcription was elevated, but expression of other Bcl-2 family proteins, such as Bcl-2, Puma, and Noxa, was not affected by the drug combination (Figure 3-6). Expression of death receptor 5 (DR5) was elevated by the drug combination in a CHOP-dependent manner (Figure 3-6) as described previously [28], while procaspase-8, recruited to the death inducing signaling complex (DISC) after DR5 activation [21], was not cleaved at all (Figure 3-6). These data suggest the crucial role of Bim expression in the drug combination.

Gamitrinib and DOX combination treatment enhances mitochondrial localization of Bim and Bax.

In contrast to 22Rv1 cells, the drug combination did not induce CHOP expression in HeLa and MDA-MB-231 cells (Fig. 3-7A). In HeLa cells, knockdown of JNK compromised the enhanced cytotoxicity of the drug combination (Fig. 3-7B) whereas knockdown of CHOP did not affect the drug synergism. To confirm proteosome degradation of CHOP or Bim, we checked the expression in presence or absence of MG132, proteosome inhibitor, and observed that CHOP and Bim protein were degraded on combination drug treatment (Fig. 3-8A). These data suggest that there are context-dependent disparate stress responses to the drug combination, and the

JNK pathway, but not CHOP, can be critically involved in the synergistic combination effect in certain cancer cell types. Previous studies have shown that JNK can activate Bim through phosphorylation to trigger Bax-dependent mitochondrial apoptosis [29-32]. Phosphorylated Bim was detectable in HeLa and MDA-MB-231 cells, but not in 22Rv1 (Fig. 3-5A and 7A). Treatment with the drug combination caused increased accumulation of Bim and Bax in the mitochondria, which was significantly reduced by the JNK inhibitor SP600125 (Fig. 3-8C, left). Bim that accumulated in mitochondria was a slow-migrating phospho-form of the protein (Fig.3-8C, right panel). The combination effect was compromised by treatment with Bim siRNA (Fig. 3-7C), further supporting the important role of the proapoptotic Bcl-2 protein in the drug-induced stress response [33]. Collectively, these data indicate that the DOX-gamitrinib combination enhances JNK-mediated Bim phosphorylation, which triggers translocation of Bax to the mitochondria and augments mitochondrial apoptosis.

Drug combination treatment effectively inhibited tumor growth in vivo

We further investigated the efficacy of the drug combination in vivo using two xenograft models for prostate and breast cancer. Firstly, gamitrinib has shown anticancer activity as a single agent against prostate cancers in vivo[11, 13, 14, 34], therefore we examined the anticancer activity of gamitrinib in the presence of DOX using a prostate cancer xenograft model with the hormone-independent relapsed human prostate cancer cell line 22Rv1[35, 36]. Single treatment with gamitrinib or DOX resulted in a slight reduction in tumor volume, whereas combination treatment dramatically suppressed tumor growth (Fig. 3-9A). Secondly, DOX is frequently used to treat early and metastatic breast cancers in the clinic [37, 38]; therefore we tested the effect of the drug combination on an orthotopic xenograft model with the triple negative (ER-negative, PR-negative, and no HER2 overexpression) metastatic breast cancer cell line MDA-MB-231 [39]. The tumor growth was strongly inhibited by the drug combination but not by single agent treatment (Fig. 3-9B). Histologic analysis of organs did not show any prominent differences among the groups except for the heart (Fig. 3-10A and 11), and there was a marginal reduction in mouse weight with the combination treatment (2.5% loss of body weight at the end of the experiment compared with the start).

In vivo cardiotoxic side effects and mode of action of the drug combination.

A close examination of heart tissues from the treated mice showed a cardiotoxic phenotype of cytoplasmic vacuolization with similar severity for DOX alone and in combination treatment (Fig. 3-10A). The serum creatine phosphokinase (CPK) level was measured as an index of

72

cardiotoxicity [40, 41] at the end of the experiment (Fig. 3-10B). DOX treatment alone increased the level of CPK; this increase was reduced with the combination treatment, but the difference between single and combination treatment was not significant (Fig. 3-10B). These data suggest that the DOX-induced cardiotoxicity is not aggravated by the drug combination. Next, we analyzed the mechanism underlying the activity of the drug combination in vivo. Consistent with the in vitro data, the drug combination synergistically increased the phosphorylation of JNK in whole tumor tissue extracts (Fig. 3-9C) and the accumulation of Bim and Bax in mitochondrial fractions (Fig. 3-9D).

3-4. Discussion

In this study, DOX, one of the most widely used anticancer drugs, was combined with the mitochondria-stress inducer, gamitrinib, to exploit disparate stress pathways in cancer therapy. Combination of these agents synergistically increased cancer-specific cytotoxic activity through stimulation of JNK and CHOP stress signalling pathways and activation of the proapoptotic protein Bim. Importantly, the drug combination did not aggravate the well-known cardiotoxic side effects of DOX in vitro or in vivo. Both gamitrinib[13, 14] and DOX [33, 35] have previously been shown to activate JNK and CHOP signalling pathways. Turning on these stress pathways activates the proapoptotic Bcl-2 family protein Bim through elevated gene expression and/or phosphorylation, leading to mitochondrial cell death [37, 42]. As a result of simultaneous stimulatory effects on the stress pathways by DOX and gamitrinib, the drug combination is able to further increase the amount of Bim protein (through CHOP elevation) and/or mitochondrial accumulation of Bim (through JNK activation), leading to enhanced mitochondrial accumulation of Bax and synergistic induction of apoptotic cell death. Combining cancer drugs with disparate mechanisms of action is a feasible strategy to increase therapeutic efficacy while avoiding unacceptable side effects of the drugs [38]. In this regard, combined treatment of DOX with other cancer drugs has been examined before and some of these combinations, for example with taxane or trastuzumab, have shown much more severe cardiotoxic side effects even at lower cumulative doses [16]. The combination of DOX and gamitrinib, however, did not aggravate cytotoxicity to cardiomyocytes in vitro or in vivo. We presume that cardiomyocytes are relatively resistant to gamitrinib because they are less dependent on mitochondrial chaperone functions to maintain protein homeostasis and cope with stresses under normal

physiologic conditions. In conclusion, combined treatment of DOX and gamitrinib showed synergistically enhanced cancer-specific toxicity without aggravating cardiotoxic side effects. The drug combination can realize the full potential of the anticancer activity of the individual drugs and broaden the application of the drugs to various cancer types.

Cell line	Origin	Drug ratio DOX : Gami	CI at ED_{50}	CI at ED_{75}
HeLa	cervix	1 : 5	0.33 ± 0.03	0.41 ± 0.03
22Rv1	prostate	1 : 10	0.81 ± 0.18	0.53 ± 0.09
A172	brain	1 : 10	0.45 ± 0.28	0.76 ± 0.27
ACHN	kidney	1 : 2	0.34 ± 0.11	0.20 ± 0.07
SK-Hep1	liver	1 : 5	0.31 ± 0.05	0.29 ± 0.03
NCI-H460	lung	1 : 5	0.32 ± 0.19	0.45 ± 0.29
SK-OV3	ovary	1 : 1	0.58 ± 0.13	0.95 ± 0.28
MDA-MB-231	breast	5 : 1	0.73 ± 0.27	0.46 ± 0.24

NOTE: Cancer cells were treated with various concentrations of drugs at a fixed ratio as indicated. CI values at 50% (ED_{50}) and 75% effective doses (ED_{75}) were calculated from isobologram analysis. Data are the mean $\pm$ 1.96 s.d. (95% confidence interval) of two independent experiments performed in triplicate.

Table 3-1. Combination Index (CI) values at ED50 and ED75 in various cancer cell lines

A

B

C

D
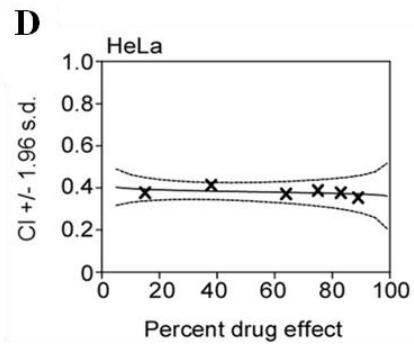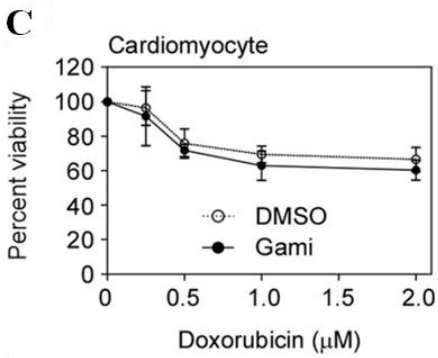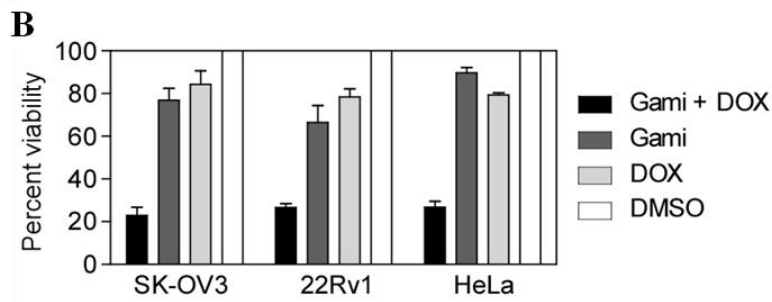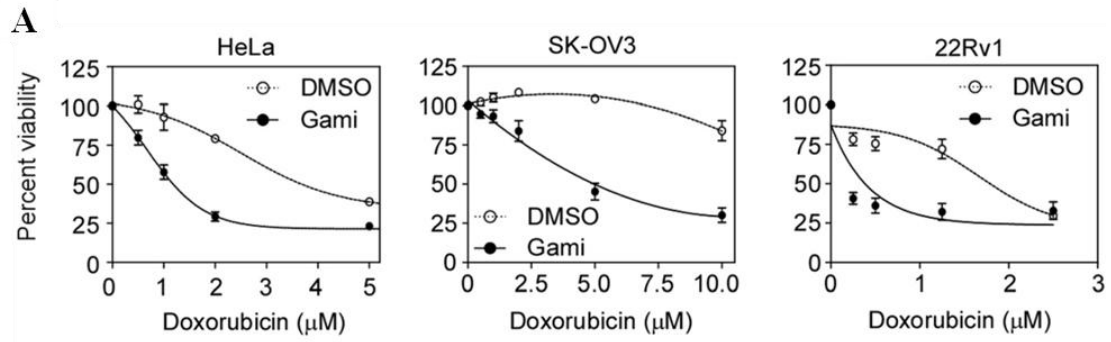
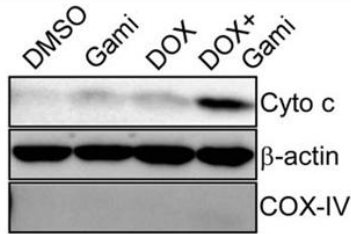**Figure 3-1. Combination treatment with DOX and gamitrinib**

(A) Gamitrinib sensitizes cancer cells to DOX treatment. HeLa, SK-OV3, and 22Rv1 cells were treated with various on centrations of DOX in the absence (open circles) or presence of 5 μM, 10 μM, and 2.5 μM gamitrinib (closed circles), respectively, for 24 hours. Cell viability was analyzed by MTT assay. Percent viability was expressed as a percentage relative to 0 μM DOX-treatment. (B) DOX and gamitrinib were added as a single agent or in combination to the following cancer cells: SKOV3 (10uM/10uM gamitrinib), 22Rv1 (0.25uM DOX/2.5uM gamitrinib), and HeLa (2uM DOX/5uM gamitrinib). Cells were treated with the drugs for 24hours and analyzed by MTT assay. The cell viability compared with that of DMSO treated control was plotted as a percentage. Data are the mean±SEM of two independent experiments performed in triplicate. (C) Effect of combination treatment on cardiomyocytes. Mouse primary cardiomyocytes were treated in the absence (open circles) or presence (closed circles) of 5 μM gamitrinib for 24 hours and analyzed by MTT assay. (D) Graphical representation of combination index (CI) for HeLa cells. The MTT data were analyzed using CalcuSyn software to generate CI values. The 95% confidence interval of CI (mean ± 1.96 × standard deviation) is depicted as dotted lines.
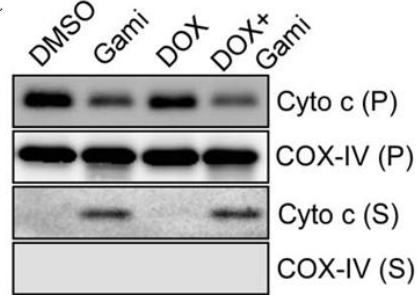
A

B

C
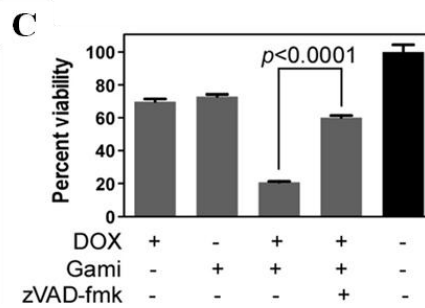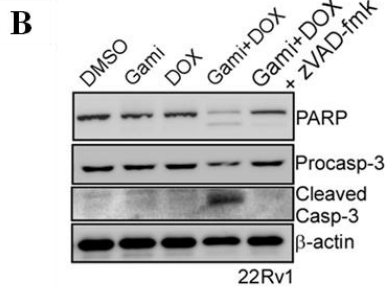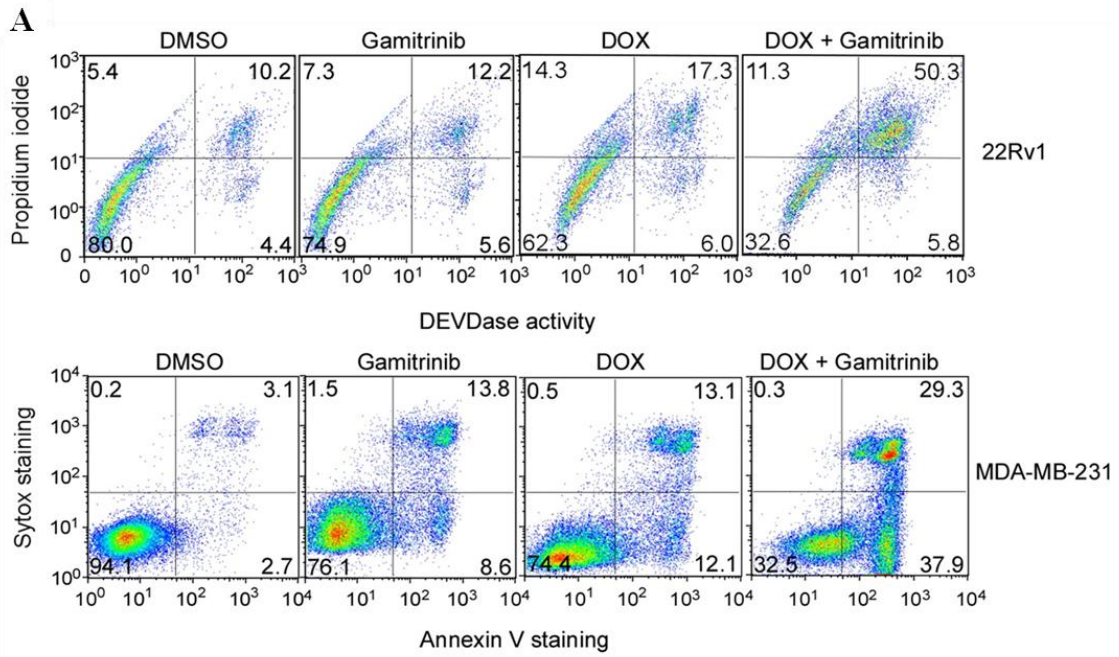
Figure 3-2. Induction of apoptosis by combination treatment

(A) Cell death analysis. 22Rv1 and MDA-MB-231 cells were treated with 0.25 μM DOX/2.5 μM gamitrinib and 10 μM DOX/5 μM gamitrinib, respectively, as single agents or combination treatment for 24 hours, and analyzed for propidium iodide, Sytox, Annexin V staining, and DEVDase activity by flow cytometry. The percentage of cells in each quadrant is indicated. (B) Caspase activation by the drug combination. 22Rv1 cells were treated with 0.25 μM DOX and 2.5 μM gamitrinib, and analyzed by western blotting. The pan-caspase inhibitor zVAD-fmk was used at a concentration of 10 μM. (C) Effect of caspase inhibitor on the drug combination treatment. 22Rv1 cells were treated with 0.25 μM DOX, 2.5 μM gamitrinib, and 10 μM zVAD-fmk as indicated and analyzed by MTT assay. Percent viability compared with DMSO-treated control is shown. Data are the mean ± SEM of duplicated three independent experiments
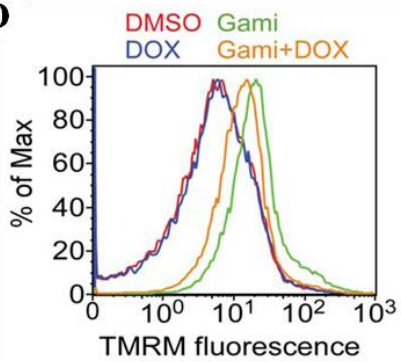
A

DMSO Gami DOX DOX+Gami

Cyto c

β-actin

COX-IV

B

DMSO — 84.6 — 14.3

Gamitrinib — 90.4 — 9.22

DOX — 67.5 — 31.6

DOX + Gamitrinib — 40.9 — 58.7

Red Fluorescence

10^3 10^2 10^1 10^0

Green Fluorescence

1 10^1 10^2 10^3 10^1 10^2 10^3

C

DMSO Gami DOX DOX+Gami

Cyto c (P)

COX-IV (P)

Cyto c (S)

COX-IV (S)

D

DMSO Gami
DOX Gami+DOX

% of Max

100 80 60 40 20 0

0 10^0 10^1 10^2 10^3

TMRM fluorescence

E

Fluorescence intensity

2500 2000 1500 1000 500 0

Mitotracker
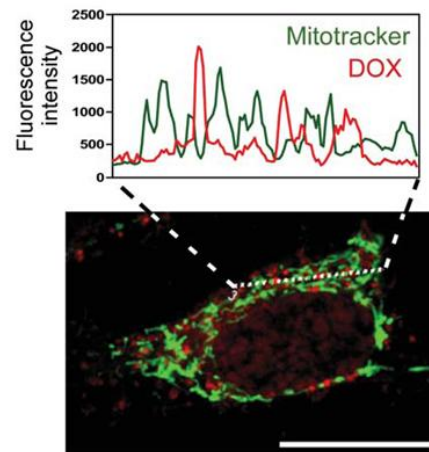DOX
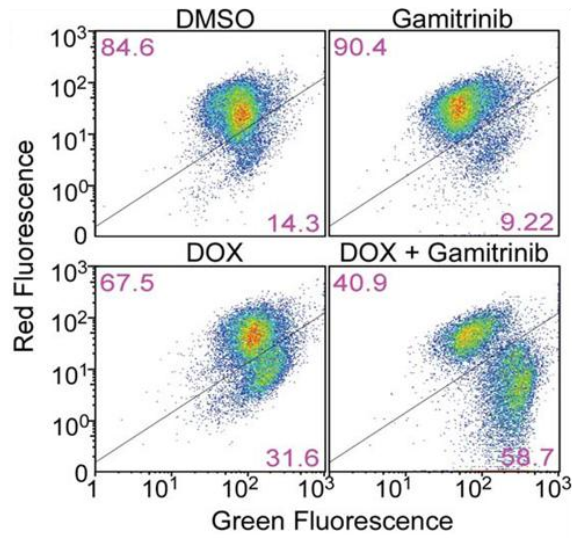
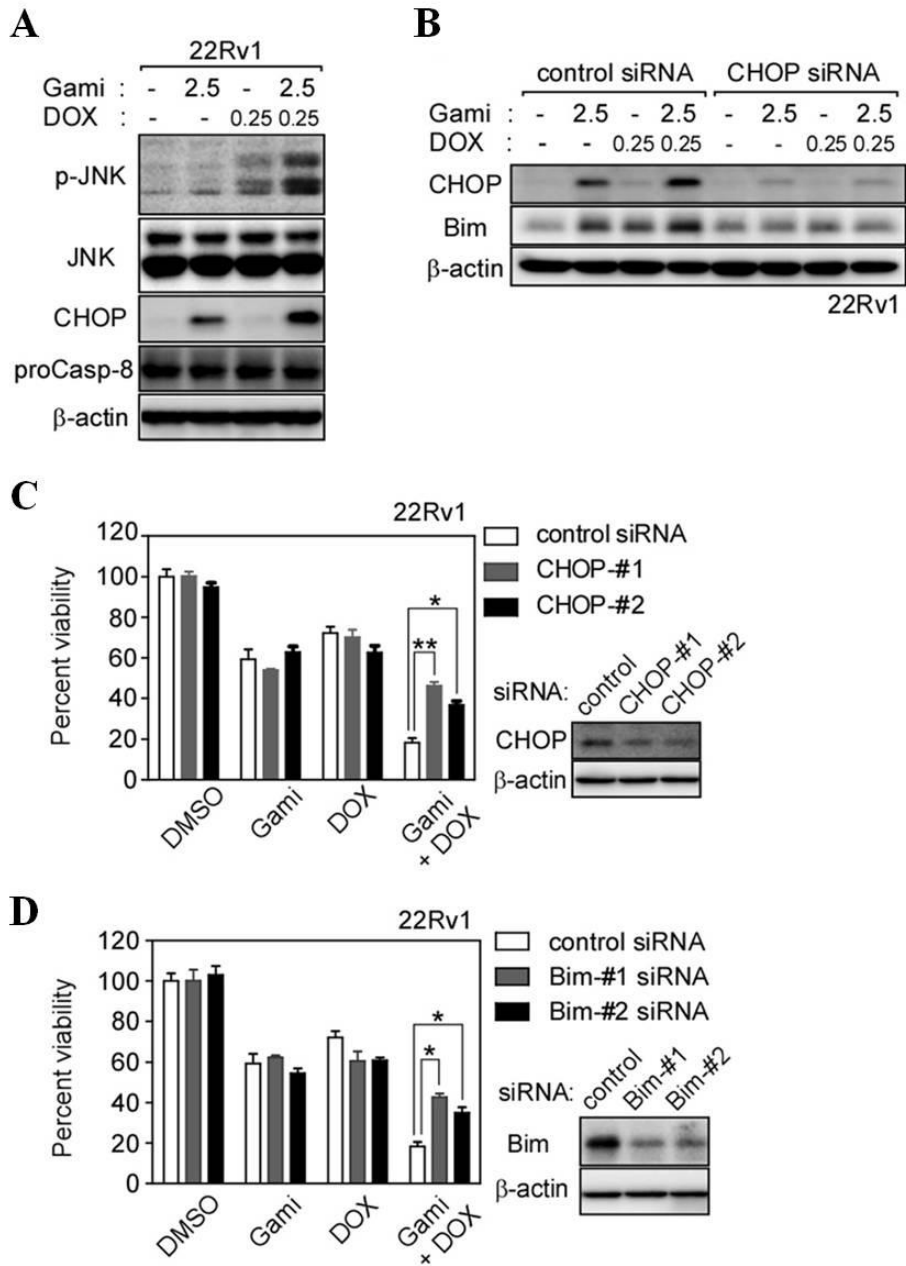**Figure 3-3. Effect of DOX on cancer cell mitochondria**

(A) Discharged cytochrome c in cytoplasm. HeLa cells were treated with 5uM gamitrinib and 0.5uM DOX alone or in combination for 24 hours and cytosolic fractions were analyzed by western blotting. (B) JC-1 staining of HeLa cells. Cells were treated as in (A) labelled by JC-1 staining[43], and analyzed by flow cytometry. The percentage of lost membrane potential is indicated (C) Cytochrome c release from isolated mitochondria. HeLa mitochondria were treated with 10uM gamitrinib and 1uM DOX alone or in combination. After centrifugation, the mitochondrial pellet (P) and supernatant (S) were analyzed by western blotting. (D) Membrane potential of isolated mitochondria. Mitochondria isolated from HeLa cells were treated with the drugs at the same concentration as in (C), stained with TMRM and analyzed by flow cytometry. (E) Confocal imaging of DOX localization. HeLa cells with stable overexpression of Bcl-2 were labelled with Mitotracker (green), treated with 10uM DOX (red) for 24hours and analyzed by confocal microscopy. Fluorescence intensity of the cytoplasm was further analyzed as a histogram (upper panel). White bar, 10um
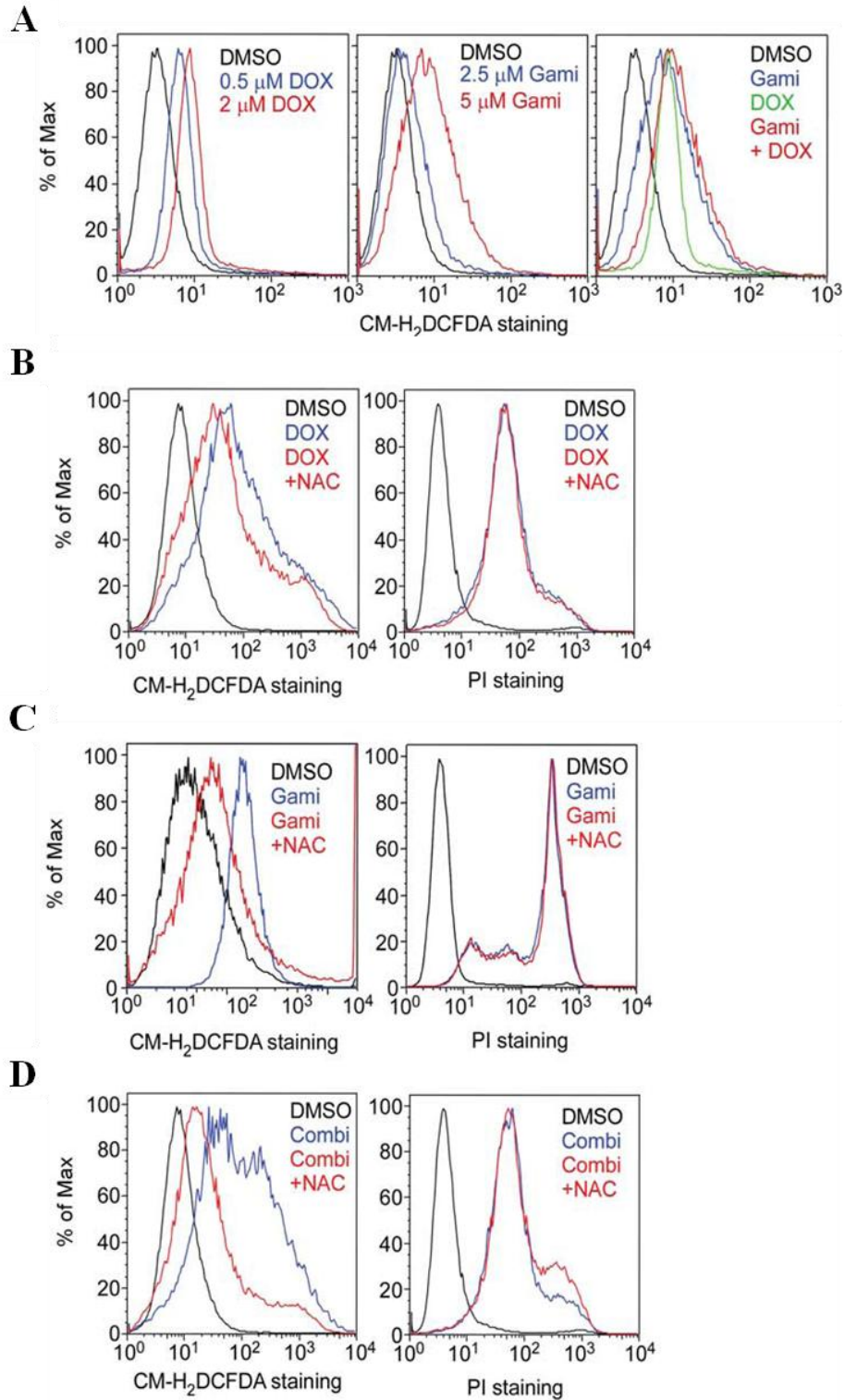
**Figure 3-4. Effect of reactive oxygen species on the drug combination effect**

(A) ROS production in HeLa cells. CM-H2DCFDA-labeled cells were treated with DOX and gamitrinib as indicated for 24 hours and anlayzed by flow cytometry. (B) Effect of ROS scavenger on DOX cytotoxicity. HeLa cells were treated with 5uM DOX in the presence or absence of 20mM N-acetylcysteine(NAC) for 24 hours. (C) Effect of ROS scavenger on gamitrinib cytotoxicity. HeLa cells were incubated with 2uM gamitrinib in the absence or presence of 20mM NAC for 24 hours. (D) Effect of ROS-scavenger on drug combination cytotoxicity. HeLa cells were co-treated with 5uM DOX and 2uM gamitrinib for 24 hours. In (A)-(D), cells stained with CM-H2DCFDA and propidium iodide were analyzed by flow cytometry.

A

22Rv1

Gami : - 2.5 - 2.5
DOX : - - 0.25 0.25

p-JNK

JNK

CHOP

proCasp-8

β-actin

B

control siRNA   CHOP siRNA

Gami : - 2.5 - 2.5   - 2.5 - 2.5
DOX : - - 0.25 0.25   - - 0.25 0.25

CHOP

Bim

β-actin

22Rv1

C

22Rv1

□ control siRNA
■ CHOP-#1
■ CHOP-#2

Percent viability

120
100
80
60
40
20
0

DMSO   Gami   DOX   Gami + DOX

*
**

siRNA: control CHOP-#1 CHOP-#2

CHOP

β-actin

D

22Rv1

□ control siRNA
■ Bim-#1 siRNA
■ Bim-#2 siRNA

Percent viability

120
100
80
60
40
20
0

DMSO   Gami   DOX   Gami + DOX

*
*

siRNA: control Bim-#1 Bim-#2

Bim

β-actin

84

Figure 3-5. Effect of drug combination on the expression of CHOP and Bim

(A) CHOP induction and JNK phosphorylation. 22Rv1 cells were treated with DOX and gamitrinib alone or in combination as indicated and the whole cell lysate was analyzed by western blotting. (B) CHOP knockdown and Bim expression. After treatment with control or CHOP-#1 siRNAs, 22Rv1 cells were incubated with DOX and gamitrinib alone or in combination for 24 hours as indicated and cell extracts were analyzed by western blotting. (C) CHOP knockdown. 22Rv1 cells were treated with control or CHOP siRNAs for 24 hours and then with 0.25 μM DOX and 2.5 μM gamitrinib for 24 hours as indicated. The cell viability was analyzed by MTT assay. Data are mean ± SEM of two independent experiments performed in triplicate.*, $p < 0.05$; **, $p < 0.004$. (D) Effect of combination drug treatment after Bim silencing. After treatment with Bim siRNA, 22Rv1 cells were incubated with 0.25 μM DOX and 2.5 μM gamitrinib for 24 hours as indicated and cell viability was analyzed by MTT assay. Data are mean ± SEM of two independent experiments performed in triplicate. *, $p < 0.05$.
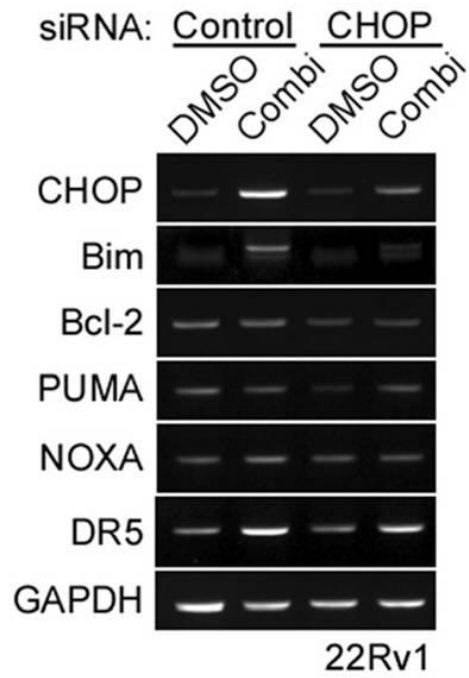
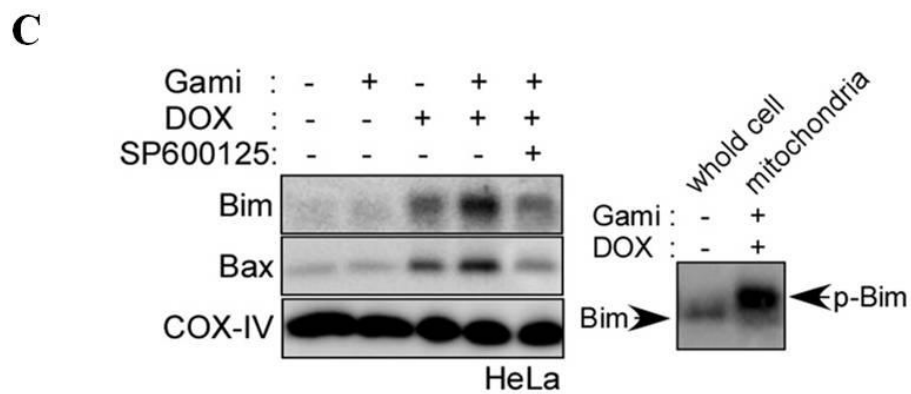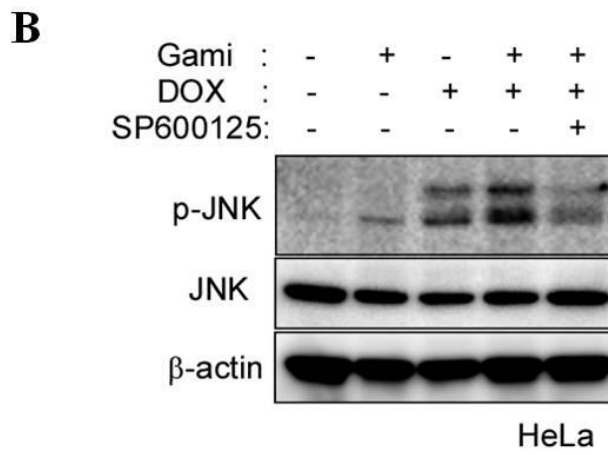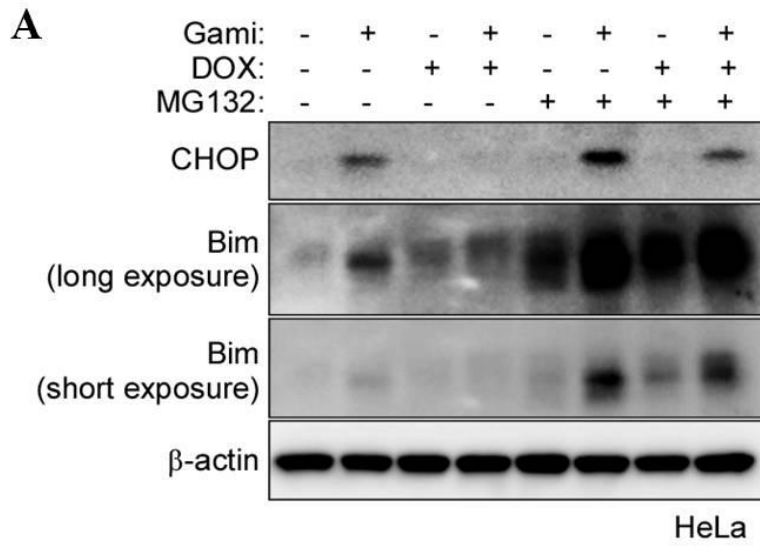**Figure 3-6. Expression of Bcl-2 family proteins and DR5**

22Rv1 cells were treated with 0.25 μM DOX and 2.5 μM gamitrinib for 24 hours as indicated. After extraction and reverse transcription of RNA, the cDNA of interest was amplified by PCR.
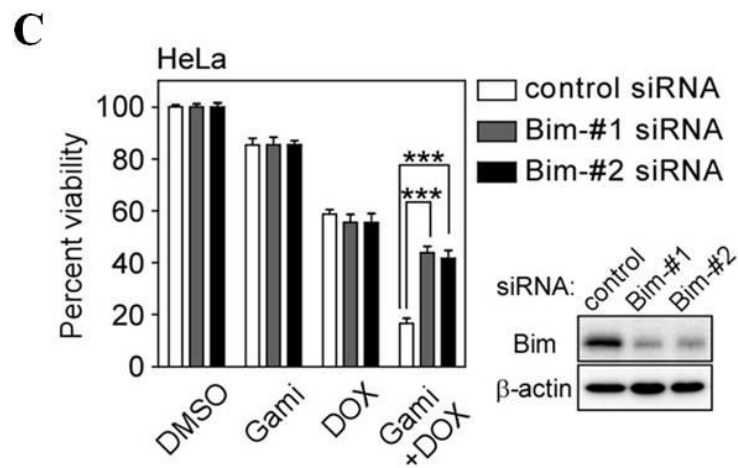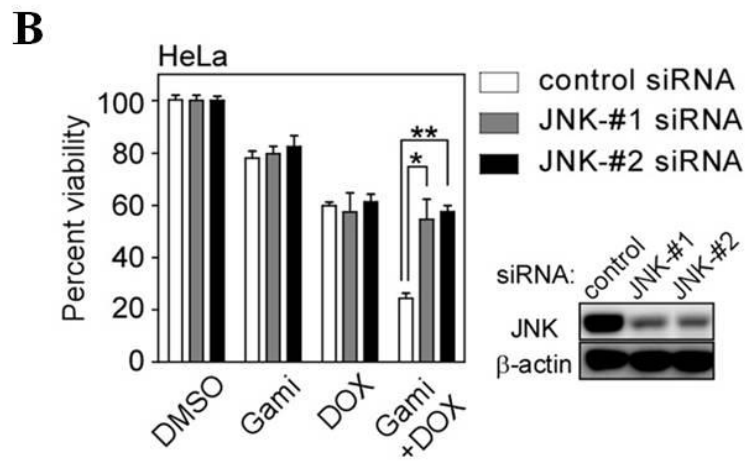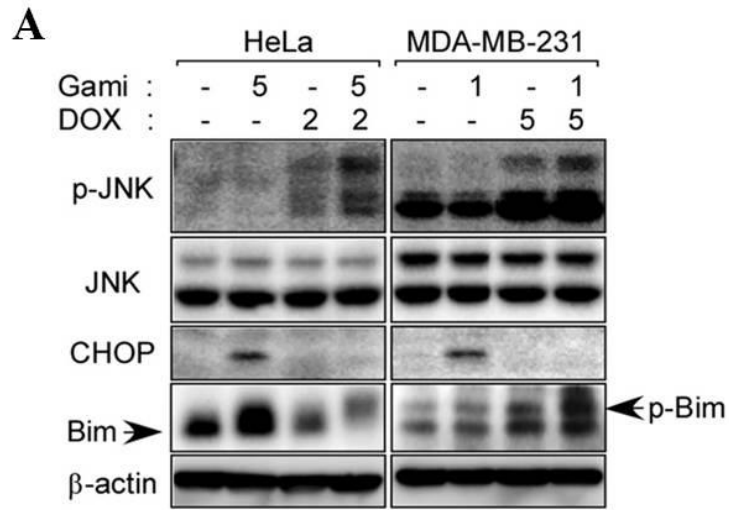
Figure 3-7. Enhancement of JNK-mediated Bim phosphorylation by drug combination treatment

(A) Phosphorylation of JNK and Bim. HeLa and MDA-MB-231 cells were treated with DOX and gamitrinib alone or in combination for 24 hours as indicated and analyzed by western blotting. (B) JNK silencing compromises the synergistic effect of combination treatment. HeLa cells were treated with JNK siRNA prior to treatment with 2 μM DOX and 5 μM gamitrinib as indicated for 24 hours. Cell viability was analyzed by MTT assay. Data are mean ± SEM of two independent experiments performed in triplicate. *, $p < 0.02$; **, $p = 0.0004$. (C) Effect of Bim silencing. After treatment with control or Bim-specific siRNAs, HeLa cells were incubated with 2 μM DOX and 5 μM gamitrinib for 24 hours as indicated and analyzed by MTT assay. Data show mean ± SEM of two independent experiments performed in triplicate. ***, $p < 0.0001$.

A

Gami:	-	+	-	+	-	+	-	+
DOX:	-	-	+	+	-	-	+	+
MG132:	-	-	-	-	+	+	+	+

CHOP

Bim
(long exposure)

Bim
(short exposure)

β-actin

HeLa

B

Gami :	-	+	-	+	+
DOX :	-	-	+	+	+
SP600125:	-	-	-	-	+

p-JNK

JNK

β-actin

HeLa

C

Gami :	-	+	-	+	+
DOX :	-	-	+	+	+
SP600125:	-	-	-	-	+

Bim

Bax

COX-IV

HeLa

|	whold cell	mitochondria
Gami :	-	+
DOX :	-	+

Bim ➤   ◄ p-Bim

Figure 3-8. Effect of MG132 and SP600125

(A) MG132 effect on Bim and CHOP expression. HeLa cells were treated with 5 μM gamitrinib, 2 μM DOX, and 30 μM MG132 as indicated, and analyzed by western blotting. (B) Inhibition of JNK activity by SP600125. HeLa cells were treated with 5 μM gamitrinib, 2 μM DOX, or 10 μM SP600125 as indicated and analyzed by western blotting. The inhibition of JNK activity reduces phosphor-form (auto-phosphorylation) of the protein. (C) Mitochondrial accumulation of Bim and Bax. After treatment of HeLa cells with 5 μM gamitrinib, 2 μM DOX, or 10 μM SP600125 as indicated, mitochondria were fractionated and analyzed by western blotting (left). Bim phosphorylation in the whole cell extract and the mitochondrial fraction (right).
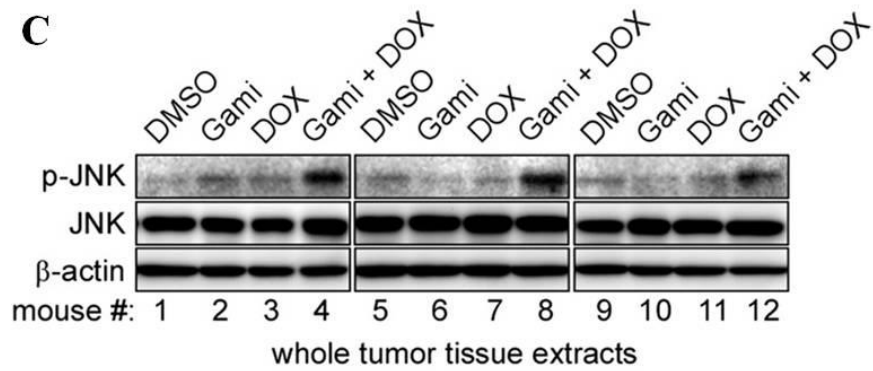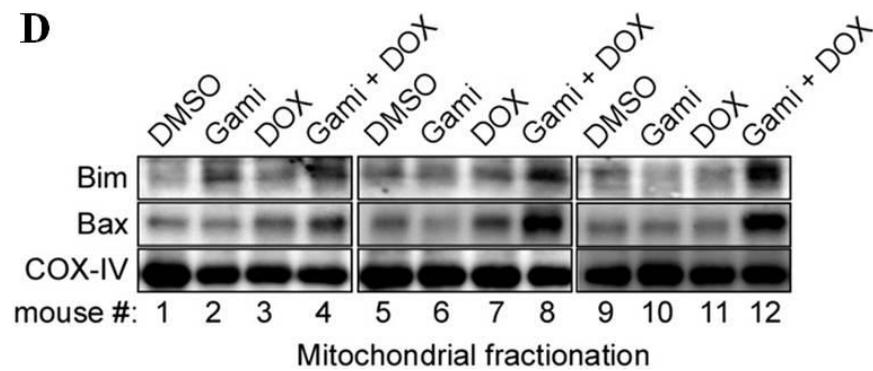
A

B

C

whole tumor tissue extracts

D

Mitochondrial fractionation
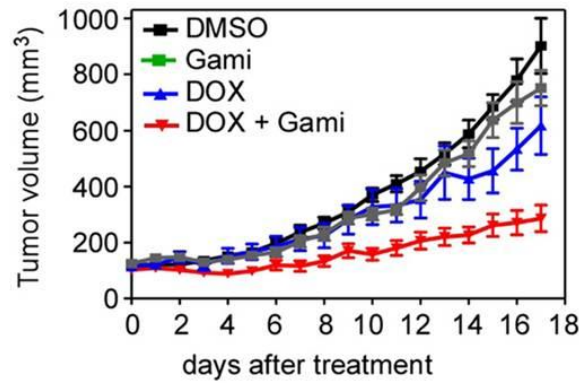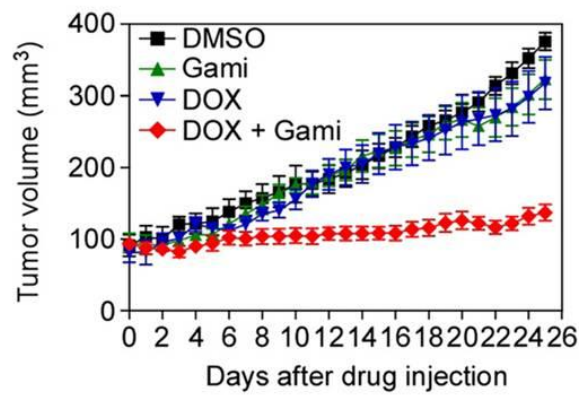
Figure 3-9. Drug combination effect in vivo

(A) Prostate cancer xenograft. 22Rv1 cells (7×10^6 cells) were injected subcutaneously into both flanks of nude mouse (5 mice/group). After tumors were established, mice were treated twice a week with 3 mg/kg DOX i.v. and 10 mg/kg gamitrinib i.p. as single agents or in combination. (B) Orthotopic xenograft of breast cancer cells. MDA-MB-231 cells (1×10^7 cells) were grown in mammary fat pads of nude mouse (3 mice/group). Mice were treated twice a week with 3 mg/kg DOX i.v. and 10 mg/Kg gamitrinib i.p. as single agents or in combination. (C) JNK phosphorylation in tumor tissue. Tumor samples collected from the xenograft mice in (B) were analyzed by western blotting. (D) Accumulation of Bim and Bax in mitochondria. Mitochondrial fractionations isolated from the tumors in (B) were analyzed by western blotting.
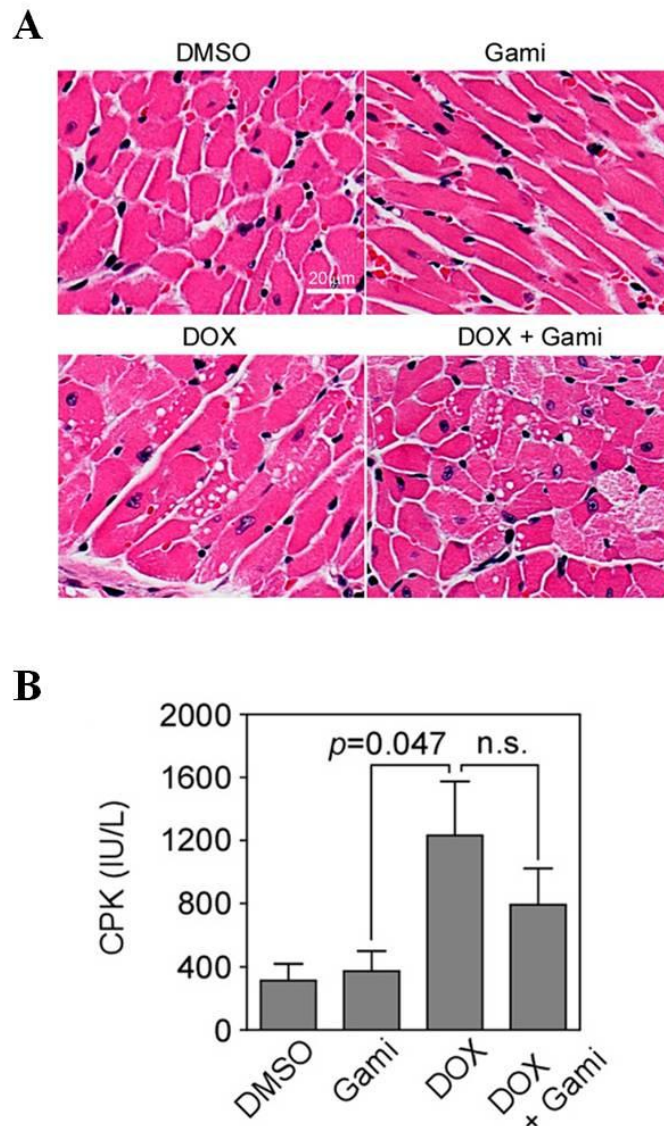
Figure 3-10. Side effect on combination drug treatment

(A) Hematoxylin and eosin staining of heart tissues. At the end of the experiment in (Fig 3-9B), heart ventricles were collected from the mice and analyzed by hematoxylin and eosin staining. Magnification, 200×. (B) Serum creatine phosphokinase activity. Blood was drawn from mice at the end of experiments in (Fig 3-9B) and serum creatine phosphokinase (CPK) activity was measured. n.s., p > 0.05.
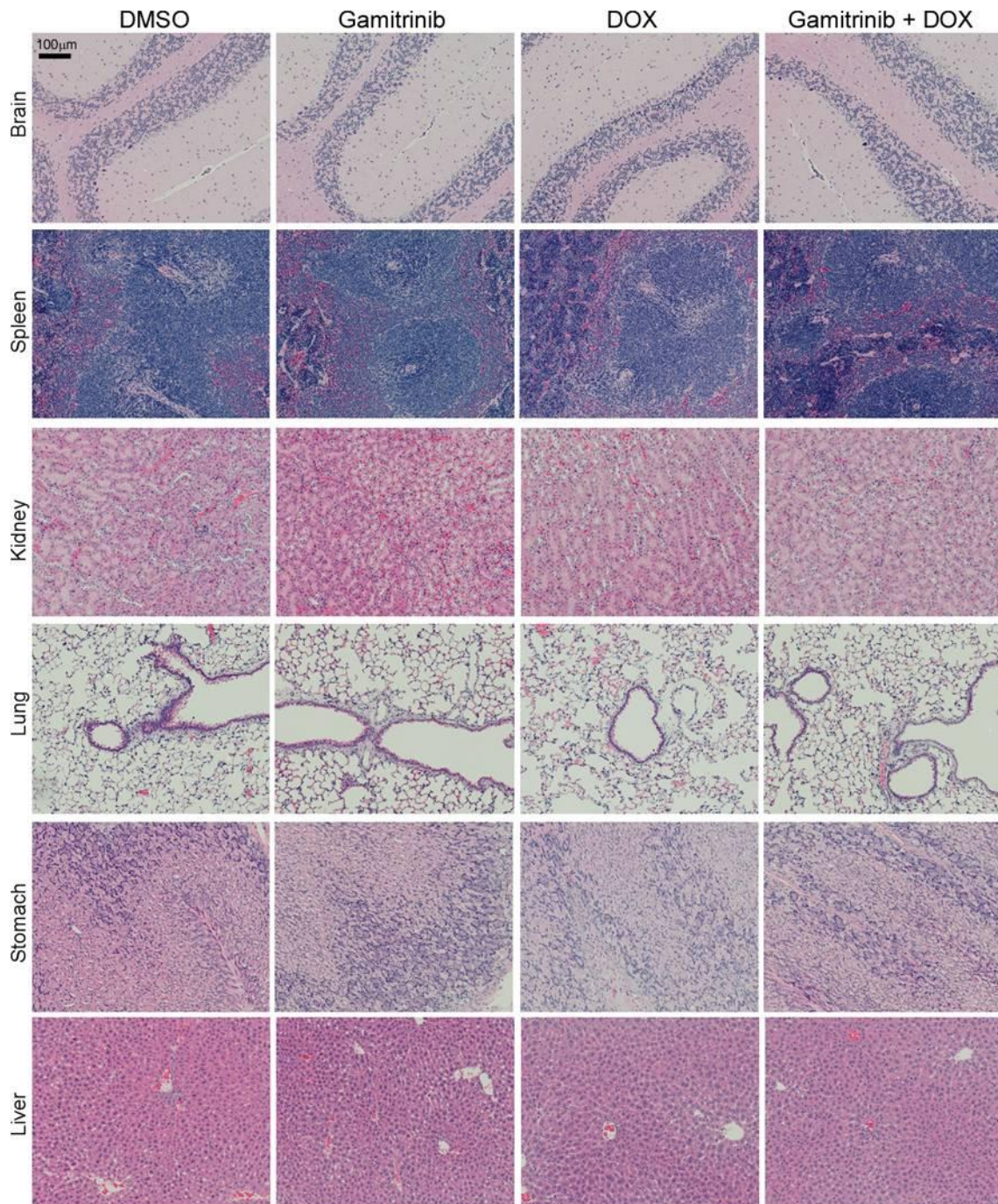
Figure 3-11. Hematoxylin and eosin staining of mouse organs [44]

At the end of the experiment shown in Fig 3-9B, mouse organs were harvested, stained with hematoxylin and eosin, and analyzed under a light microscope. Scale bar, 100 um

3-5. References

1. Taipale, M., D.F. Jarosz, and S. Lindquist, *HSP90 at the hub of protein homeostasis: emerging mechanistic insights.* Nat Rev Mol Cell Biol, 2010. **11**(7): p. 515-28.

2. Trepel, J., et al., *Targeting the dynamic HSP90 complex in cancer.* Nat Rev Cancer, 2010. **10**(8): p. 537-49.

3. Kang, B.H., et al., *Regulation of tumor cell mitochondrial homeostasis by an organelle-specific Hsp90 chaperone network.* Cell, 2007. **131**(2): p. 257-70.

4. Felts, S.J., et al., *The hsp90-related protein TRAP1 is a mitochondrial protein with distinct functional properties.* J Biol Chem, 2000. **275**(5): p. 3305-12.

5. Sciacovelli, M., et al., *The mitochondrial chaperone TRAP1 promotes neoplastic growth by inhibiting succinate dehydrogenase.* Cell Metab, 2013. **17**(6): p. 988-99.

6. Yoshida, S., et al., *Molecular chaperone TRAP1 regulates a metabolic switch between mitochondrial respiration and aerobic glycolysis.* Proc Natl Acad Sci U S A, 2013. **110**(17): p. E1604-12.

7. Chae, Y.C., et al., *Landscape of the mitochondrial Hsp90 metabolome in tumours.* Nat Commun, 2013. **4**: p. 2139.

8. Caino, M.C., et al., *Metabolic stress regulates cytoskeletal dynamics and metastasis of cancer cells.* J Clin Invest, 2013. **123**(7): p. 2907-20.

9. Matassa, D.S., et al., *Translational control in the stress adaptive response of cancer cells: a novel role for the heat shock protein TRAP1.* Cell Death Dis, 2013. **4**: p. e851.

10. Kang, B.H., et al., *Combinatorial drug design targeting multiple cancer signaling networks controlled by mitochondrial Hsp90.* J Clin Invest, 2009. **119**(3): p. 454-64.

11. Kang, B.H., *TRAP1 regulation of mitochondrial life or death decision in cancer cells and mitochondria-targeted TRAP1 inhibitors.* BMB Rep, 2012. **45**(1): p. 1-6.

12. Kang, B.H. and D.C. Altieri, *Compartmentalized cancer drug discovery targeting mitochondrial Hsp90 chaperones.* Oncogene, 2009. **28**(42): p. 3681-8.

13. Kang, B.H., et al., *Preclinical characterization of mitochondria-targeted small molecule hsp90 inhibitors, gamitrinibs, in advanced prostate cancer.* Clin Cancer Res, 2010. **16**(19): p. 4779-88.

14. Kang, B.H., et al., *Targeted inhibition of mitochondrial Hsp90 suppresses localised and metastatic prostate cancer growth in a genetic mouse model of disease.* Br J Cancer, 2011. **104**(4): p. 629-34.

15. Kroemer, G., L. Galluzzi, and C. Brenner, *Mitochondrial membrane permeabilization in*

cell death. Physiol Rev, 2007. **87**(1): p. 99-163.

16.   Siegelin, M.D., et al., *Exploiting the mitochondrial unfolded protein response for cancer therapy in mice and human cells.* J Clin Invest, 2011. **121**(4): p. 1349-60.

17.   Minotti, G., et al., *Anthracyclines: molecular advances and pharmacologic developments in antitumor activity and cardiotoxicity.* Pharmacol Rev, 2004. **56**(2): p. 185-229.

18.   Wang, J.C., *DNA topoisomerases.* Annu Rev Biochem, 1996. **65**: p. 635-92.

19.   Smith, L.A., et al., *Cardiotoxicity of anthracycline agents for the treatment of cancer: systematic review and meta-analysis of randomised controlled trials.* BMC Cancer, 2010. **10**: p. 337.

20.   Lefrak, E.A., et al., *A clinicopathologic analysis of adriamycin cardiotoxicity.* Cancer, 1973. **32**(2): p. 302-14.

21.   Chou, T.C., *Drug Combination Studies and Their Synergy Quantification Using the Chou-Talalay Method.* Cancer Research, 2010. **70**(2): p. 440-446.

22.   Chou, T.C., *Theoretical basis, experimental design, and computerized simulation of synergism and antagonism in drug combination studies.* Pharmacological Reviews, 2006. **58**(3): p. 621-681.

23.   Kim, S.J., et al., *Doxorubicin prevents endoplasmic reticulum stress-induced apoptosis.* Biochemical and Biophysical Research Communications, 2006. **339**(2): p. 463-468.

24.   Lu, M., et al., *Prevention of Doxorubicin cardiopathic changes by a benzyl styryl sulfone in mice.* Genes Cancer, 2011. **2**(10): p. 985-92.

25.   Panaretakis, T., et al., *Doxorubicin requires the sequential activation of caspase-2, protein kinase C delta, and c-Jun NH2-terminal kinase to induce apoptosis.* Molecular Biology of the Cell, 2005. **16**(8): p. 3821-3831.

26.   Haynes, C.M. and D. Ron, *The mitochondrial UPR - protecting organelle protein homeostasis.* J Cell Sci, 2010. **123**(Pt 22): p. 3849-55.

27.   Puthalakath, H., et al., *ER stress triggers apoptosis by activating BH3-only protein Bim.* Cell, 2007. **129**(7): p. 1337-1349.

28.   Ewer, M.S. and S.M. Lippman, *Type II chemotherapy-related cardiac dysfunction: time to recognize a new entity.* J Clin Oncol, 2005. **23**(13): p. 2900-2.

29.   Lei, K. and R.J. Davis, *JNK phosphorylation of Bim-related members of the Bcl2 family induces Bax-dependent apoptosis.* Proceedings of the National Academy of Sciences of the United States of America, 2003. **100**(5): p. 2432-2437.

30.   Putcha, G.V., et al., *JNK-mediated BIM phosphorylation potentiates BAX-dependent*

apoptosis. Neuron, 2003. **38**(6): p. 899-914.

31. Okuno, S., et al., *The c-Jun N-terminal protein kinase signaling pathway mediates Bax activation and subsequent neuronal apoptosis through interaction with Bim after transient focal cerebral ischemia.* Journal of Neuroscience, 2004. **24**(36): p. 7879-7887.

32. Sunayama, J., et al., *JNK antagonizes Akt-mediated survival signals by phosphorylating 14-3-3.* Journal of Cell Biology, 2005. **170**(2): p. 295-304.

33. Youle, R.J. and A. Strasser, *The BCL-2 protein family: opposing activities that mediate cell death.* Nat Rev Mol Cell Biol, 2008. **9**(1): p. 47-59.

34. Leav, I., et al., *Cytoprotective mitochondrial chaperone TRAP-1 as a novel molecular target in localized and metastatic prostate cancer.* Am J Pathol, 2010. **176**(1): p. 393-401.

35. Sramkoski, R.M., et al., *A new human prostate carcinoma cell line, 22Rv1.* In Vitro Cell Dev Biol Anim, 1999. **35**(7): p. 403-9.

36. Nagabhushan, M., et al., *CWR22: The first human prostate cancer xenograft with strongly androgen-dependent relapsed strains both in vivo and in soft agar.* Cancer Research, 1996. **56**(13): p. 3042-3046.

37. Gogineni, K. and A. DeMichele, *Current approaches to the management of Her2-negative metastatic breast cancer.* Breast Cancer Research, 2012. **14**(2).

38. Liedtke, C., et al., *Response to neoadjuvant therapy and long-term survival in patients with triple-negative breast cancer.* J Clin Oncol, 2008. **26**(8): p. 1275-81.

39. Brinkley, B.R., et al., *Variations in Cell Form and Cytoskeleton in Human-Breast Carcinoma-Cells Invitro.* Cancer Research, 1980. **40**(9): p. 3118-3129.

40. Kang, Y.J., Y. Chen, and P.N. Epstein, *Suppression of doxorubicin cardiotoxicity by overexpression of catalase in the heart of transgenic mice.* J Biol Chem, 1996. **271**(21): p. 12610-6.

41. Kang, Y.J., et al., *Overexpression of metallothionein in the heart of transgenic mice suppresses doxorubicin cardiotoxicity.* Journal of Clinical Investigation, 1997. **100**(6): p. 1501-1506.

42. Nagabhushan, M., et al., *CWR22: the first human prostate cancer xenograft with strongly androgen-dependent and relapsed strains both in vivo and in soft agar.* Cancer Res, 1996. **56**(13): p. 3042-6.

43. Zuliani, T., et al., *Sensitive and reliable JC-1 and TOTO-3 double staining to assess mitochondrial transmembrane potential and plasma membrane integrity: interest for cell death investigations.* Cytometry A, 2003. **54**(2): p. 100-8.

44.   Fischer, A.H., et al., *Hematoxylin and eosin staining of tissue and cell sections.* CSH Protoc, 2008. **2008**: p. pdb prot4986.

Conclusion

This study shows a new the function of mitochondrial Hsp90s regulating the calcium-mediated interplay between the permeability transition pore (PTP) in mitochondria and the ryanodine receptor (RyR) in the endoplasmic reticulum (ER). The two calcium channels, PTP and RyR, are coordinated to propagate and amplify calcium signal-evoking stress responses, which consequently increases susceptibility to additional organelle stresses. The pathway is very active in cancer cells unless mitochondrial Hsp90s are elevated to suppress it, and we have therefore exploited this to selectively kill cancer cells in vivo in this study. The mitochondrial Hsp90s plays a critical regulatory role in mitochondrial stress signalling and protects the cell by suppressing mitochondria-initiated, calcium-mediated stress signals in cancer cells. Though the calcium signal has been intensively studied so far, "mitochondria-initiated" calcium cross-talk between mitochondria (PTP) and the ER (RyR) has not been reported before. This will be appreciated not only as a novel calcium signaling pathway but also as a part of the largely unknown retrograde signaling from the mitochondria to nucleus. The sequential events including in PTP opening, RyR opening, ER calcium depletion and UPRER induce CHOP expression and sensitize cancer cells to cell death. We provide here a rationale for combination cancer therapeutics development lowering the cell death threshold exclusively in cancer cells by targeting the coordinated calcium pathway. The importance of the novel calcium signaling was further proved by exploiting combination cancer therapy. We found that doxorubicin (trade name Adriamycin) or Thapsigargin together with mitochondrial UPR inducer, G-TPP, showed strong synergism through the mitochondria and ER crosstalk. The rationale can be exploited to find effective and better multicomponent anticancer regimen combining antitumor drugs or even non-antitumor drugs, and thereby to benefit the cancer patients in the future.

Acknowledgements

학문에 대한 호기심과 열정으로 다소 늦게 시작했던 박사과정을 마치기까지 여러모로 도움을 주셨던 많은 분들께 진심으로 감사의 마음을 전합니다. 제일 먼저, 부족했던 저를 첫 제자로 받아주시고, 아낌없는 조언과 연구를 지도해 주신 강병헌 교수님께 진심으로 감사드립니다. 늘 한결 같은 마음으로 존경하며, 교수님의 연구에 대한 열정과 청렴함을 본받겠습니다. 그리고 바쁘신 일정에도 학위 논문 심사에 시간을 내주신 박찬영 교수님, 박태주 교수님, 이창욱 교수님, 백승훈 교수님께 진심으로 감사드립니다. 사랑하는 우리 가족, 힘든 과정을 견딜 수 있도록, 아낌없는 격려로 저를 믿고 지켜봐 주신 주신 아버지, 어머니께 진심으로 감사드리고, 늘 같이 걱정해주고, 위로해 준 오빠와 동생에게도 고맙다는 말을 전합니다. 5년이라는 박사과정 동안, 많은 후배들과 박사님들, 연구원 선생님들을 알게 되어서, 좋은 인연을 만들 수 있었던 시간들이었습니다. 저의 하소연들을 다 들어 주고, 저를 가장 잘 도와준 야무지고, 알뜰한 지은씨, 뛰어난 유머 감각과 센스 소유자인 다은이 너무 너무 고맙고, 많은 유행어를 창출하며 먼저 졸업한 주형씨, 삶의 밸런스를 잘 맞춰가며 인생을 즐기는 재화씨, 조용한 학명이, 너무나 많은 연예인(?)과 사물, 동물(?)을 닮은 안중이, 베스트 드라이버 근영이, 모두들 힘든 실험실 생활에도 활력소가 되어주고, 부족한 선배를 믿고 따라줘서 너무 고맙습니다. 비슷한 시기에 대학원을 입학해서, 함께 수업을 듣고, 많은 시간을 함께 가졌던, 창식쌤, 영지, 늘 이해해주어서 고맙고, 늘 건강하고, 앞으로도 자주 연락하며 지냈으면 좋겠습니다. 부지런하고, 책임감이 강해서 뭐든 잘하는 은경이, 현아, 효진이, 준선이 앞으로도 열심히 해서 좋은 연구 성과로 졸업하길 바랍니다. 멀리서 늘 지켜 봐주고 도움이 필요할 때는 언제든 달려와 주신 언화 언니 너무 고맙습니다. 꼼꼼히 잘 챙겨주고, 서로 힘이 되었

던 해영이 더욱 건강해지길 바라며, 실험실 생활에 여유를 가질 수 있게 해주었던, 지금은 미국에서 열심히 연구하고 있는 유일한 친구 같은 정민씨에게 고맙다는 말을 전합니다. 일일이 언급하지는 못했지만, 저를 도와주신 많은 분들께 다시 한번 진심으로 감사의 마음을 표합니다. 앞으로도 더욱 정진하여 좋은 연구 성과와 배움을 나눔으로, 여러분들에 대한 감사의 마음에 보답 드리겠습니다.

부족하나마 이 논문을 완성할 수 있도록 지혜와 건강을 허락해주신 은혜로우신 하나님께 진심으로 감사드립니다.